Annex I: Global to Regional Atlas

Coordinating Editors: Hans-Otto Pörtner (Germany), Andrés Alegría (Germany/Honduras)

Editorial Team: Vincent Möller (Germany), Elvira S. Poloczanska (United Kingdom/Australia), Katja Mintenbeck (Germany), Sandra Götze (Germany)

AR6 WGII Chapter Representatives: Aditi Mukherji (Chapter 4), Carolina Adler (Chapter 17/CCP5), Christopher H. Trisos (Chapter 9), Christopher Lennard (Chapter 9), David S. Gutzler (Chapter 14), David Wrathall (Chapter 8), Delphine Deryng (Chapter 5), Donovan Campbell (Chapter 15), Elham Ali (Chapter 4), Gerald Nelson (Chapter 5), Guéladio Cissé (Chapter 7), Jamon Van Den Hoek (Chapter 8), Jeff Price (Chapter 2/CCP1), Joanna McMillan (Chapter 8), Joern Birkmann (Chapter 8), John Pinnegar (Chapter 15), Kevin Hennessy (Chapter 11), Kirstin Holsman (Chapter 14/CCP6), Laura Ramajo Gallardo (Chapter 12), Laurent Bopp (Chapter 3), Lea Berrang Ford (Chapter 16), M. Silvia Muylaert de Araujo (Chapter 18), Marie-Fanny Racault (Chapter 3), Marjolijn Hassnoot (Chapter 13), Mark Costello (Chapter 11/CCP1) Mark Pelling (Chapter 6), Nicholas P. Simpson (Chapter 9), Nicola Stevens (Chapter 2/CCP4), Piero Lionello (Chapter 13/CCP4), Rebecca Harris (Chapter 2/CCP3), Richard Dawson (Chapter 6/CCP2), Tabea Katharina Lissner (Chapter 4), Timon McPhearson (Chapter 6), Valeria Moreno Rudloff (CCP5) Veruska Muccione (Chapter 13), Winston Chow (Chapter 6/CCP2), Wolfgang Cramer (Chapter 1/CCP4), Wolfgang Kiessling (Chapter 3/CCP1), Yukiko Hirabayashi (Chapter 4), Zelina Zaiton Ibrahim (Chapter 16)

Date of Draft: 1October 2021

Notes: TSU Compiled Version

Table of Contents

AI.1 Introduction

The WGII Global to Regional Atlas integrates and expands on the key messages in WGII Chapters and Cross-Chapter Papers to provide summaries of vulnerability, impacts, exposure, adaptation and risk complementing the narrative in the Summary for Policymakers. Where useful for a more complete storyline, complementary maps and figures from the three AR6 Special Reports are included. Figures are grouped in topical clusters: 1. Biodiversity, Biogeography, Habitability, Health, a: Wild Species, b: Humans, c: Livestock and Crop Production, d: Fish Stocks and Fisheries (AI.2.1), 2. Water-related Challenges for Cities, Settlements and Key Infrastructure, a: Drought, b: Flooding (AI.2.2), 3. Global to Regional Risks (incl. economic), Vulnerabilities, and Adaptive Capacities (AI.2.3), and 4. From Adaptation to Climate Resilient Development (AI.2.4). Within each topical cluster, the SPM storyline is followed depending on the material available, from observed impacts (and adaptation) and projected impacts and risks, adaptation and enabling conditions to climate resilient development.

The Atlas provides visual support to key findings of the Assessment Report allowing a broader display of material and case studies. The Atlas is not intended to be comprehensive. The underlying scientific basis for each map is indicated by references to sections of the underlying report.

AI.1.1 Risk Framework

The Atlas includes mapping of the different components of risk. Risk in this report is defined as the potential for adverse consequences for human or ecological systems, recognizing the diversity of values and objectives associated with such systems. In the context of climate change impacts, risks result from dynamic interactions between climate-related hazards with the exposure and vulnerability of the affected human or ecological system. In the context of climate change responses, risks result from the potential for such responses not achieving the intended objective(s), or from potential trade-offs or negative side-effects (see Annex II: Glossary). Risk management is defined as plans, actions, strategies or policies to reduce the likelihood and/or magnitude of adverse potential consequences, based on assessed or perceived risks (see Annex II: Glossary). {1.2.1.1}

Vulnerability is a component of risk, but also an important focus independently. Vulnerability in this report is defined as the propensity or predisposition to be adversely affected. Vulnerability encompasses a variety of concepts and elements including sensitivity or susceptibility to harm and lack of capacity to cope and adapt (see Annex II: Glossary). Over the past several decades, approaches to analysing and assessing vulnerability have evolved. An early emphasis on top-down, biophysical evaluation of vulnerability included—and often started with—exposure to climate hazards in assessing vulnerability. From this starting point, attention to bottom-up, social and contextual determinants of vulnerability, which often differ, has emerged, although this approach is incompletely applied or integrated across contexts (Rufat et al., 2015; Spielman et al., 2020; Taberna et al., 2020). Vulnerability is now widely understood to differ within communities and across societies, also changing through time (Jurgilevich et al., 2017; Kienberger et al., 2013; see also Chapter 16). In the WGII AR6, assessment of the vulnerability of people and ecosystems encompasses the differing approaches that exist within the literature, both critiquing and harmonizing them based on available evidence. In this context, **exposure** is defined as the presence of people; livelihoods; species or ecosystems; environmental functions, services, and resources; infrastructure; or economic, social, or cultural assets in places and settings that could be adversely affected (Annex II: Glossary). Potentially affected places and settings can be defined geographically, as well as more dynamically, for example through transmission or interconnections through markets or flows of people. {1.2.1.1}

The WGII AR6 assessment focuses primarily on *adverse* consequences of climate change. However, climate change also has *positive* implications (benefits and opportunities) for certain people and systems. {16.1.2}

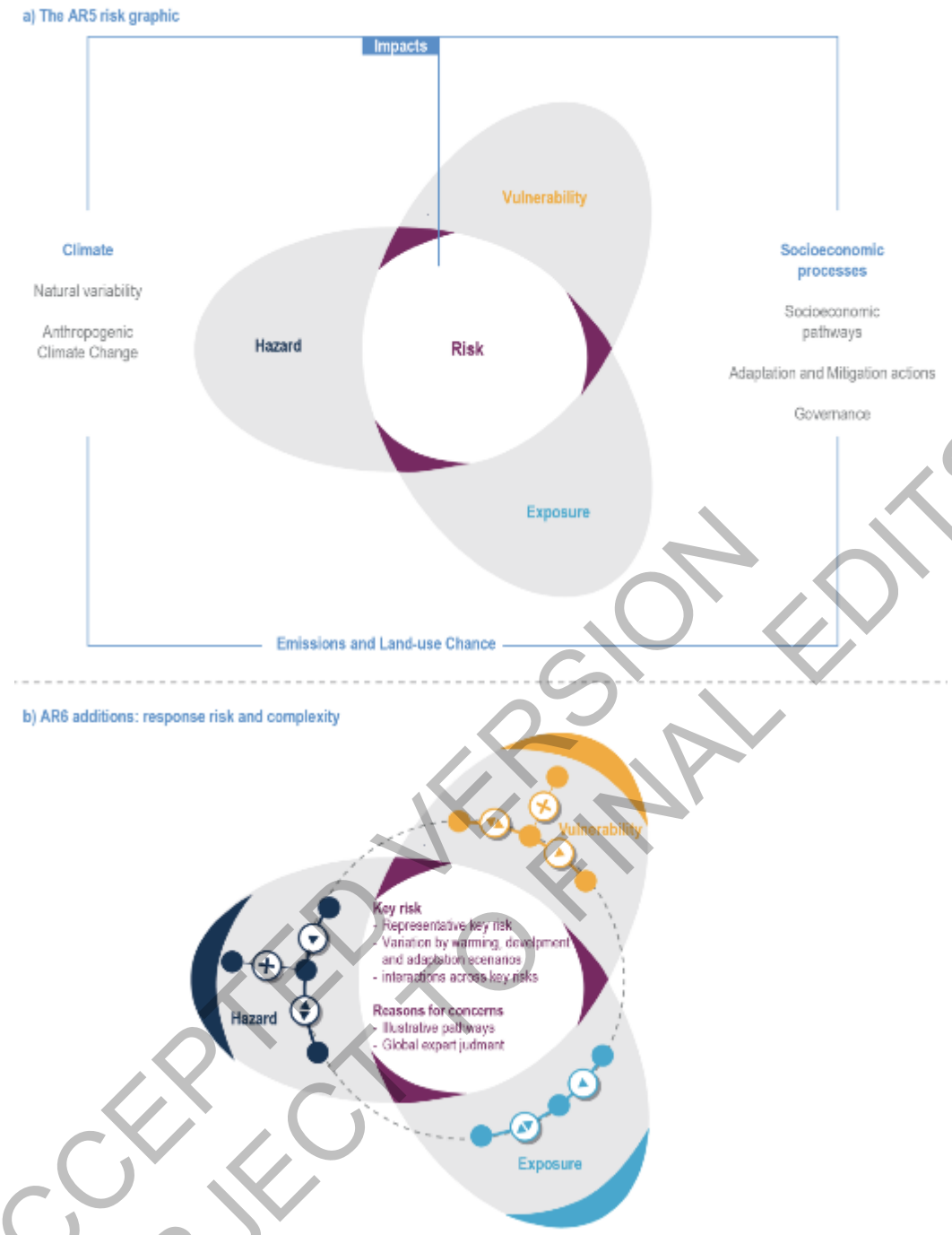

Figure AI.1: Risk in IPCC assessments. (a) An explicit risk framing emerged in the IPCC SREX and WGII AR5. (b) In the current AR6 assessment, the role of responses in modulating the determinants of risk is a new emphasis (the "wings" of the hazard, vulnerability, and exposure "propellers" represents the ways in which responses modulate each of these risk determinants {Figure 1.5}

AI.1.2 Regionalisation

As climate change is a multiscale phenomenon from the local to the global, the assessment of climate risks and climate change impacts is strongly spatial, with a focus on regional climate change. The term "regions" is used in different ways throughout the interdisciplinary AR6 assessment as the use of the term varies across disciplines. It is alternately used to point to a particular geography, relate physical distance or proximity, or categorize areas based on common biological, topographical characteristics, or elevation in relation to sea level. Its meaning depends on context. {1.3.3}

First, there are chapters dedicated to regional assessment in AR6 WGII (Chapters 9-14 and Cross-Chapter Paper 4), and within the content of these and other chapters of AR6, the term region is often used to describe continental and sub-continental regions, oceanic regions, hemispheres, or more specific localities within these geographic areas. Building on the continental domains defined in AR5 WGII and to ensure consistency with the AR6 WGI Atlas, AR6 WGII uses a Continental Set of Regions, namely Africa, Asia, Australasia, Europe, North America, Central & South America, Small Islands, Polar Regions, and the Ocean. For AR6, the continental regions include the land together with the coastal ocean. {1.3.3}

Second, the term regions is used to categorize areas around the globe with common topographical characteristics or biological characteristics. For example, Chapter 2 introduces regions in its discussion of biomes, as in arid, grassland, savanna, tundra regions, tropical, temperate, and boreal forested regions. Chapter 3 adds reference to an area's orientation with bodies of water, using terms such as deltaic, coastal, intercoastal, freshwater, and salty. On top of this, Cross-Chapter 2 uses a coastal region typology based on physical geomorphology considering elevation, coastal type, and topography (see CCP 2, pg. 5; Barragán and de Andrés, 2015; Haasnoot et al., 2019a; Kay and Adler, 2017). {1.3.3}

Third, cross-chapter papers are dedicated to *typological regions*, defined in the AR6 Glossary as regions that share one or more specific features (known as 'typologies'), such as geographic location (e.g., *coastal*), physical processes (e.g., *monsoons*), and biological (e.g., coral reefs, tropical *forests*), geological (e.g., mountains) or *anthropogenic* (e.g., megacities) formation, and for which it is useful to consider the common climate features. Typological regions are generally discontinuous (such as monsoon areas, mountains, and megacities) and are specifically used to integrate across similar climatological, geological and human domains. {1.3.3}

Fourth, the IPCC-WGI reference regions have been used for the regional synthesis of historical trends and future climate change projections. A recent update of these regions presented in AR6 WGI Atlas and used throughout AR6, offer an opportunity for refinement due to the higher atmospheric model resolution (including CMIP6). The number of land and ocean regions is 46 and 15, respectively, representing consistent regional climate features.

AI.1.3 Links to Working Group I

The WGII Atlas links to WGI through global and regional climate information {WGI Chapter 12, WGI Atlas}. Regional climate change information for impacts and for risk assessment draws on analysis of global and regional climatic variables that link climate conditions to sectors.

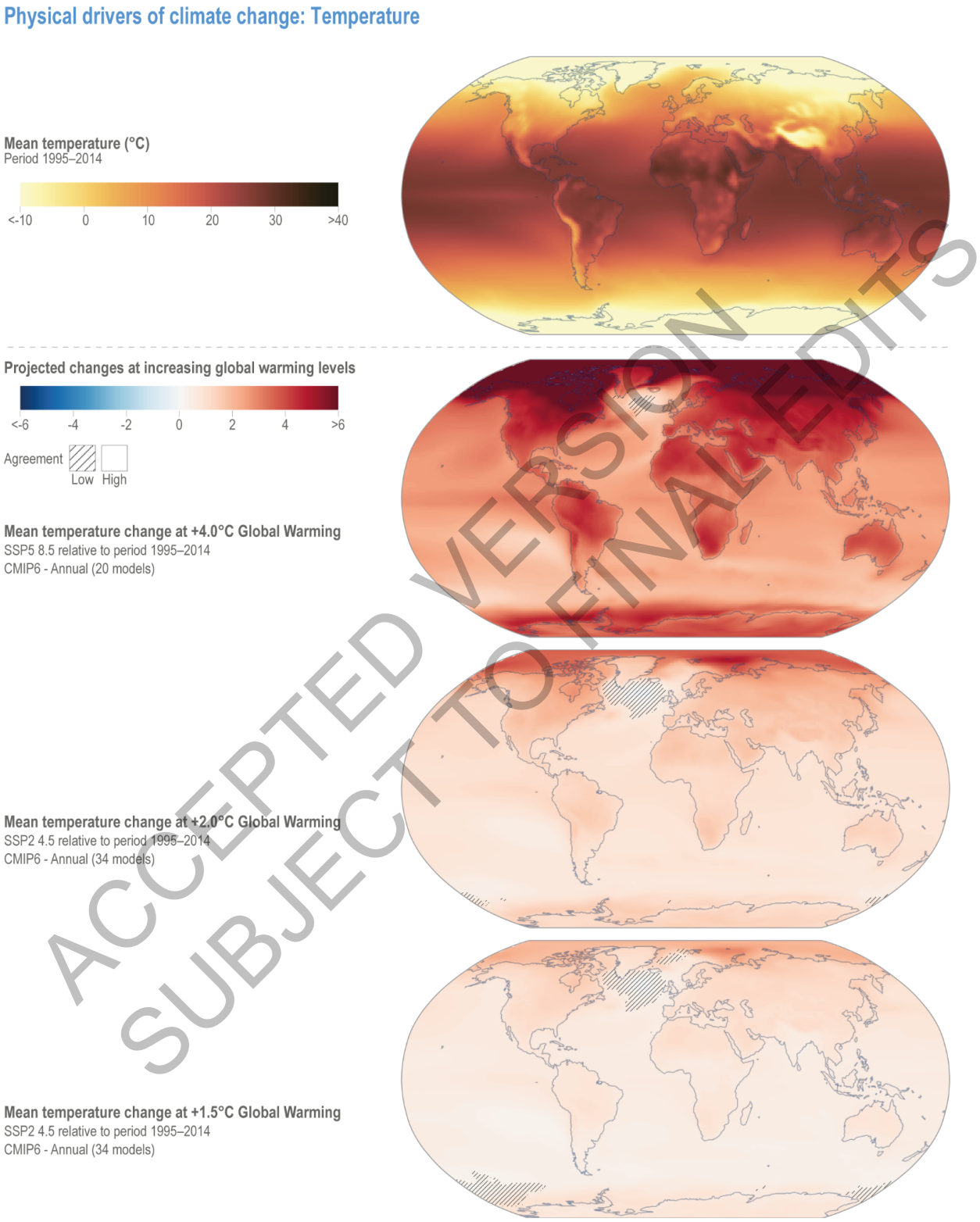

Figure AI.2 [INSERT CAPTION HERE]

Physical drivers of climate change: Precipitation

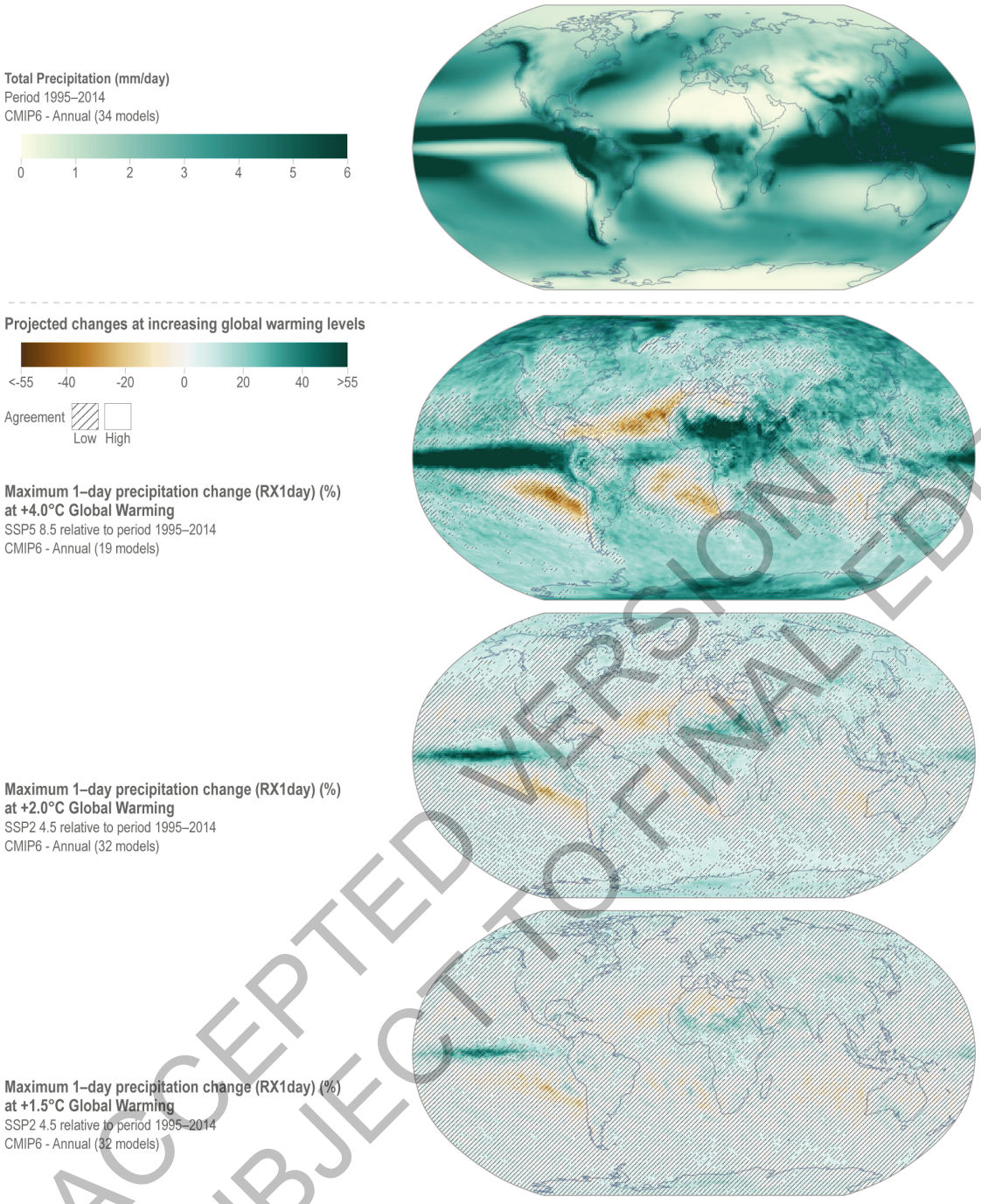

Figure AI.3 [INSERT CAPTION HERE]

Physical drivers of climate change: Dissolved oxygen in the ocean

Oxygen concentrations affect aerobic processes, such as energy metabolism, and anaerobic microbial processes, such as denitrification. Hence, projected decreases in dissolved oxygen concentration will impact organisms and their geographic distribution patterns in ways that depend upon their oxygen requirements, which are highest for large, multicellular organisms.

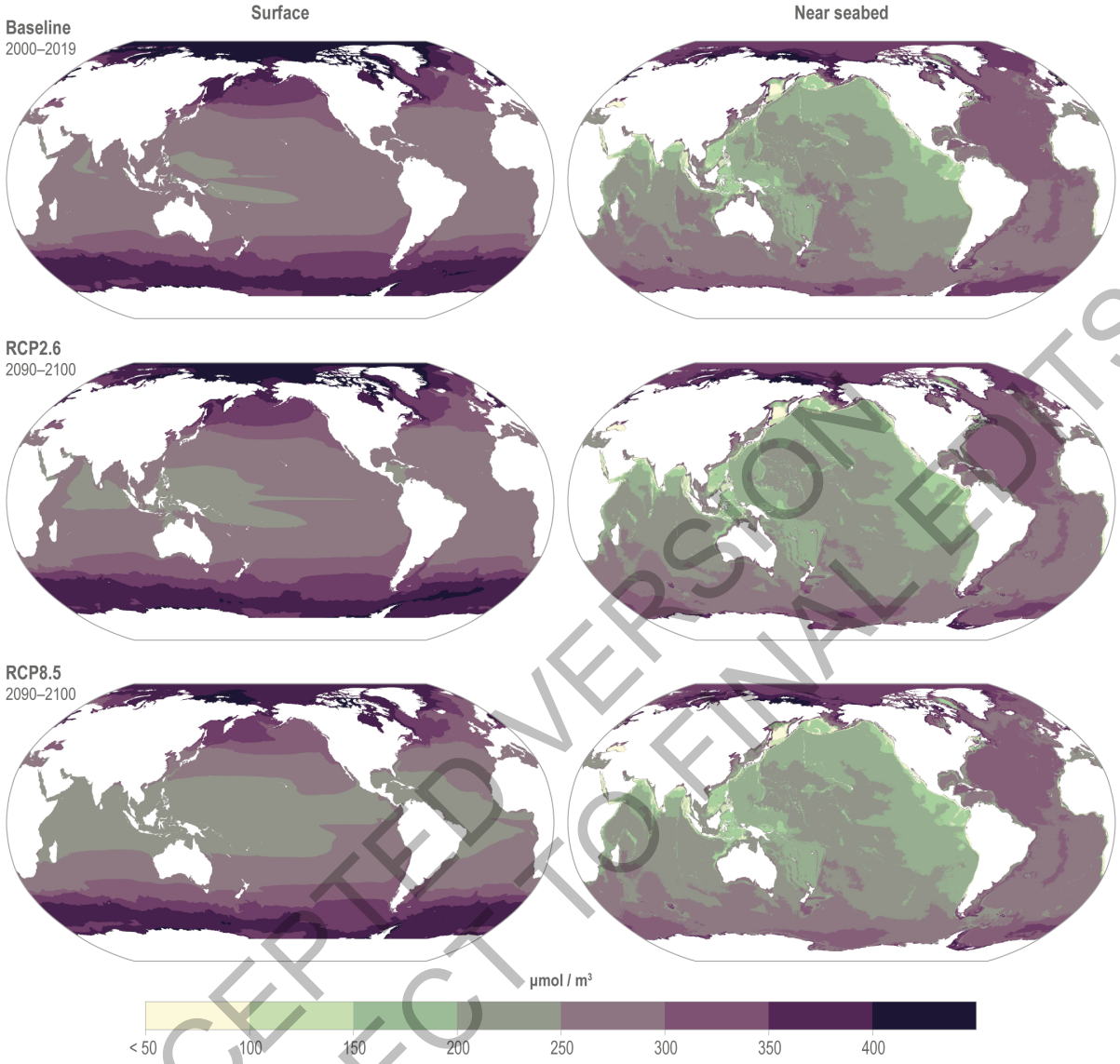

Figure AI.4 [INSERT CAPTION HERE]

Evidence of climate change impacts in many regions of the world

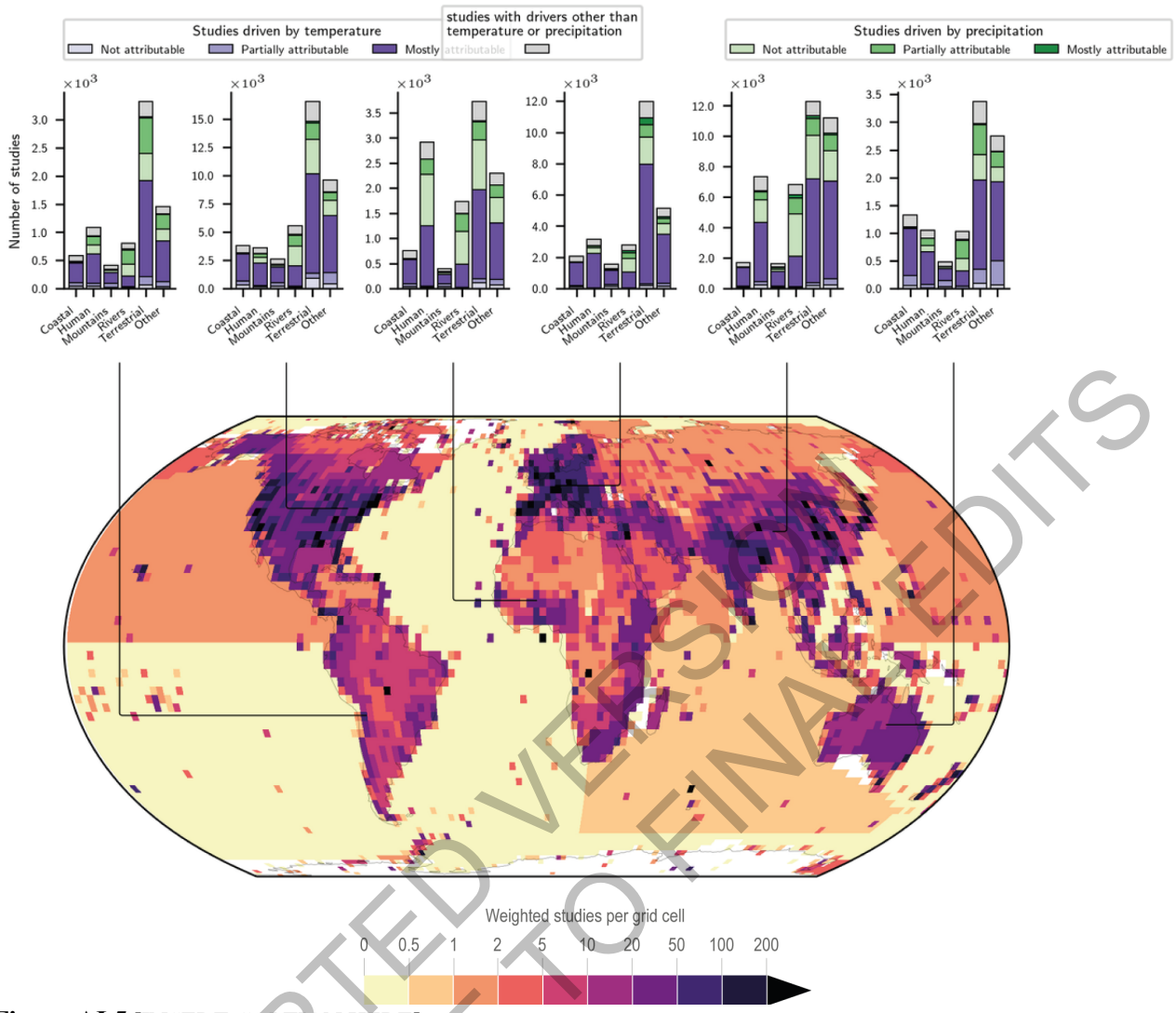

Figure AI.5 [INSERT CAPTION HERE]

AI.2 Global to Regional Maps

AI.2.1 Biodiversity, Biogeography, Habitability, Health

AI.2.1.1 Wild Species

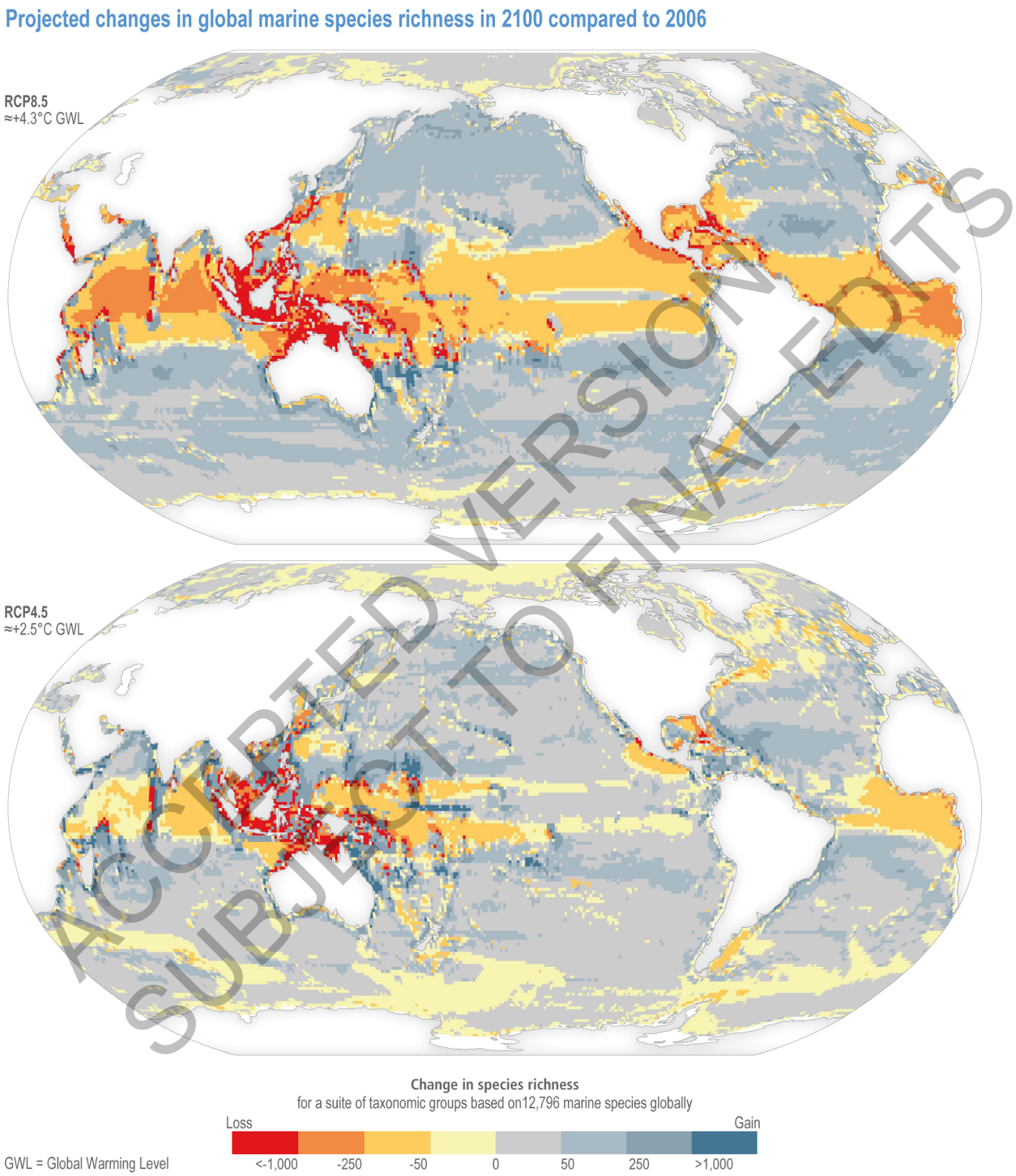

Figure AI.6 [INSERT CAPTION HERE]

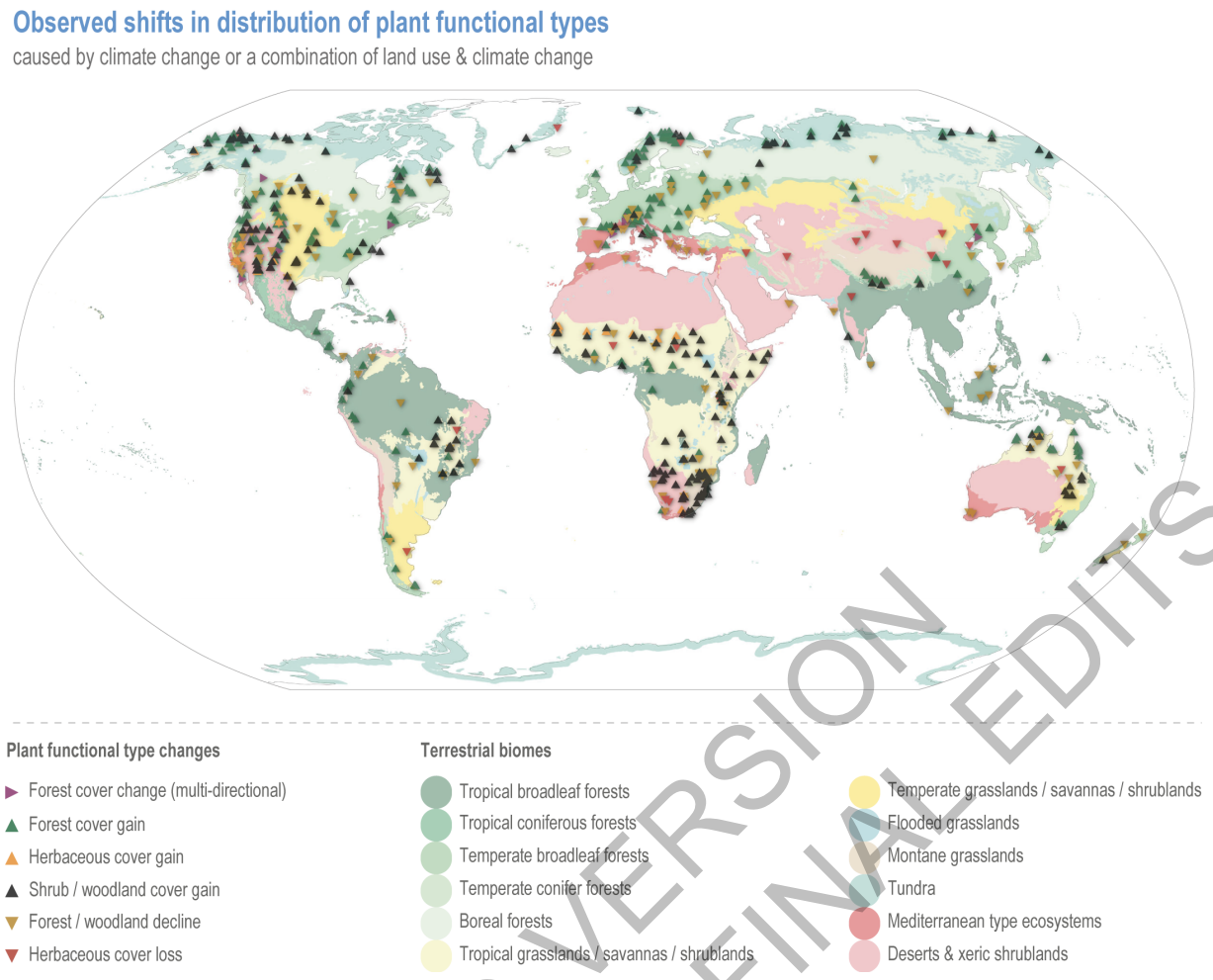

Figure AI.7 [INSERT CAPTION HERE]

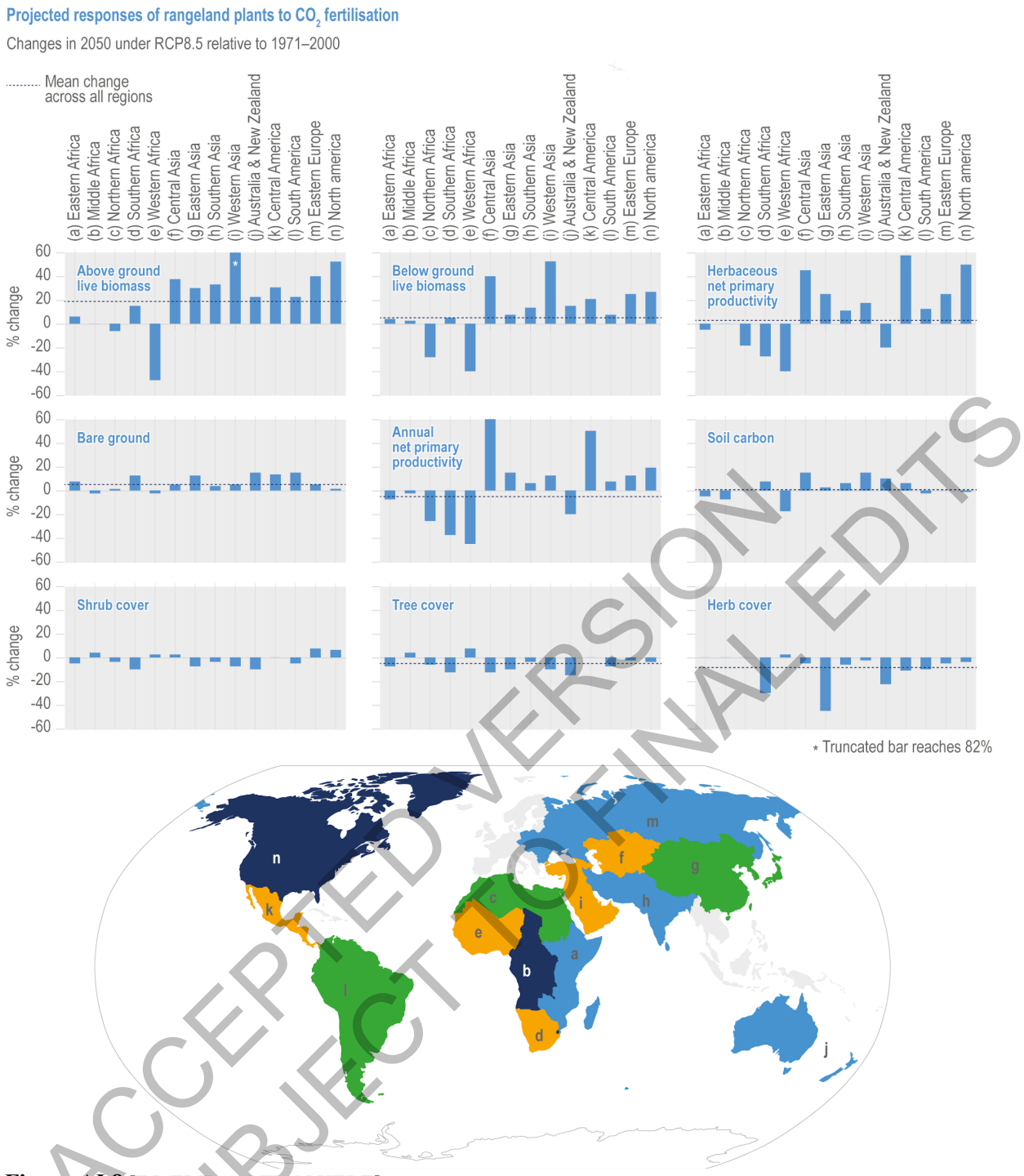

Figure AI.8 [INSERT CAPTION HERE]

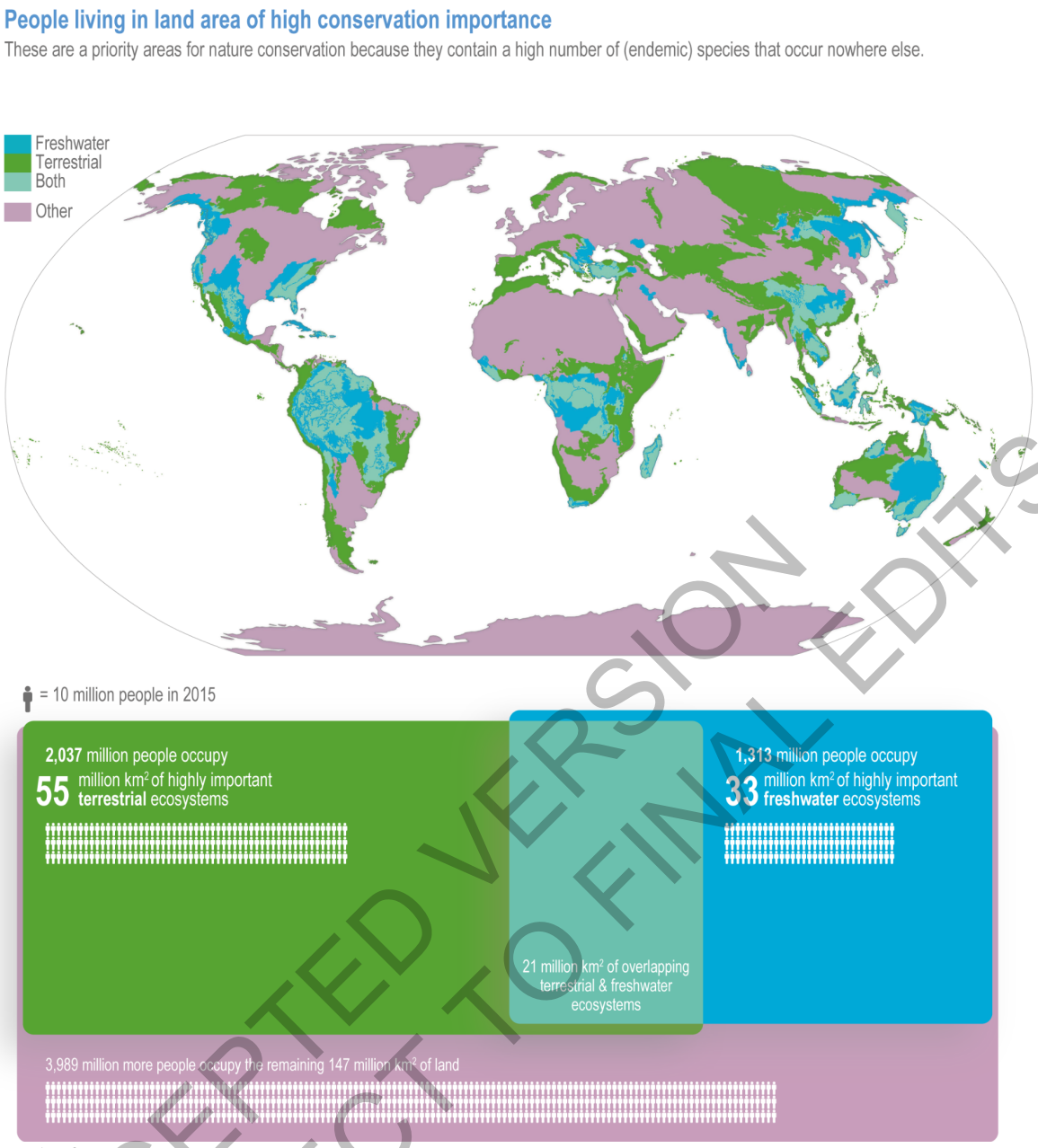

Figure AI.9 [INSERT CAPTION HERE]

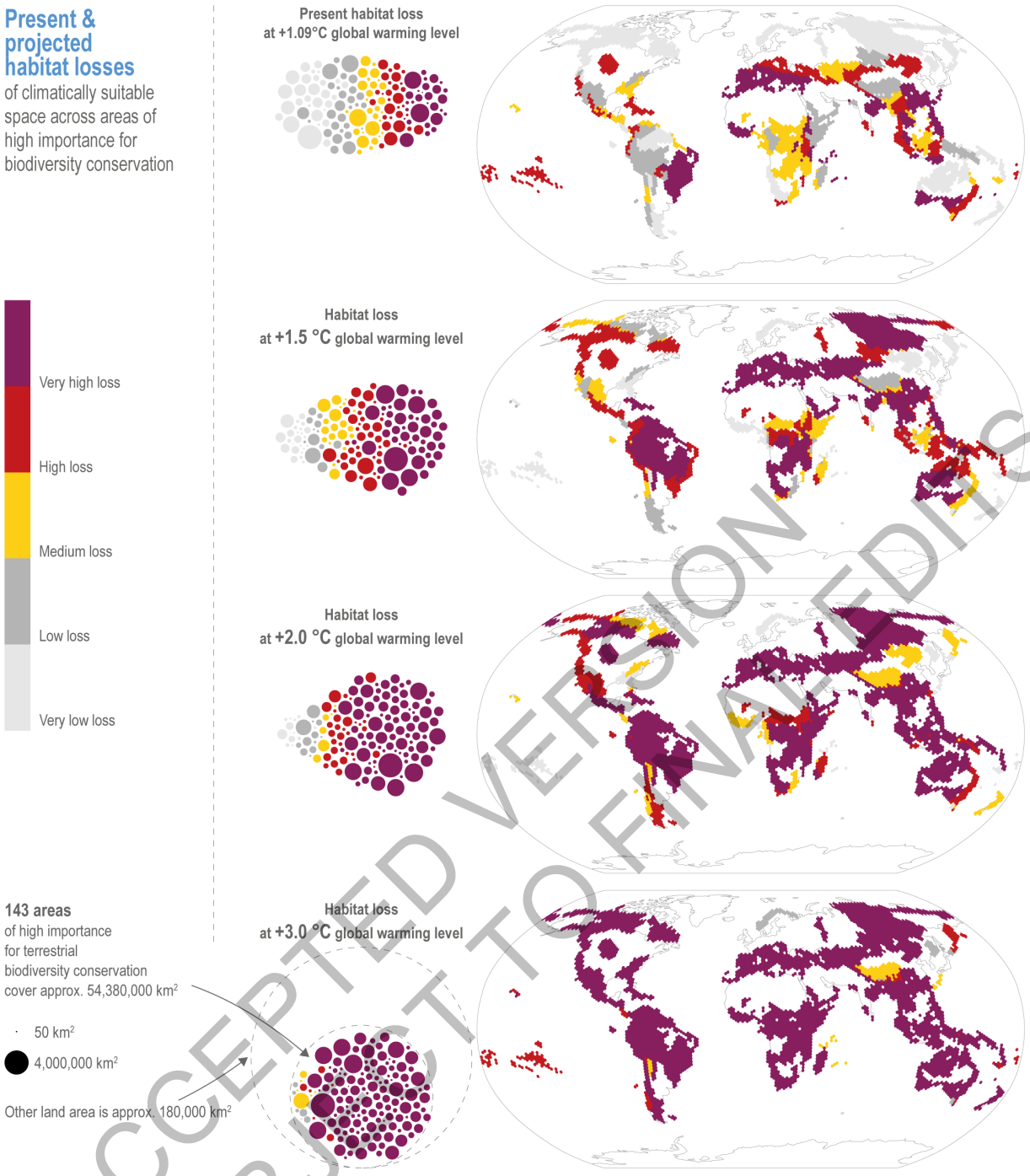

Figure AI.10 [INSERT CAPTION HERE]

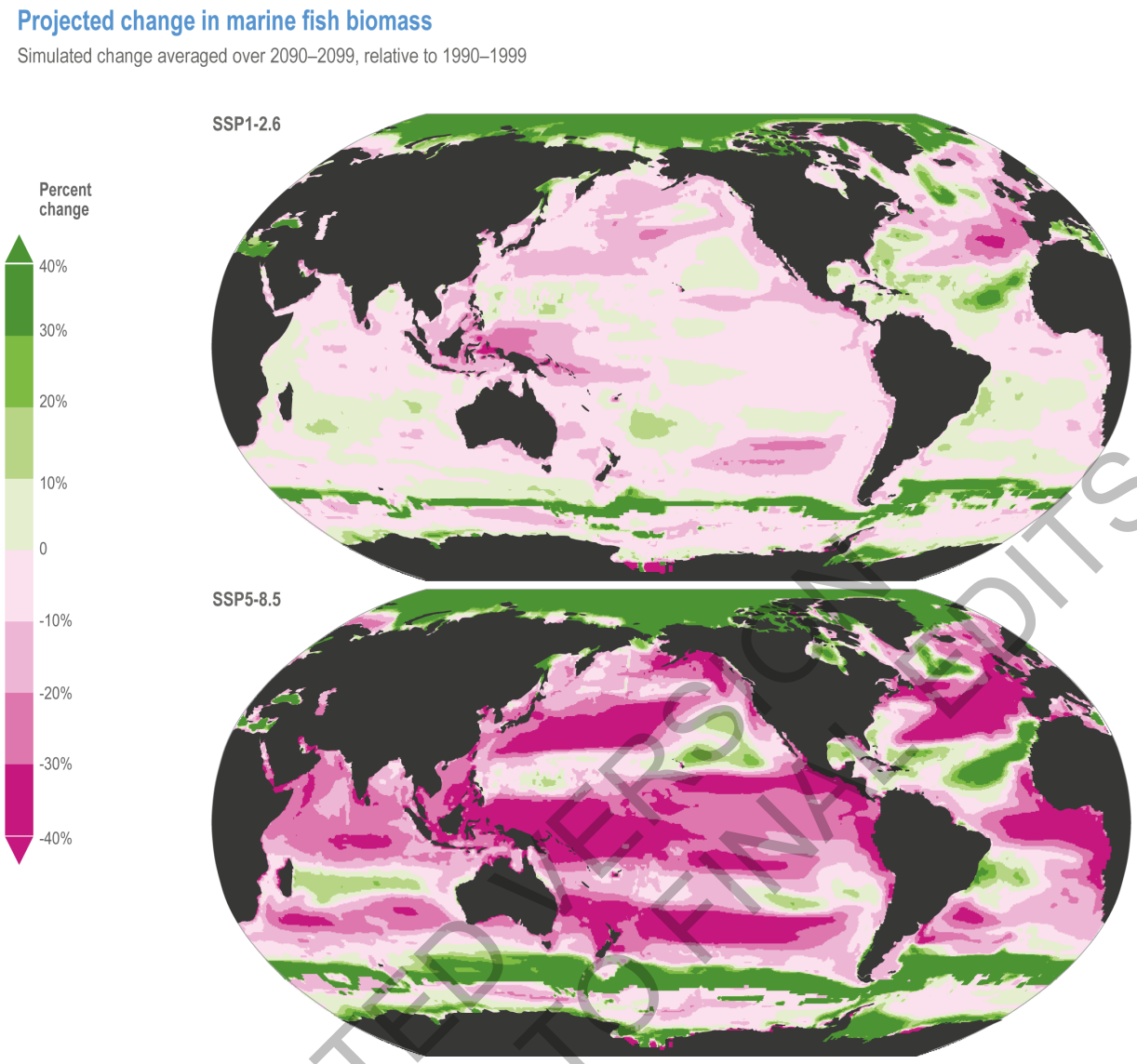

Figure AI.11 [INSERT CAPTION HERE]

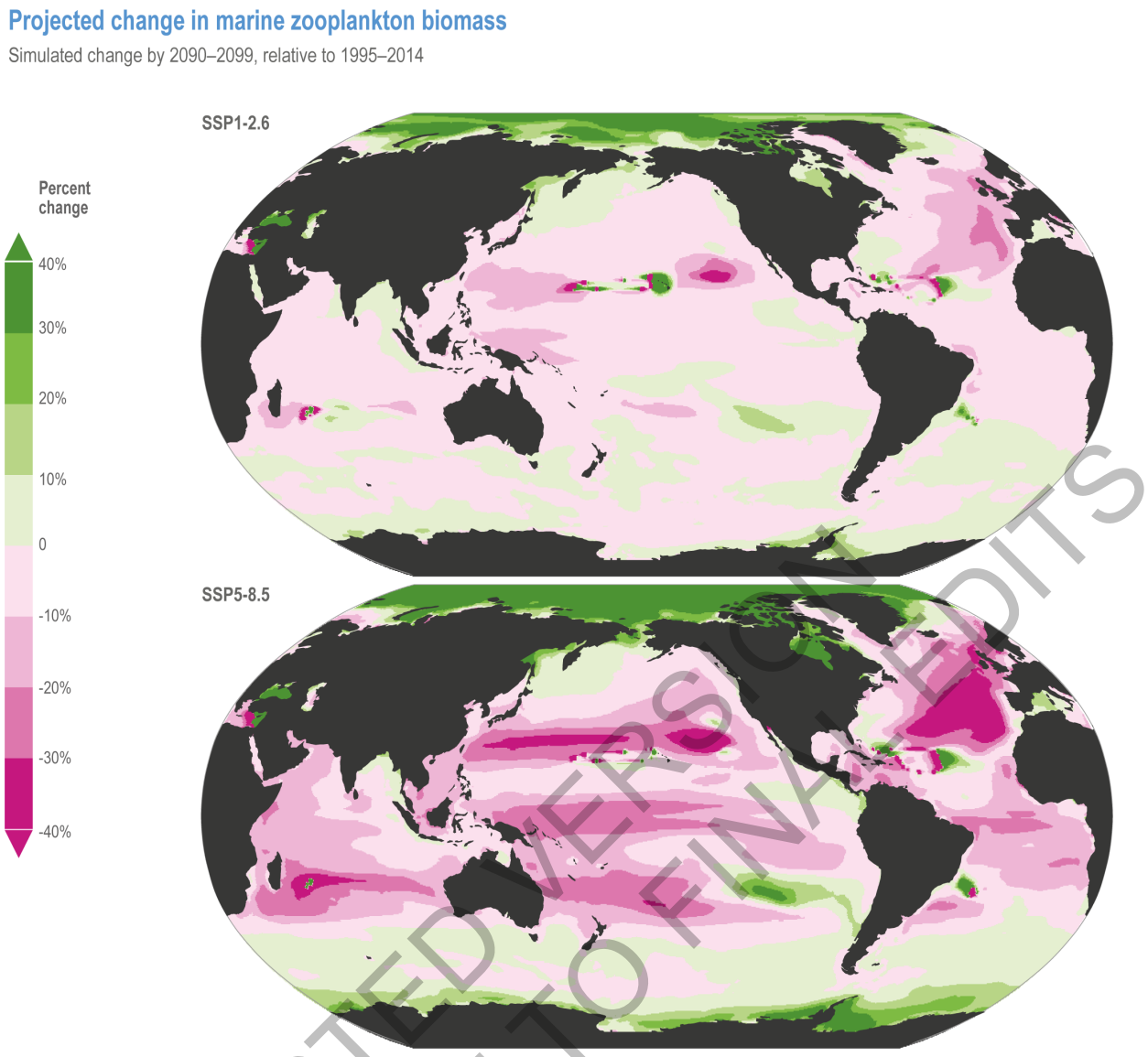

Figure AI.12 [INSERT CAPTION HERE]

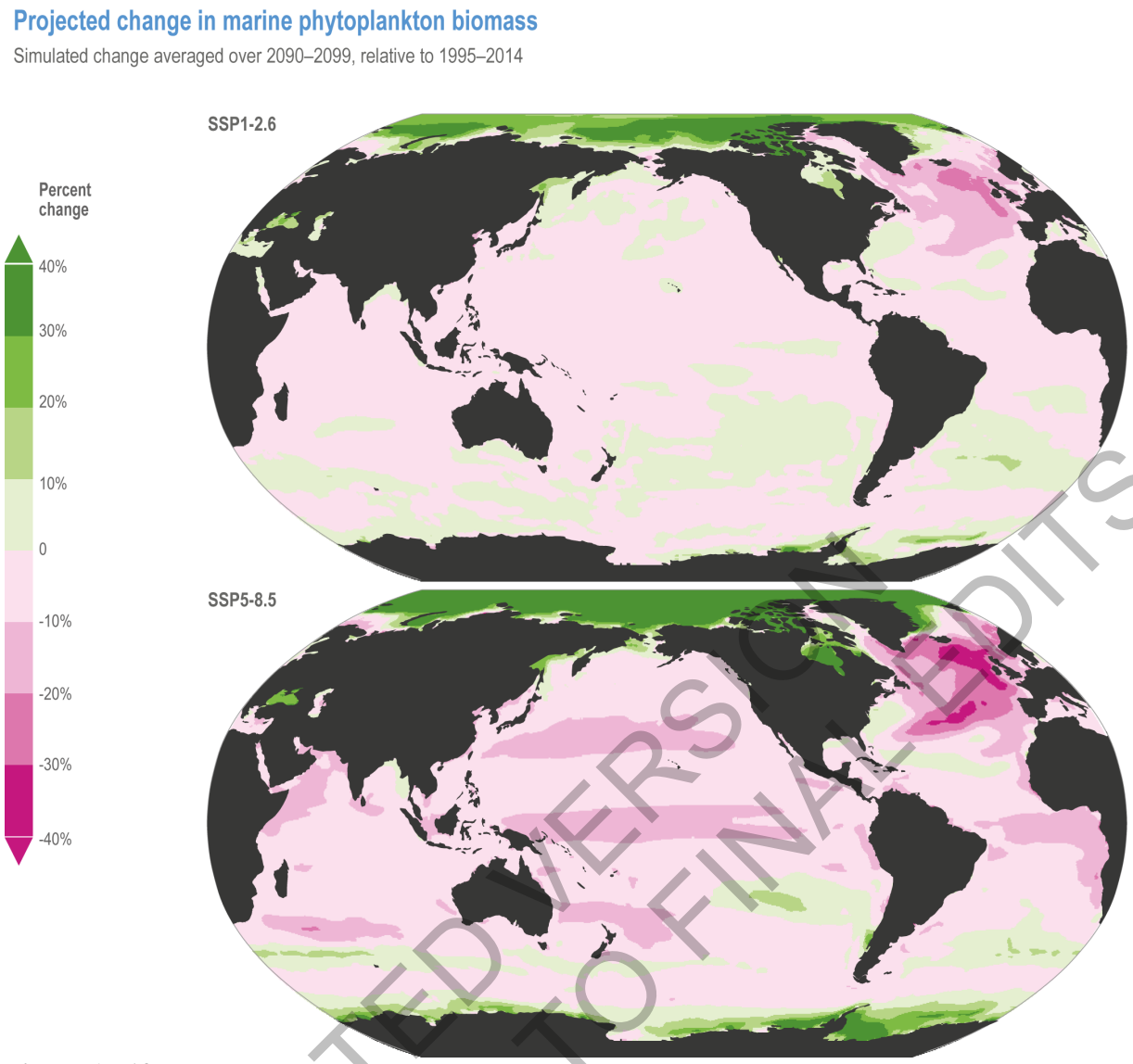

Figure AI.13 [INSERT CAPTION HERE]

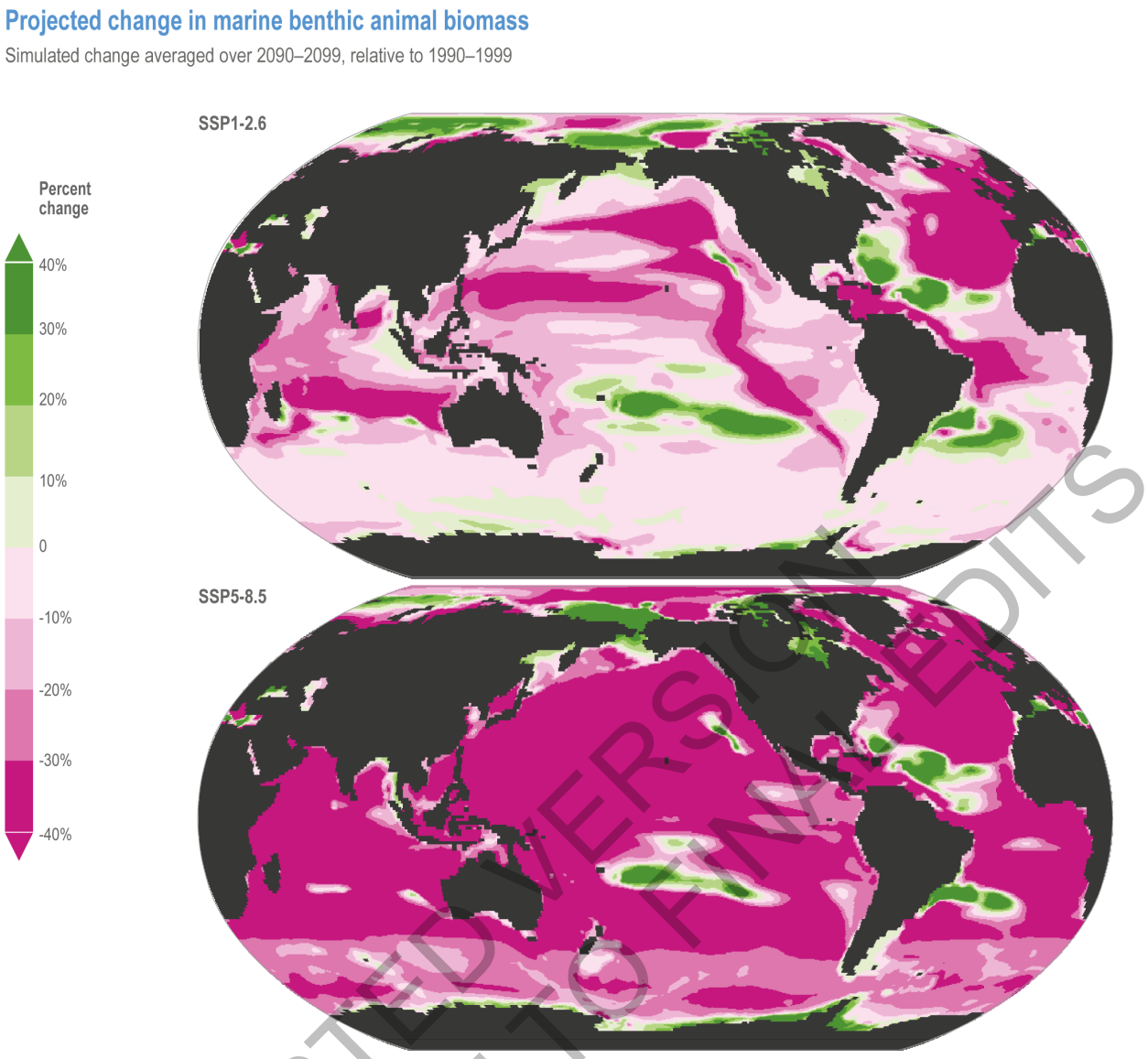

Figure AI.14 [INSERT CAPTION HERE]

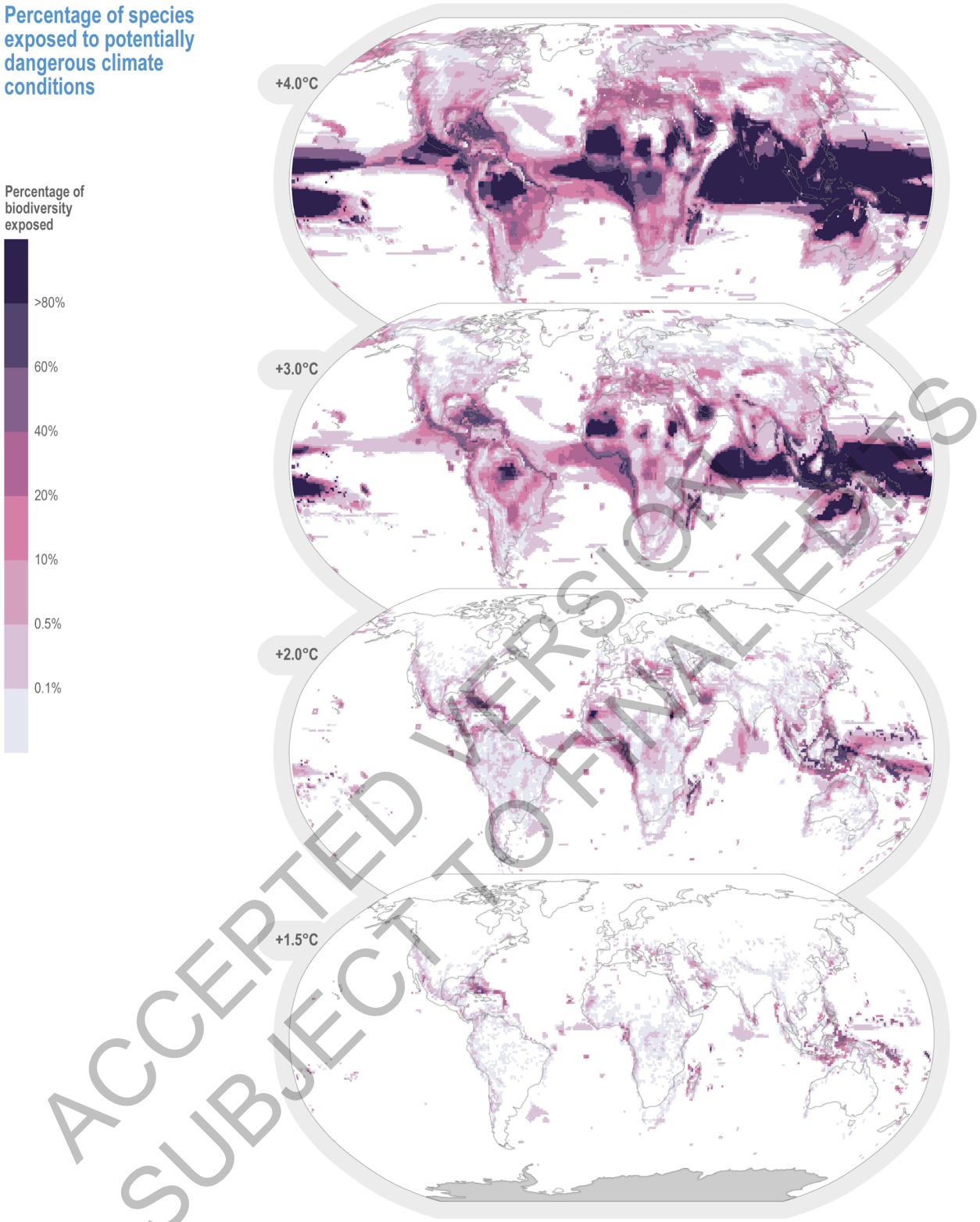

Figure AI.15 [INSERT CAPTION HERE]

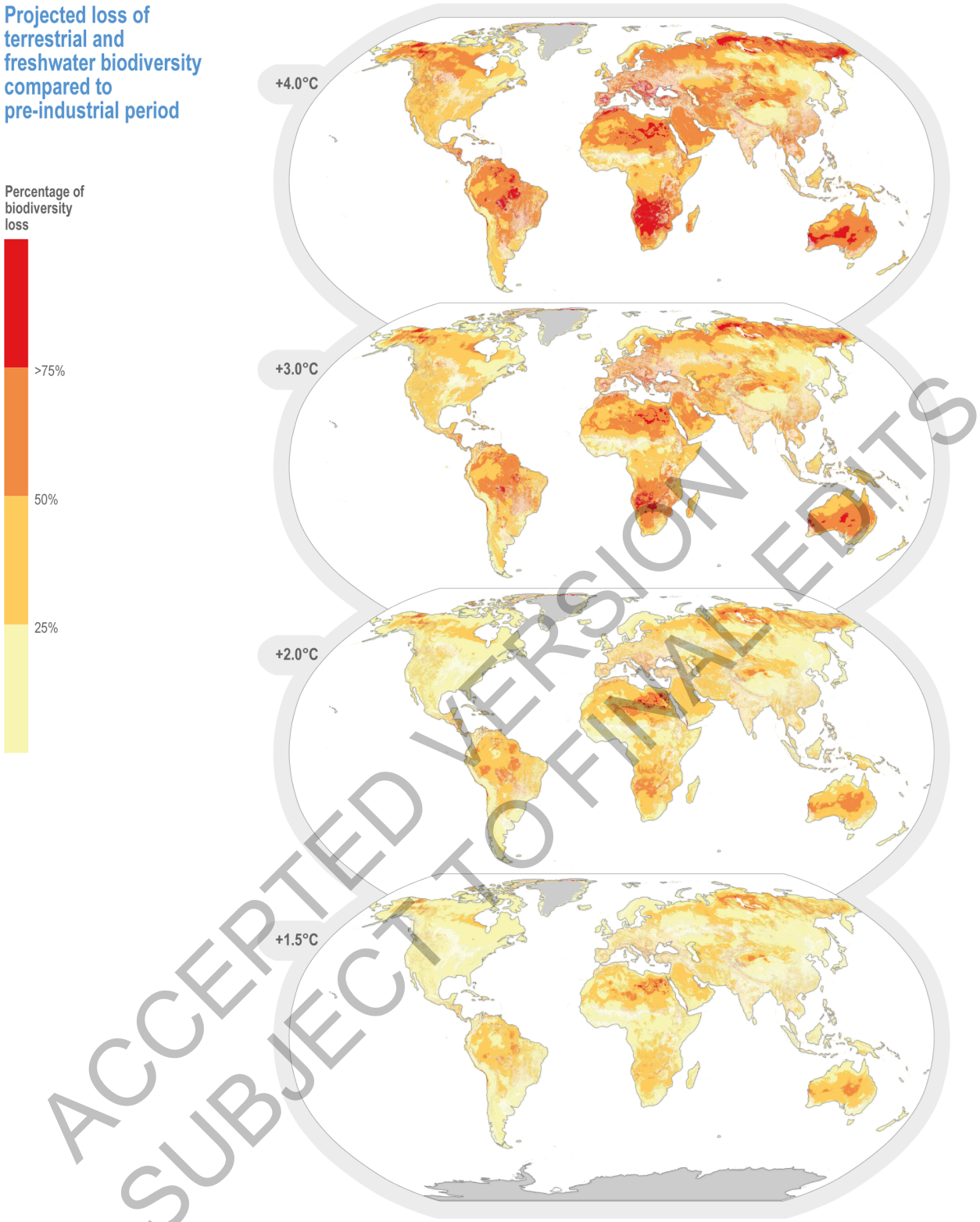

Figure AI.16 [INSERT CAPTION HERE]

AI.2.1.2 Livestock and Crop Production

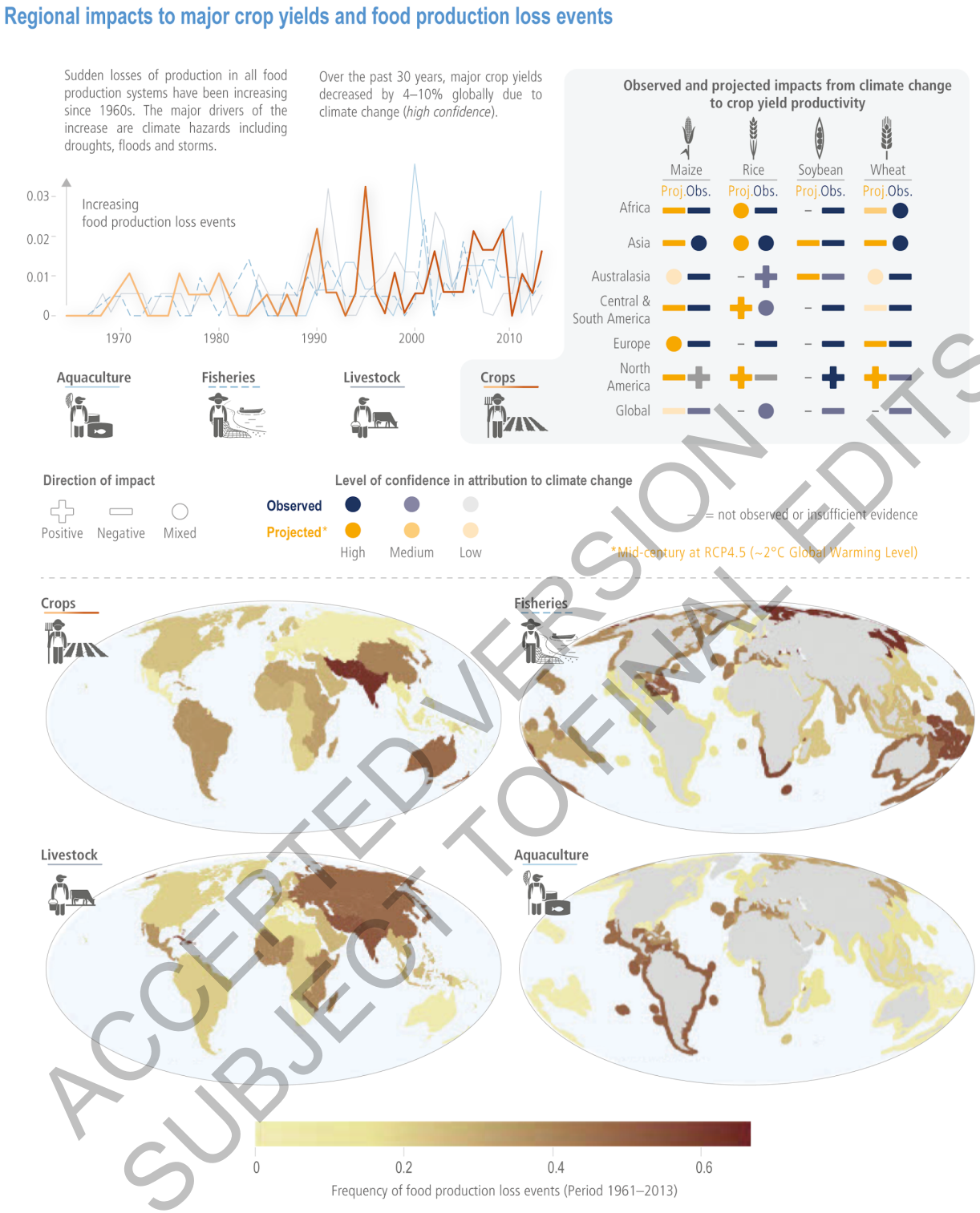

Figure AI.17 [INSERT CAPTION HERE]

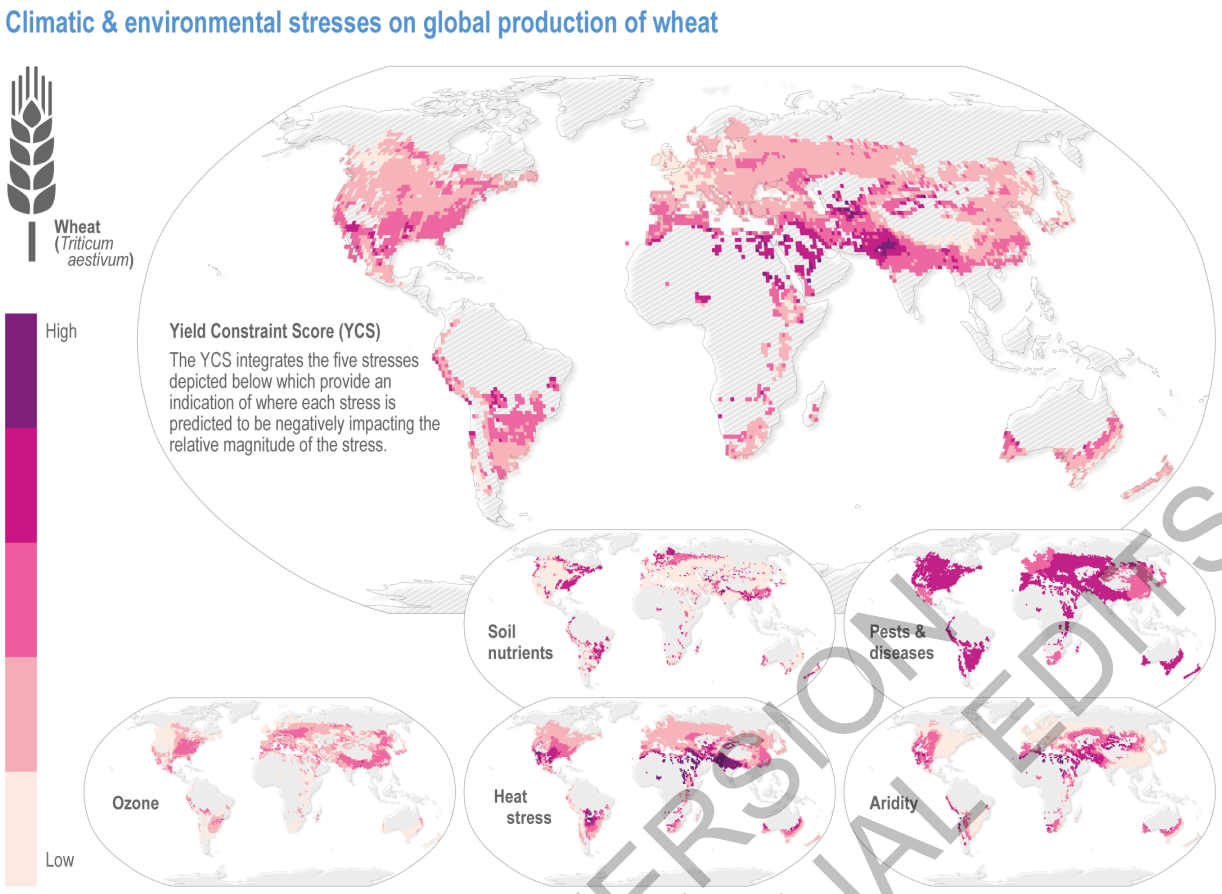

Figure AI.18 [INSERT CAPTION HERE]

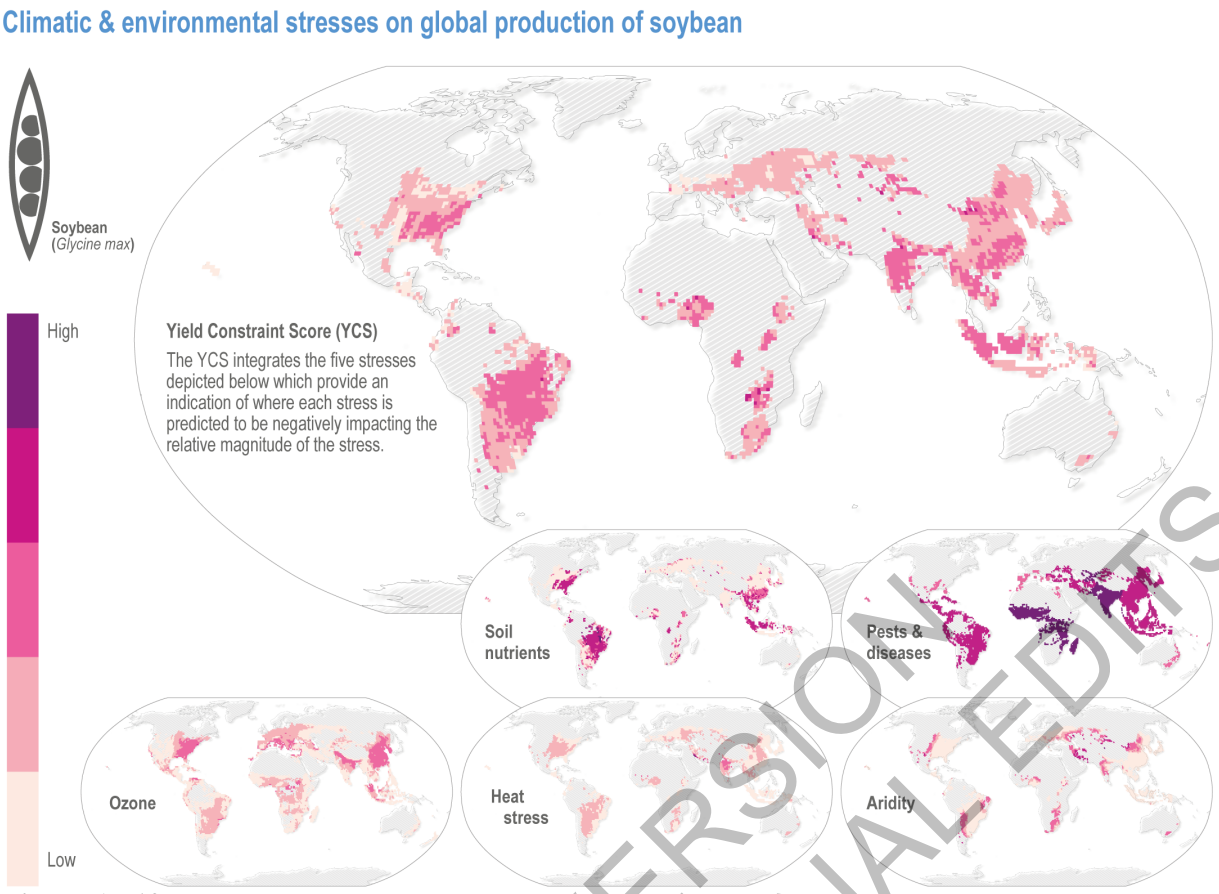

Figure AI.19 [INSERT CAPTION HERE]

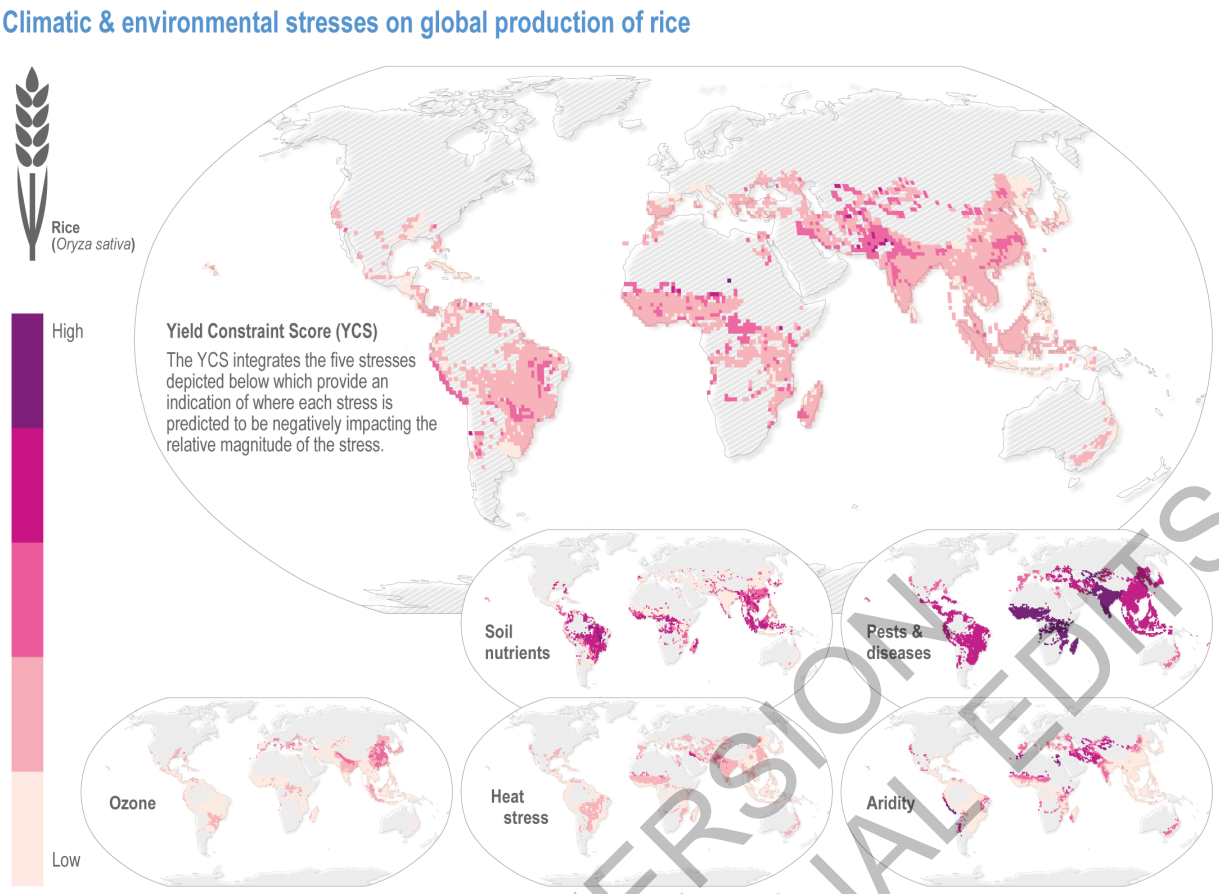

Figure AI.20 [INSERT CAPTION HERE]

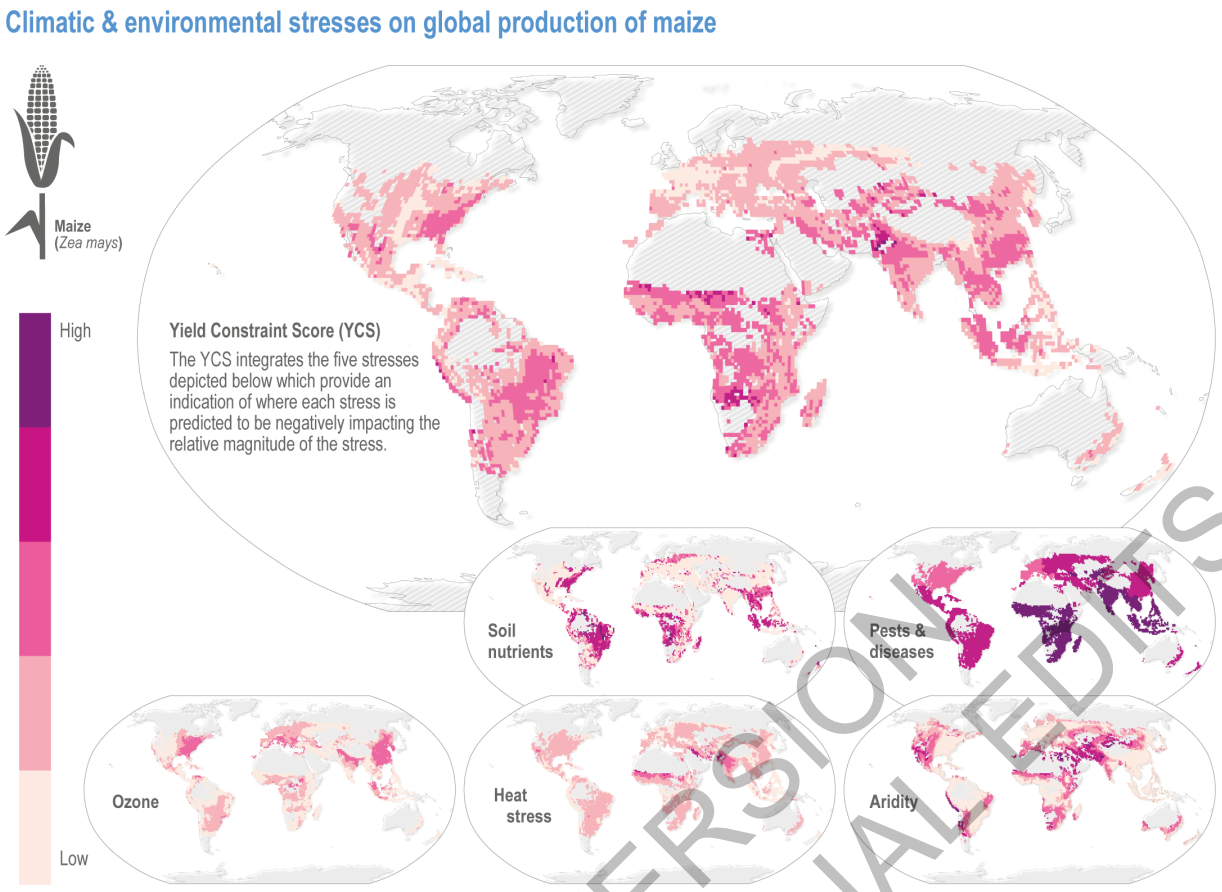

Figure AI.21 [INSERT CAPTION HERE]

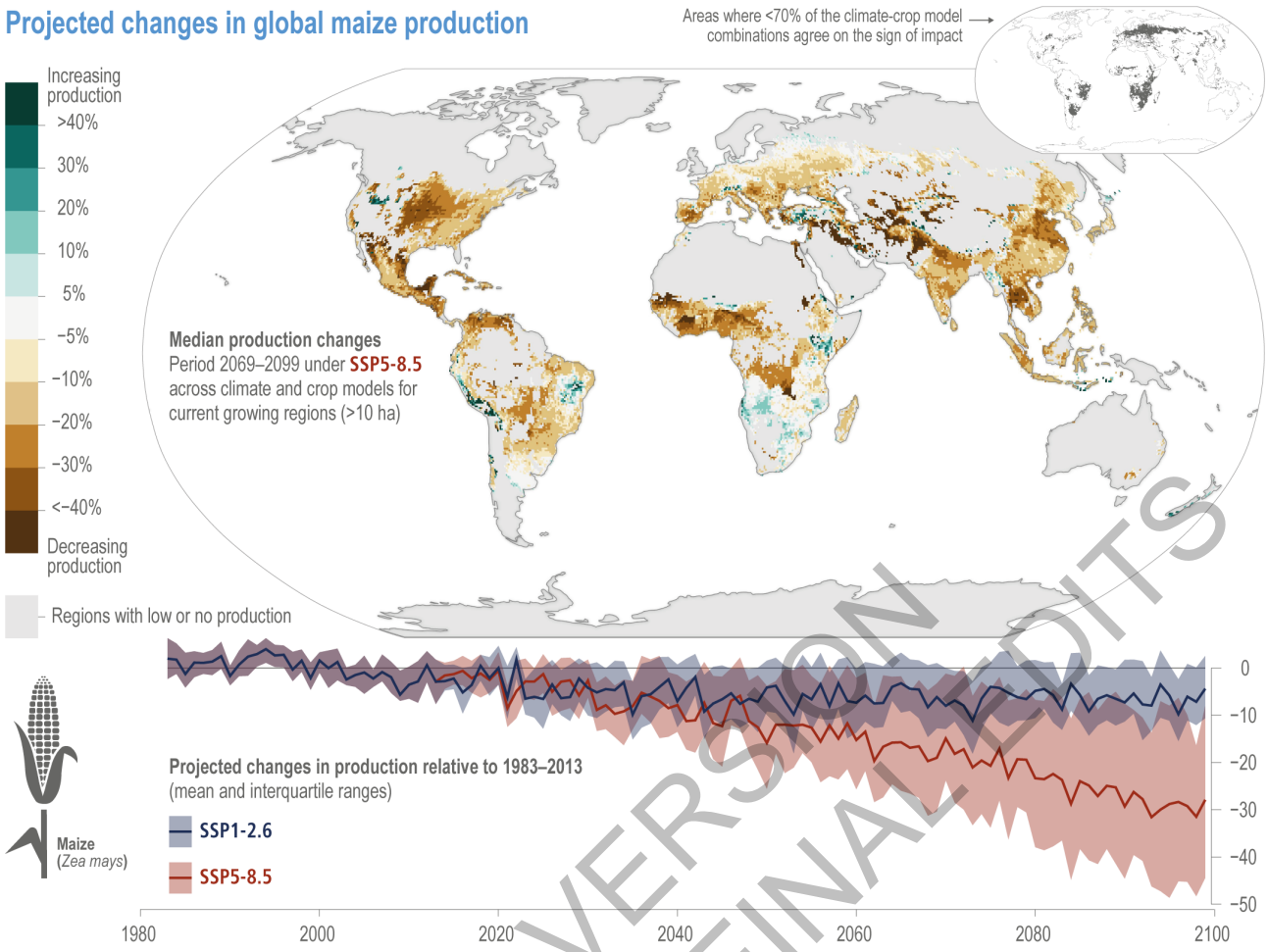

Figure AI.22 [INSERT CAPTION HERE]

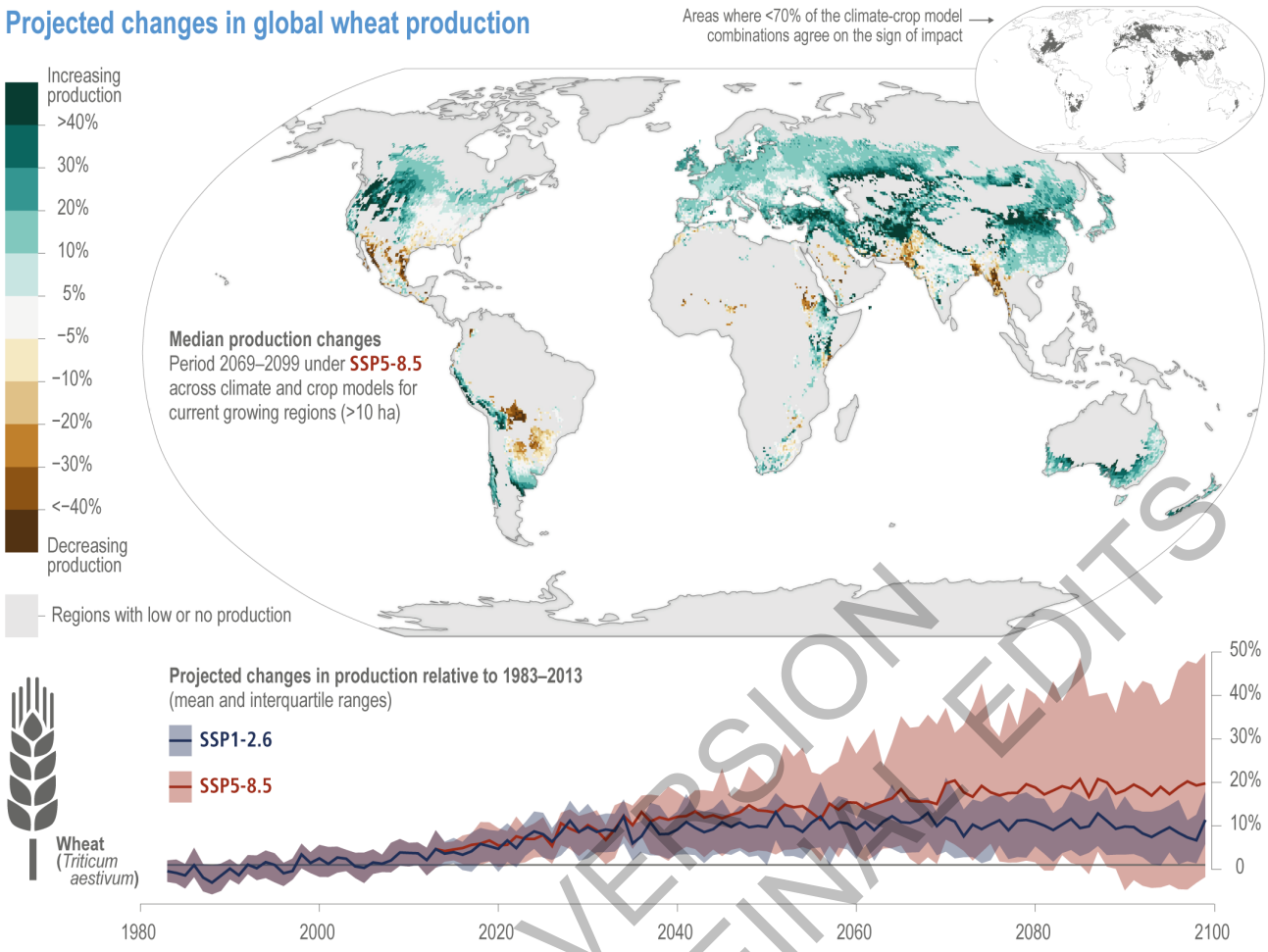

Figure AI.23 [INSERT CAPTION HERE]

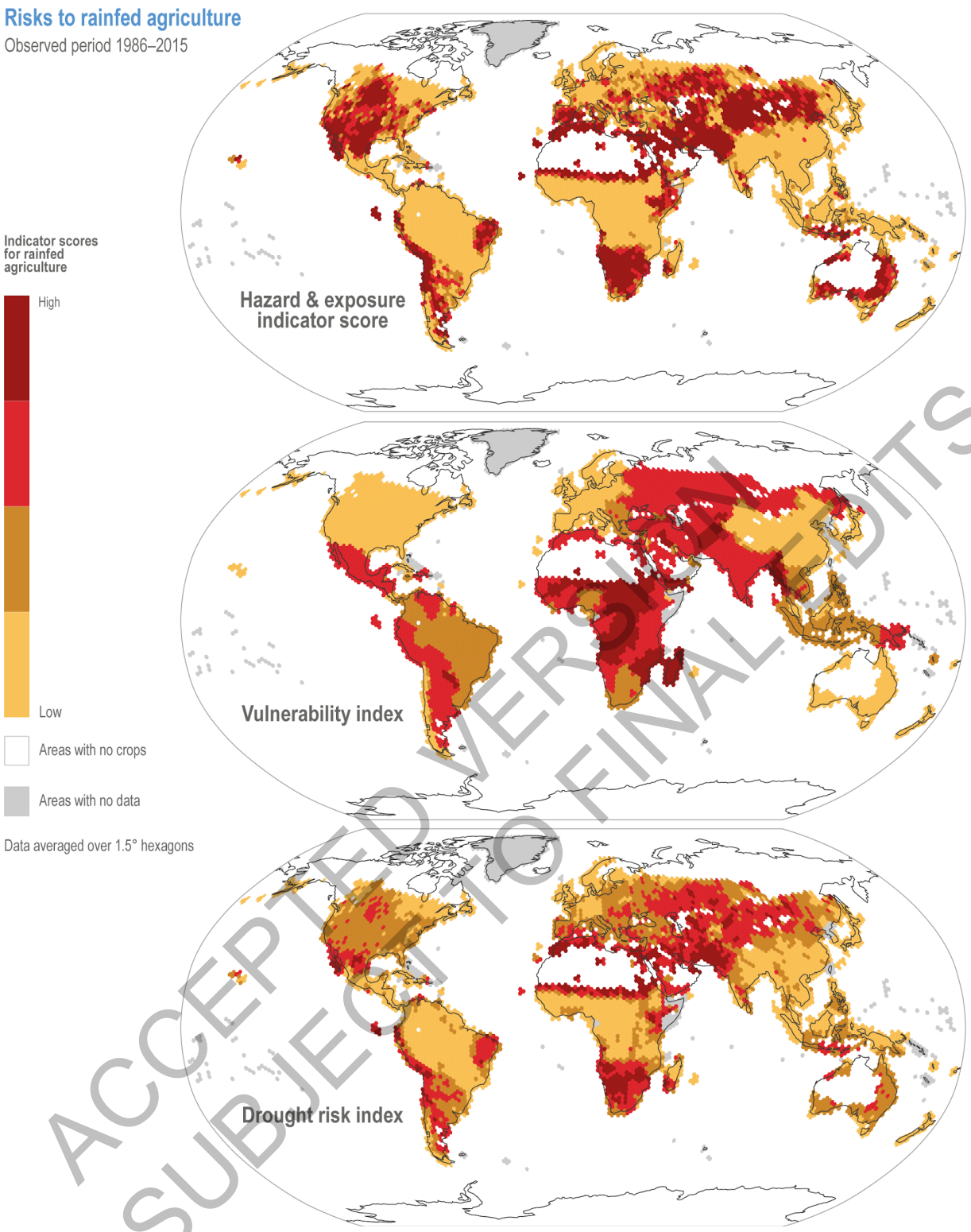

Figure AI.24 [INSERT CAPTION HERE]

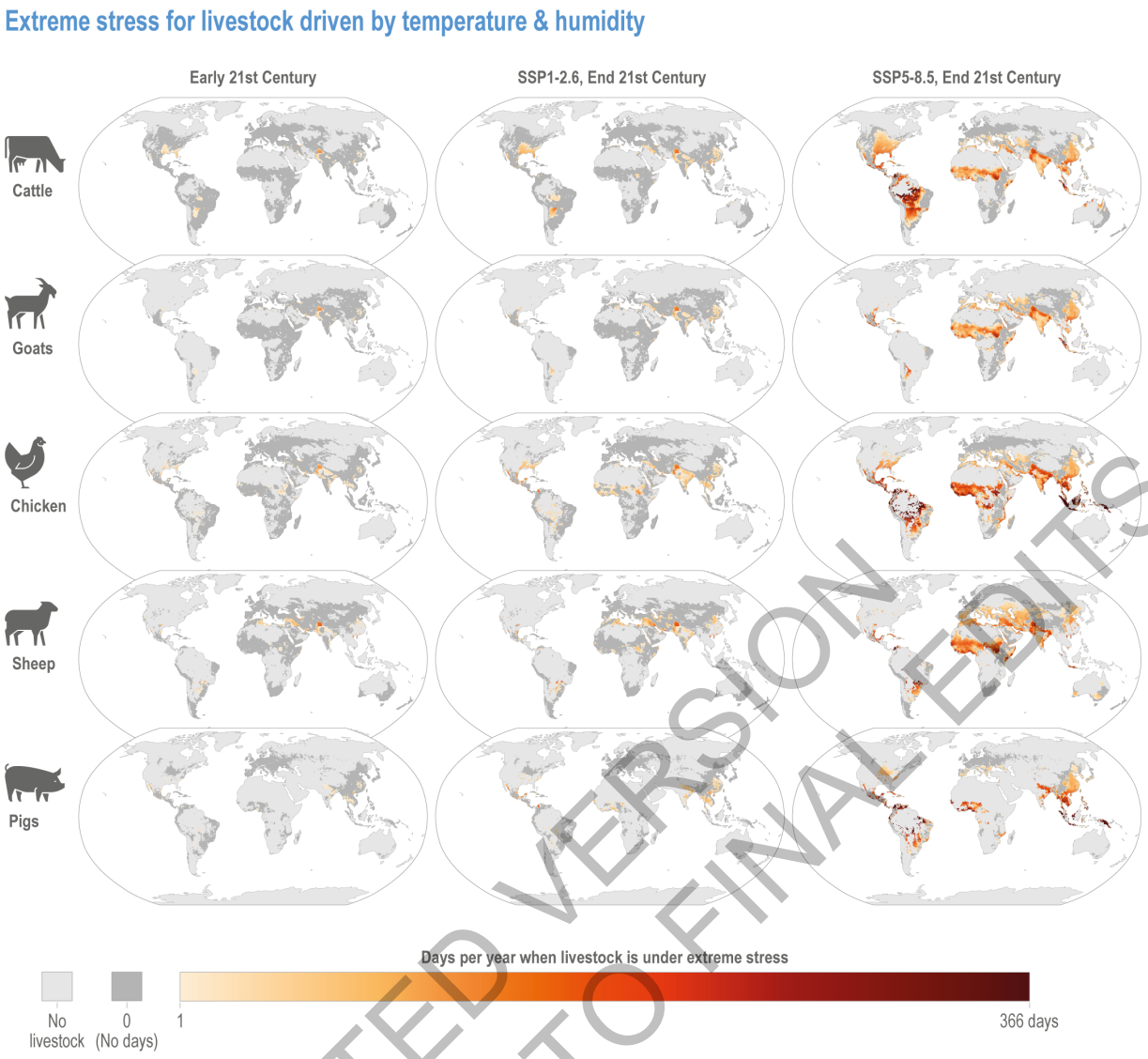

Figure AI.25 [INSERT CAPTION HERE]

AI.2.1.3 Humans

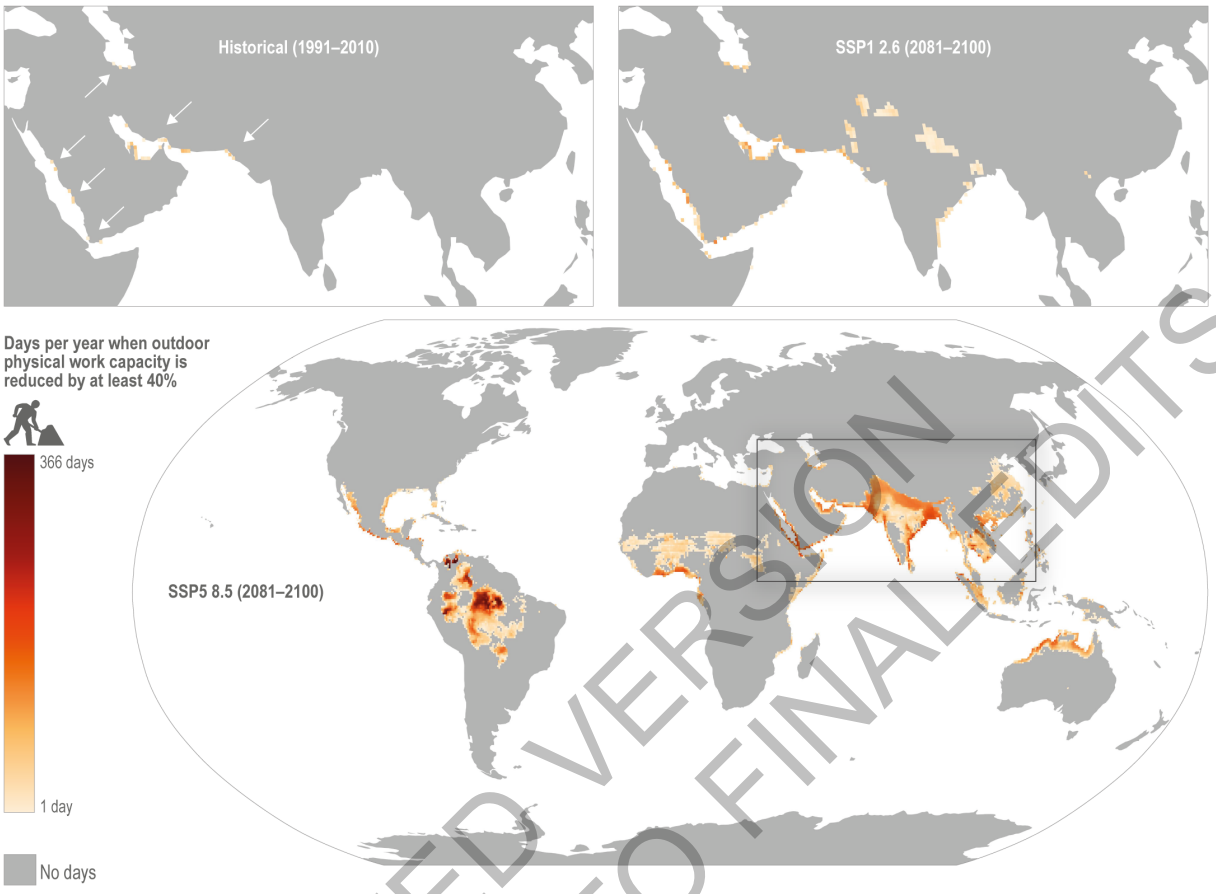

Figure AI.26 [INSERT CAPTION HERE]

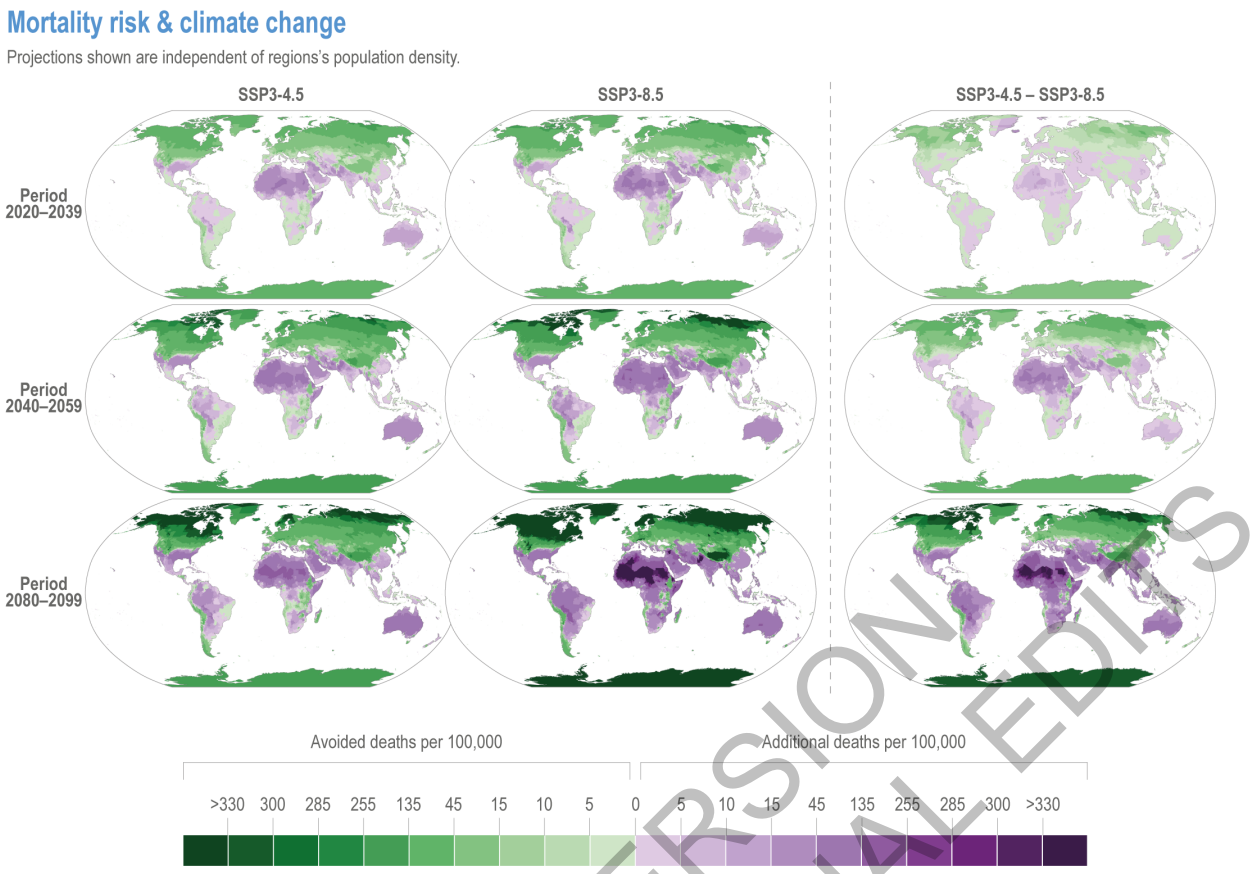

Figure AI.27 [INSERT CAPTION HERE]

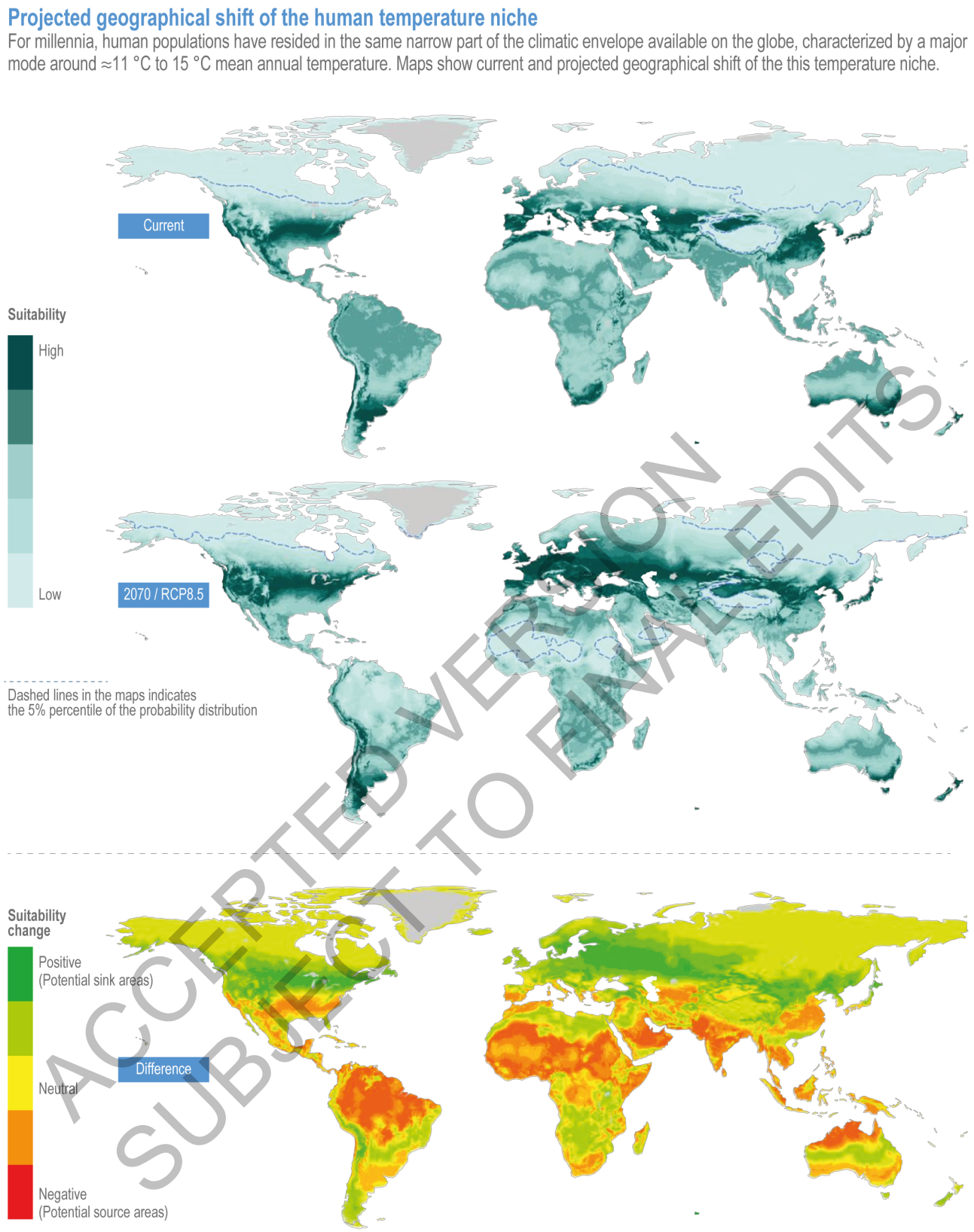

Figure AI.28 [INSERT CAPTION HERE]

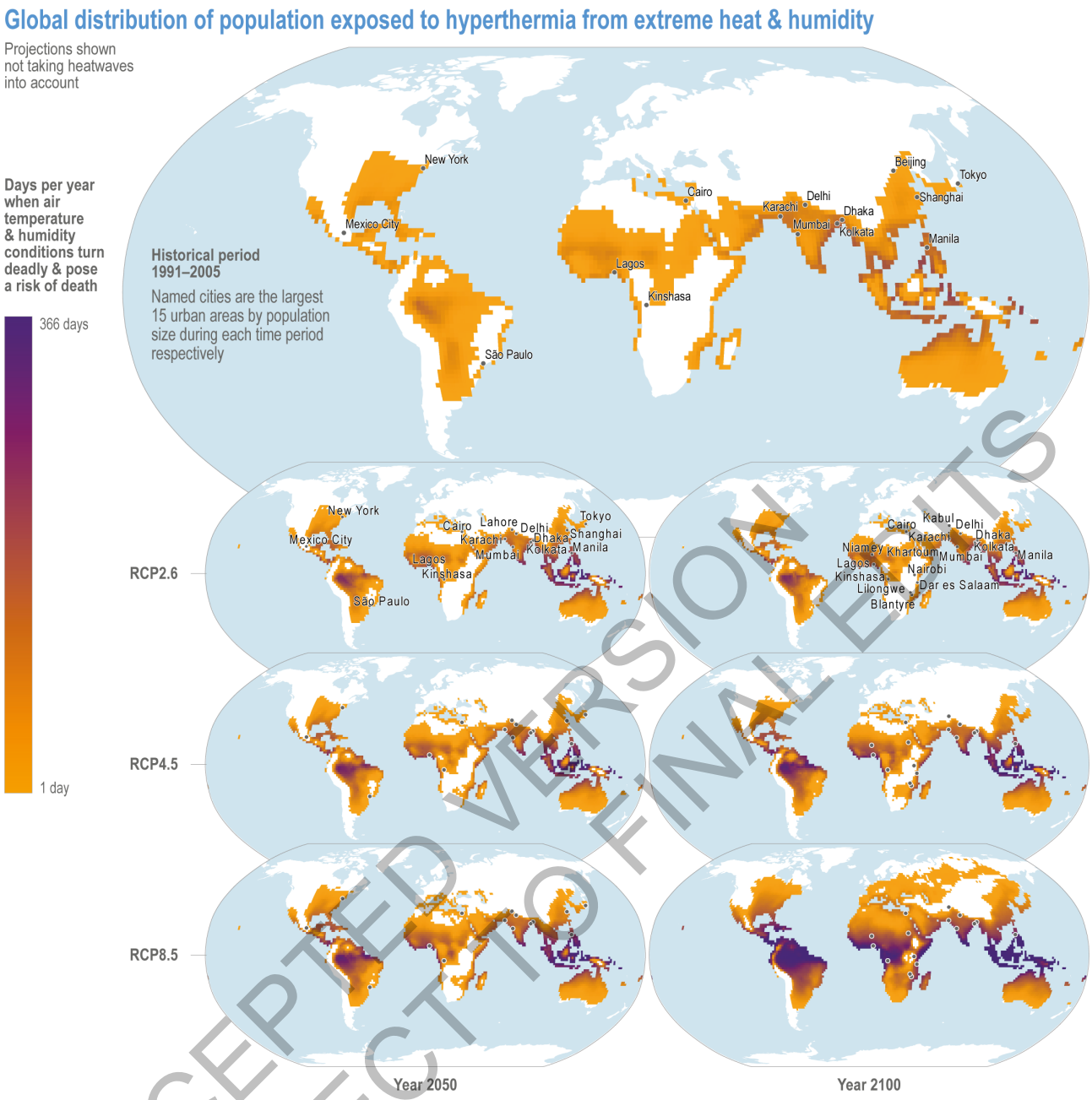

Figure AI.29 [INSERT CAPTION HERE]

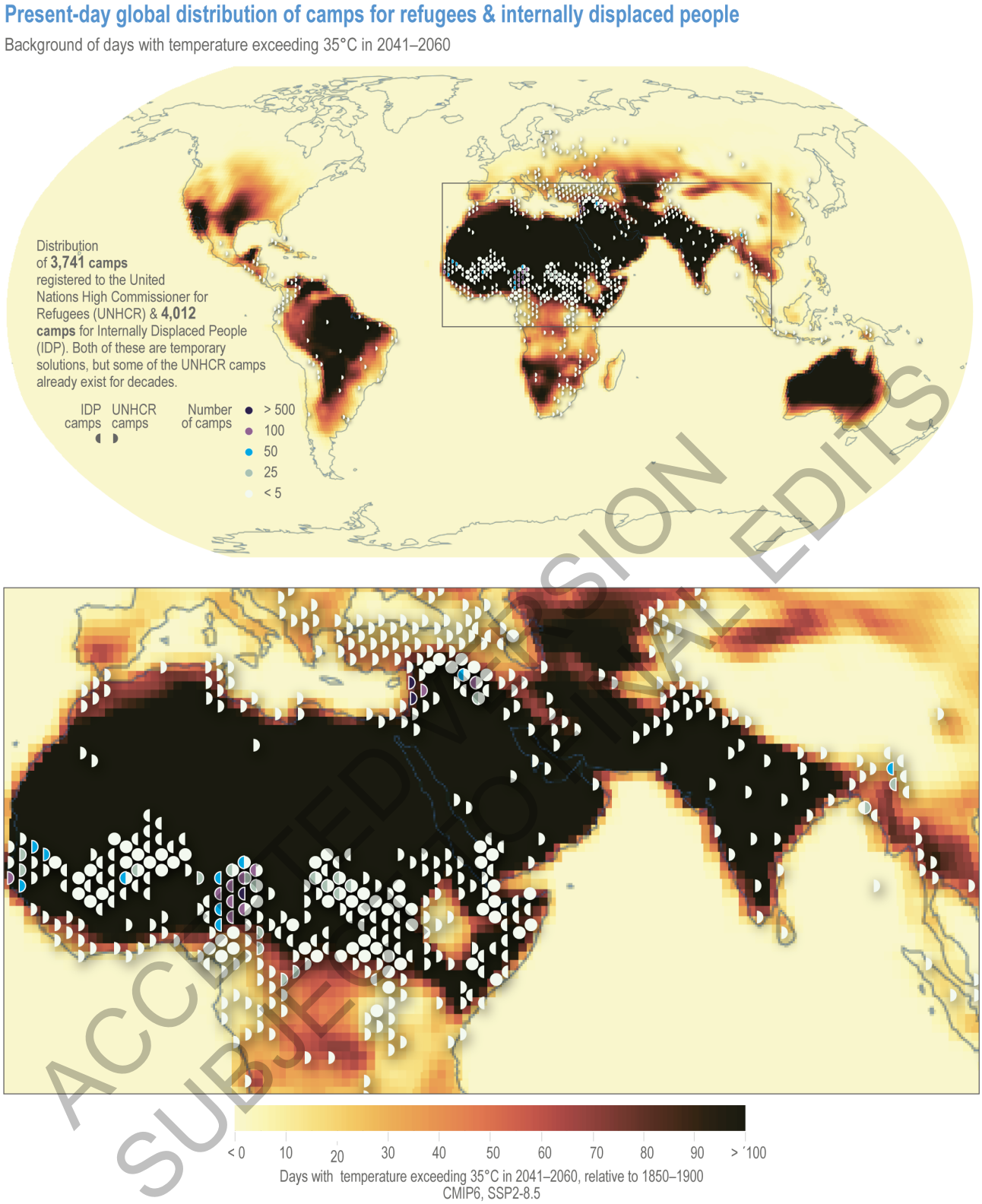

Figure AI.30 [INSERT CAPTION HERE]

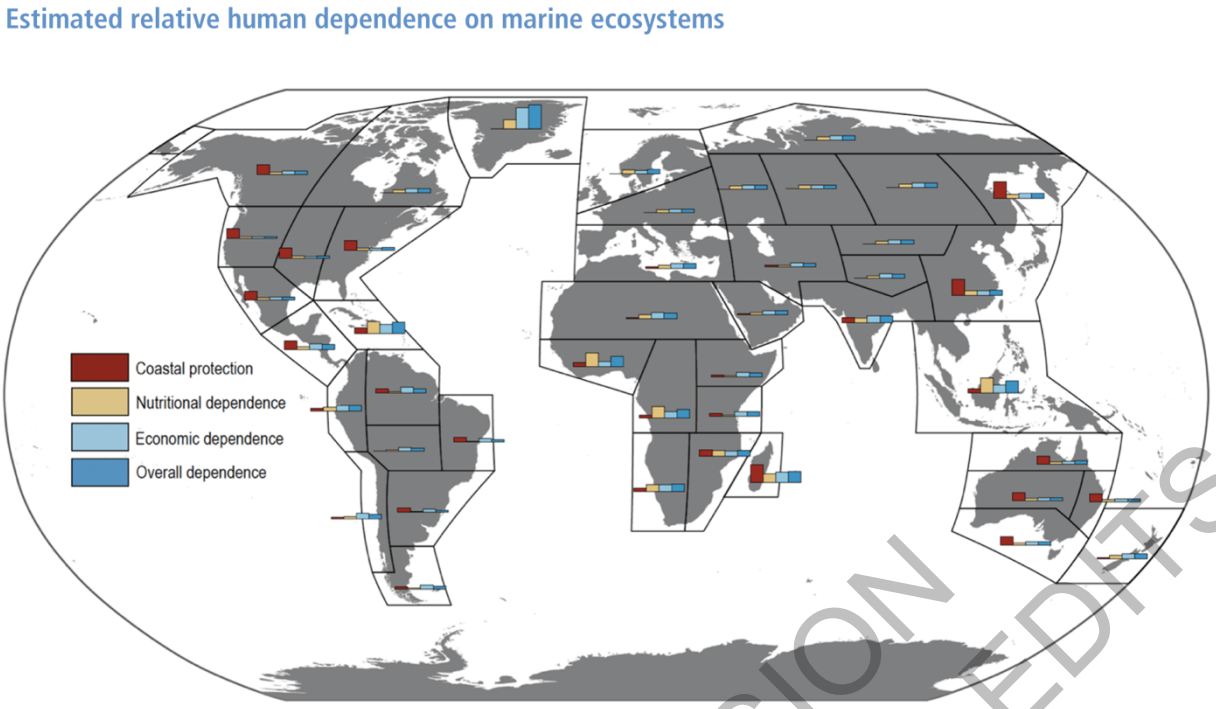

Figure AI.31 [INSERT CAPTION HERE]

AI.2.1.4 Fish Stocks and Fisheries

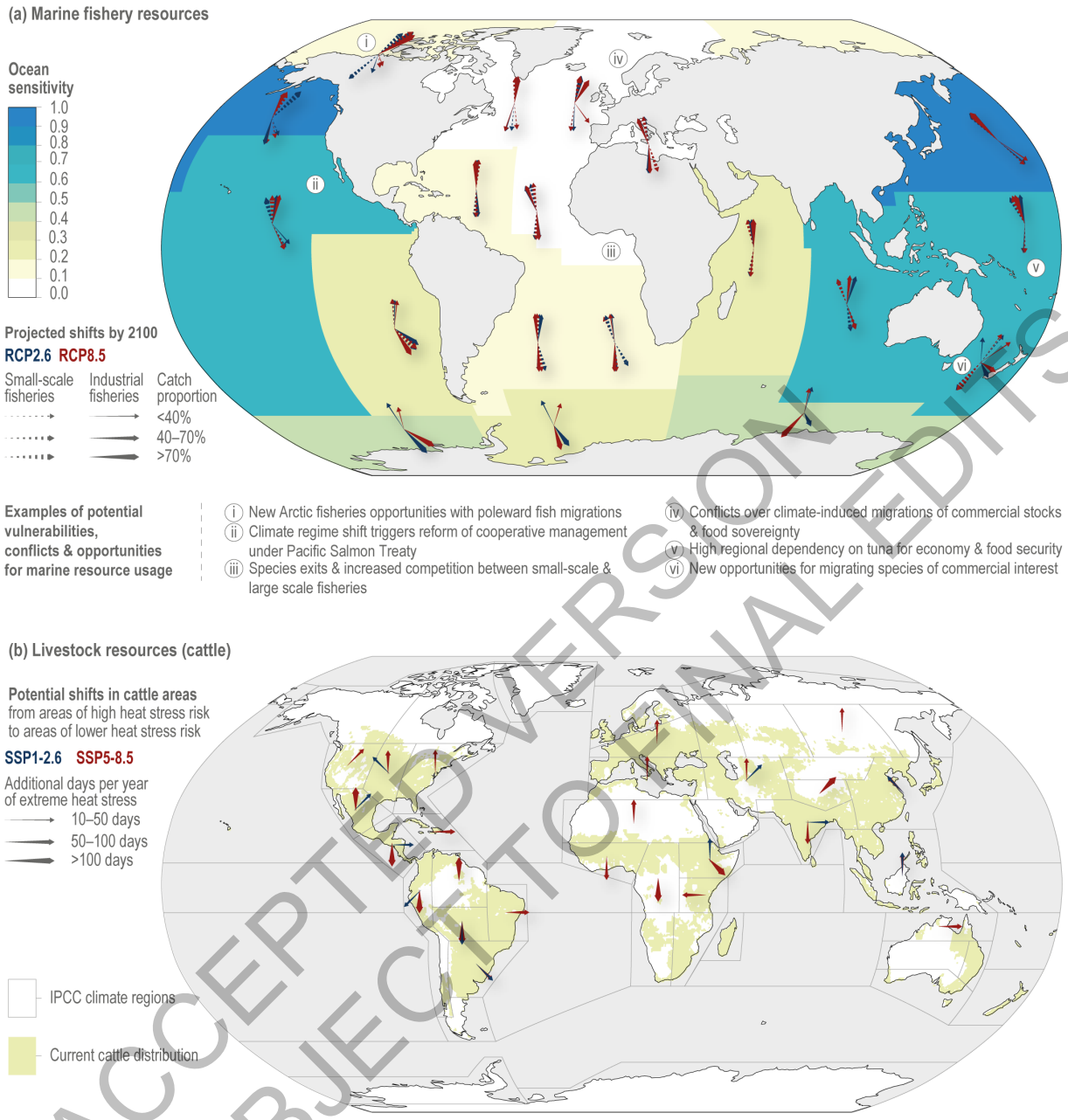

Figure AI.32 [INSERT CAPTION HERE]

Current fisheries adaptive capacity & regional micronutrient deficiency risks related to seafood-relevant micronutrients in human diets

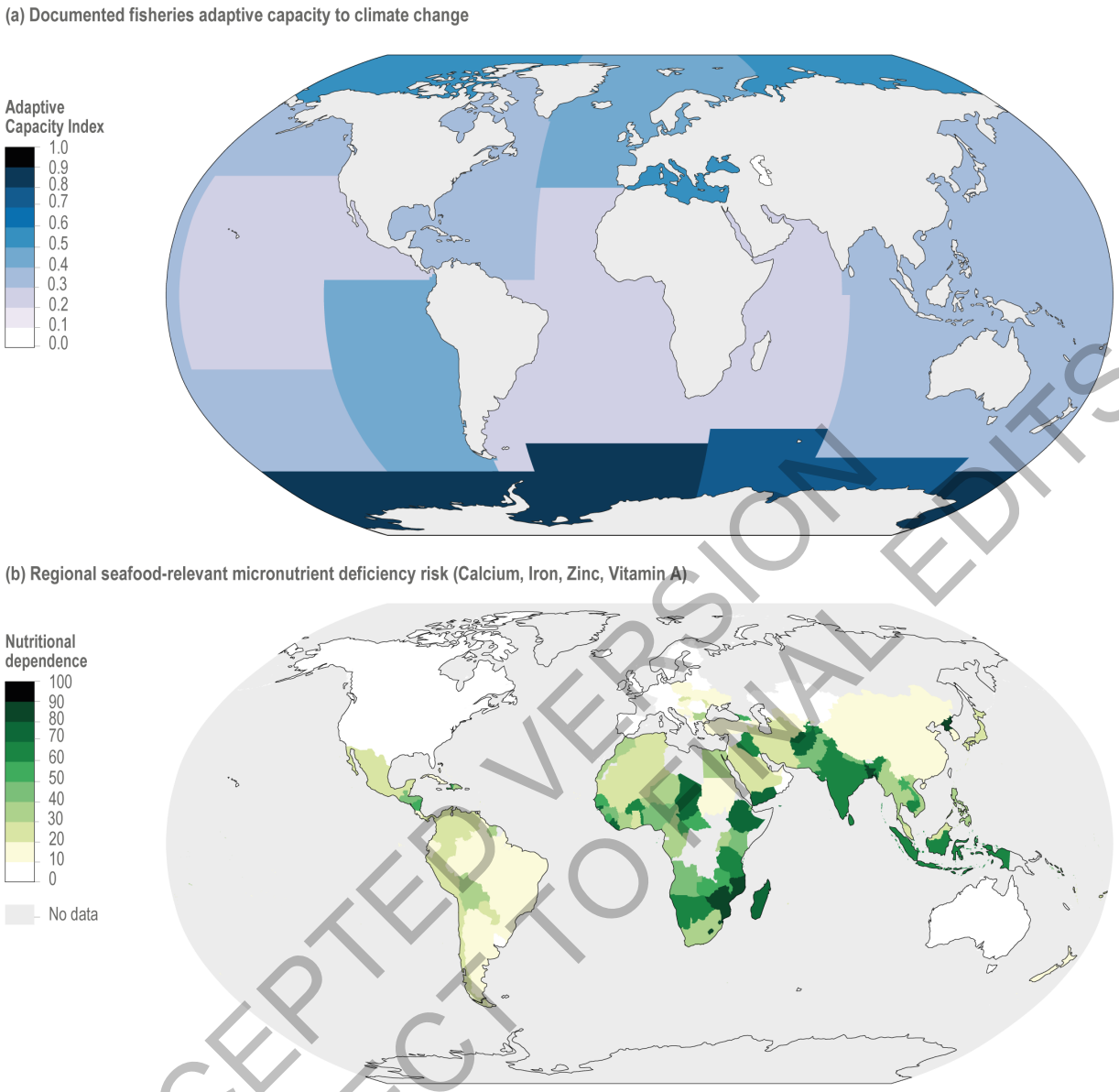

Figure AI.33 [INSERT CAPTION HERE]

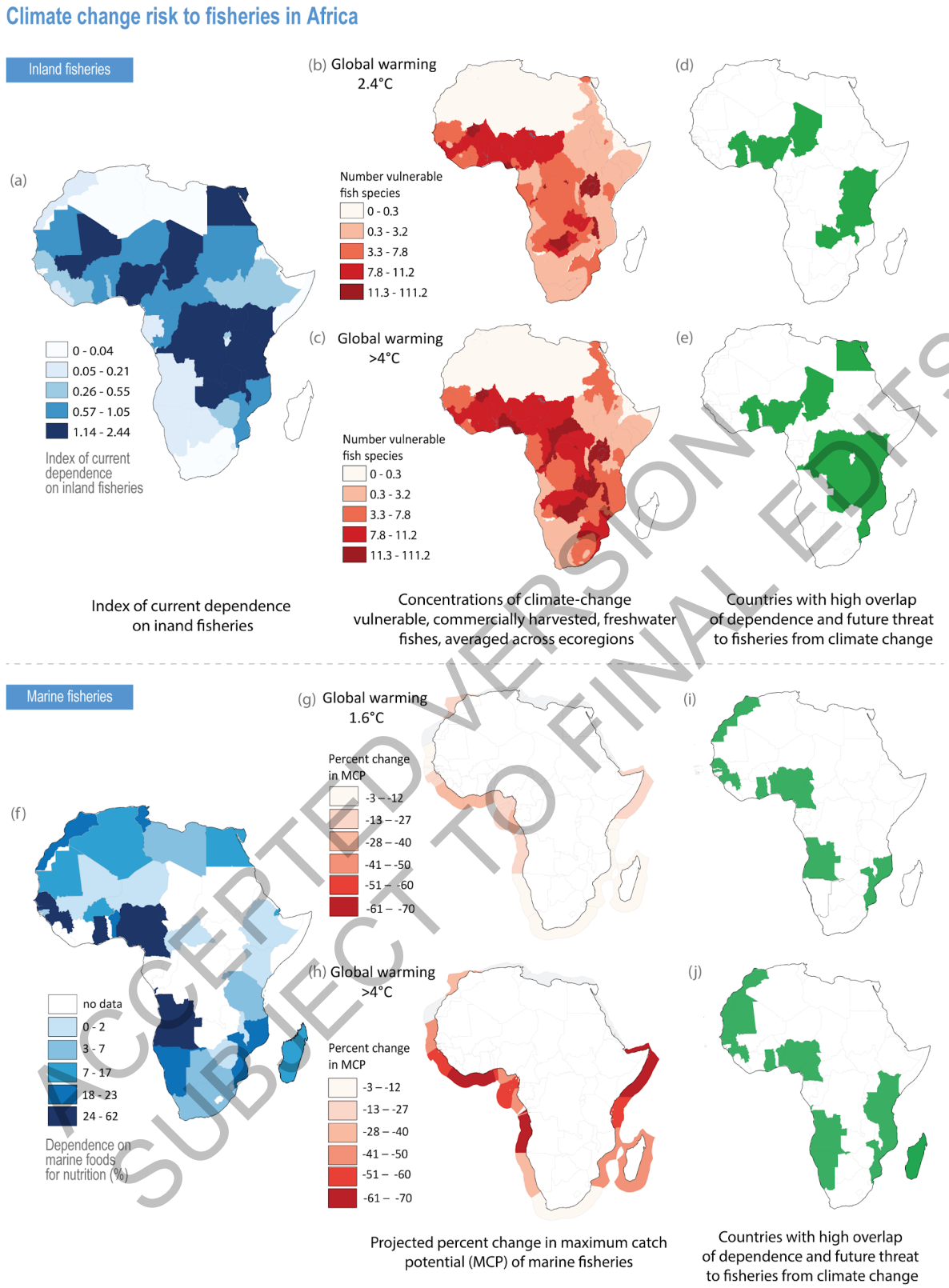

Figure AI.34 [INSERT CAPTION HERE]

AI.2.2 Water-related Challenges

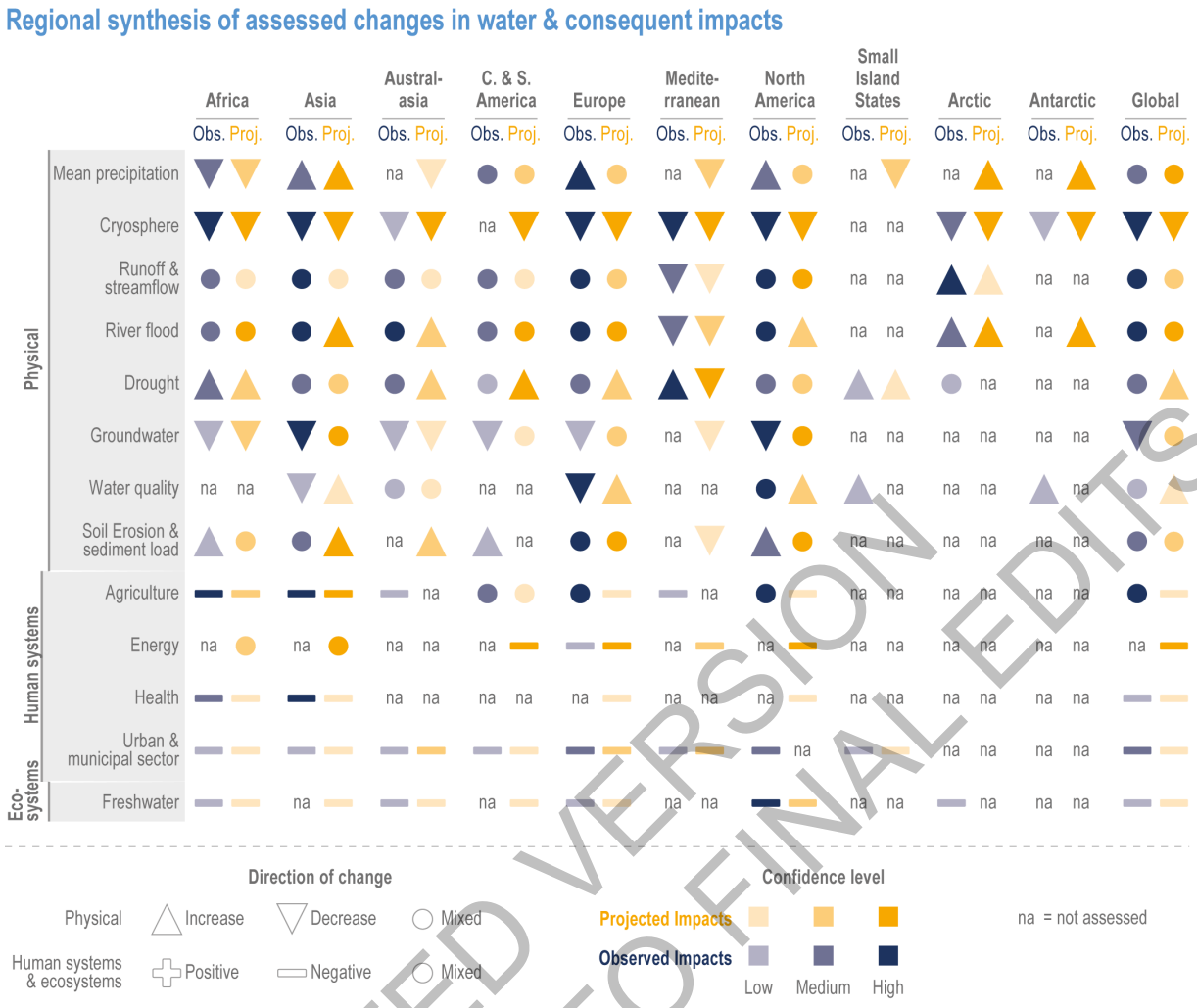

Figure AI.35 [INSERT CAPTION HERE]

AI.2.2.1 Drought

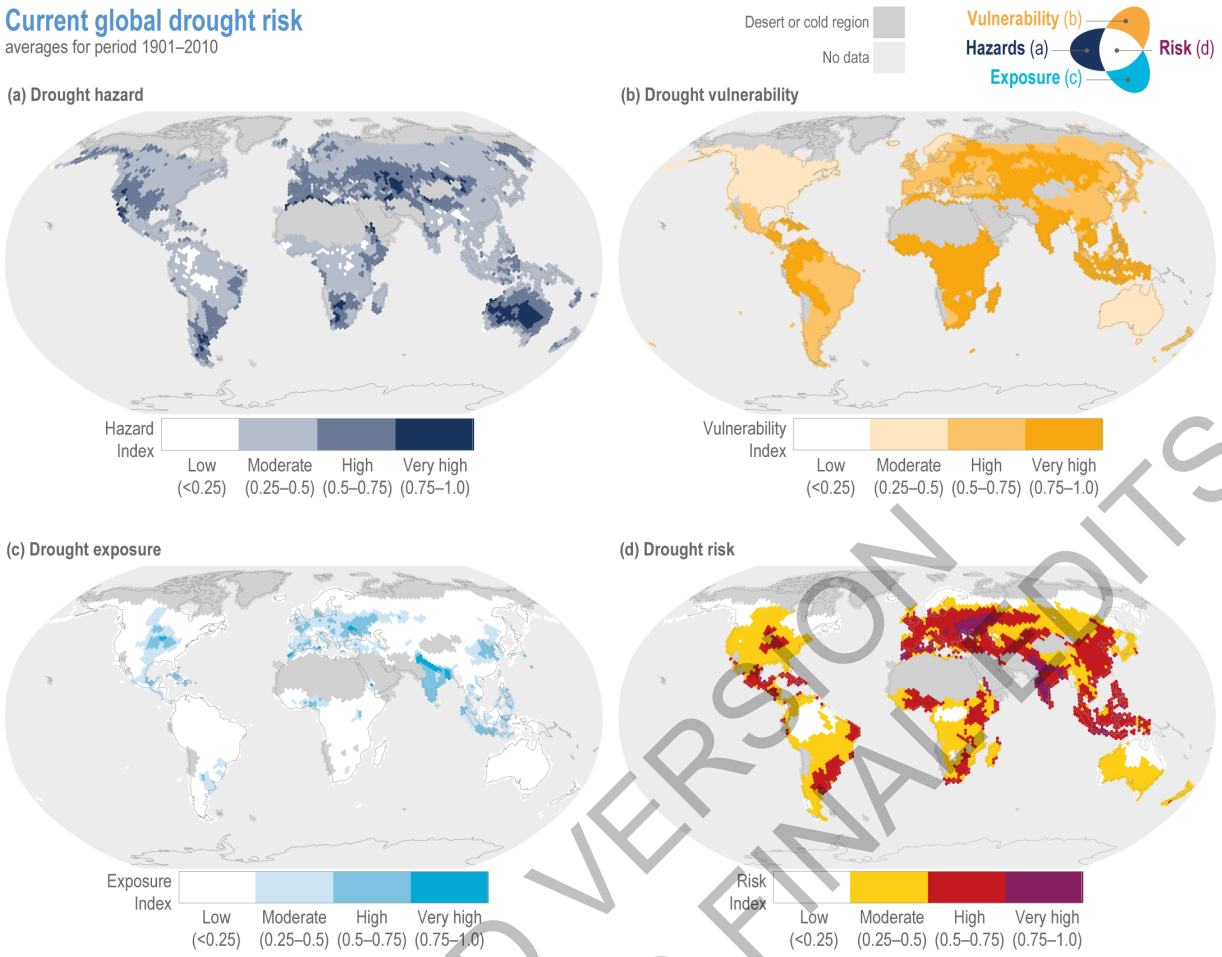

Figure AI.36 [INSERT CAPTION HERE]

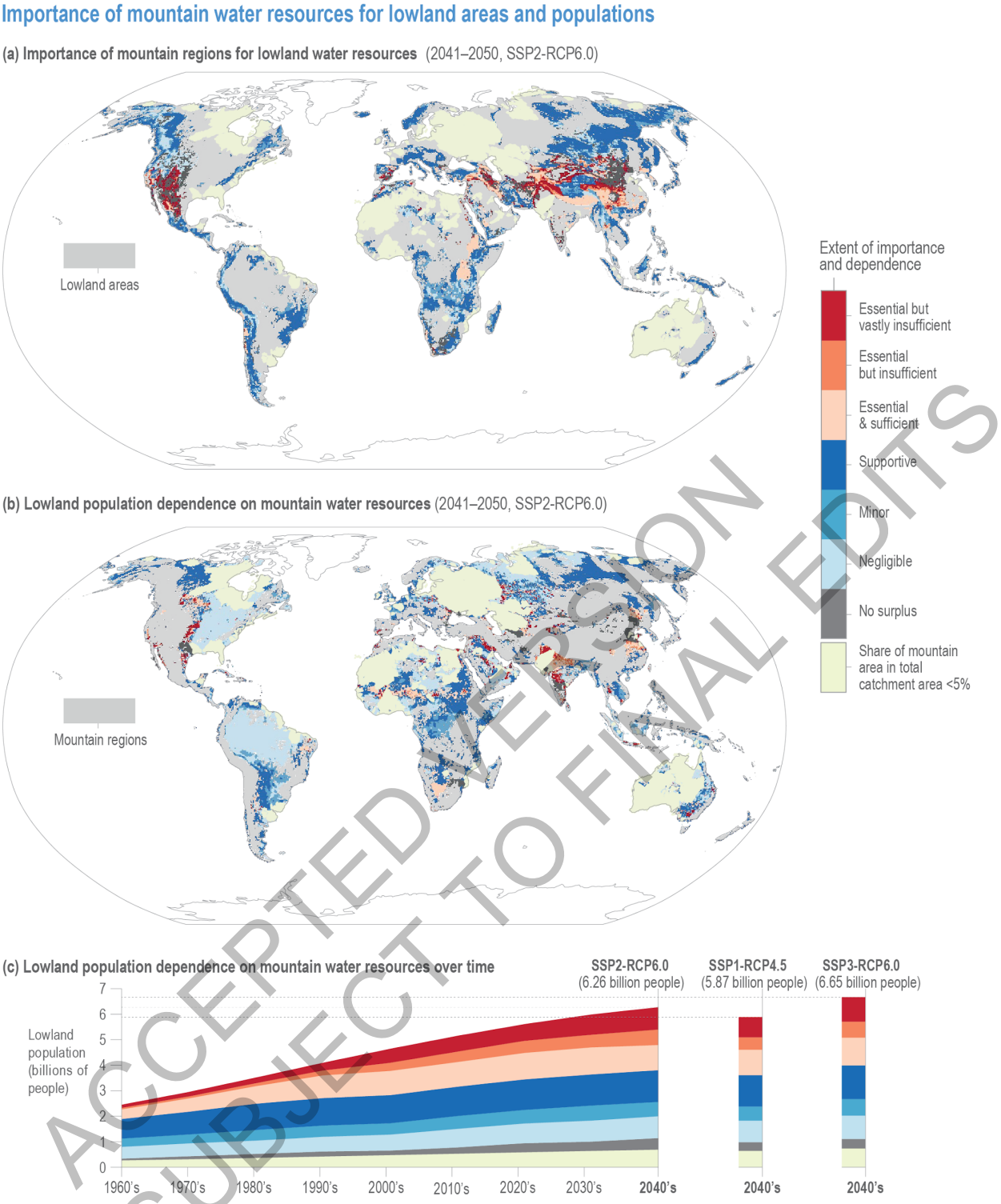

Figure AI.37 [INSERT CAPTION HERE]

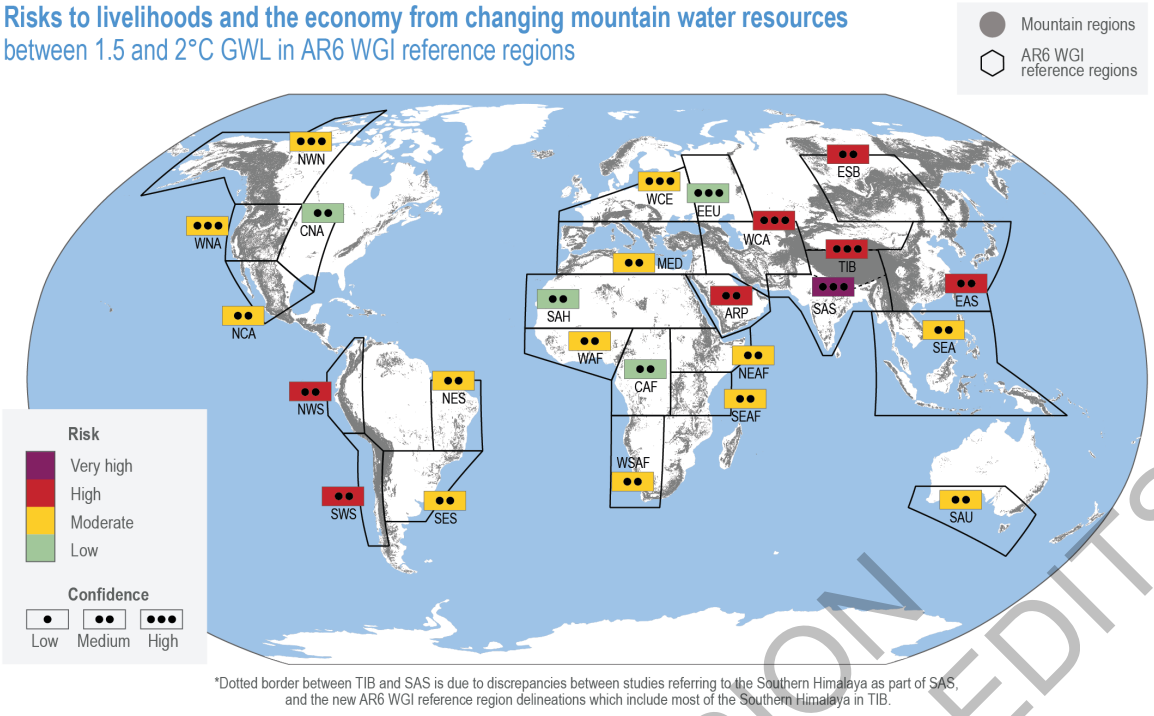

Figure AI.38 [INSERT CAPTION HERE]

AI.2.2.2 Flooding

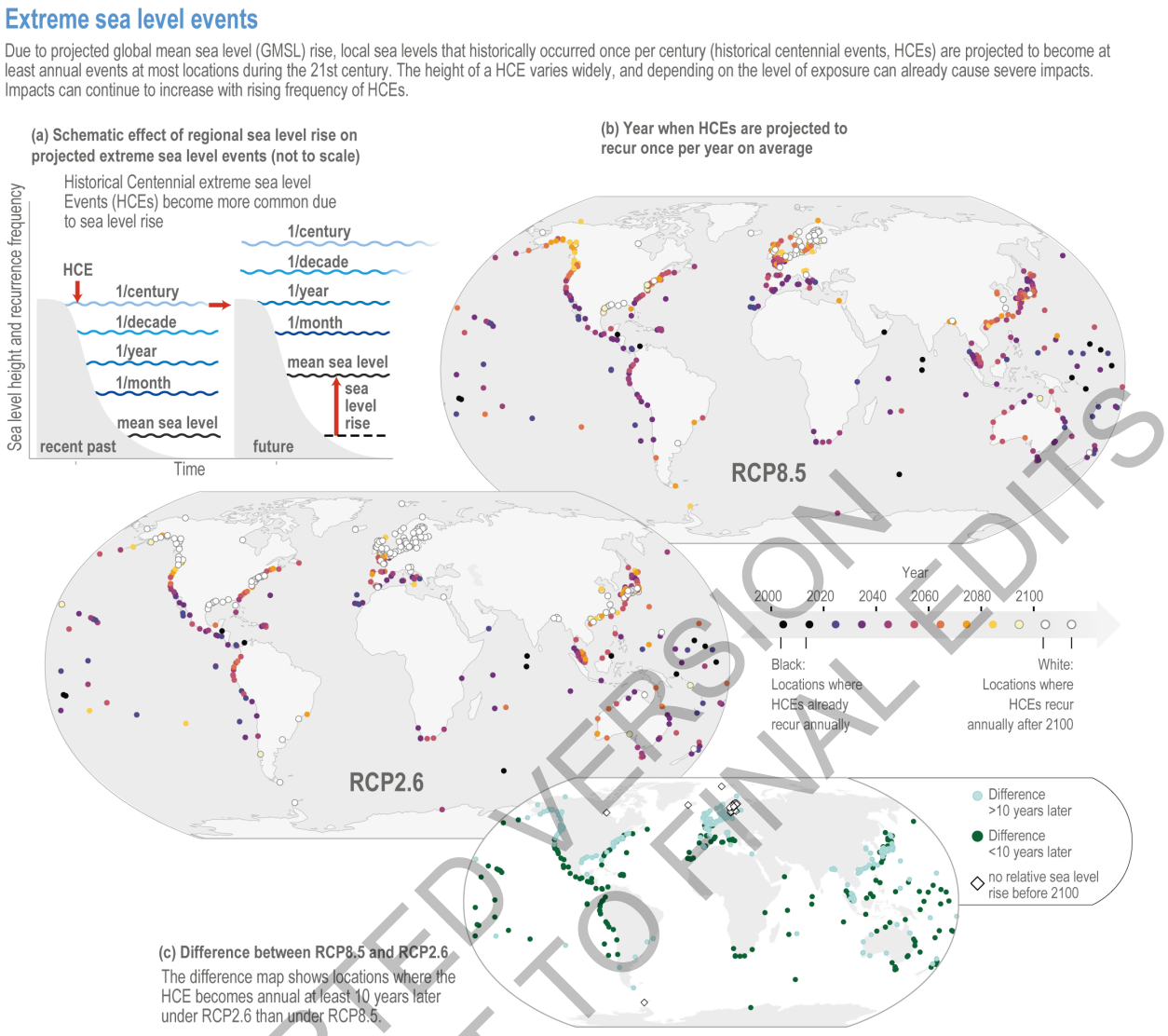

Figure AI.39 [INSERT CAPTION HERE]

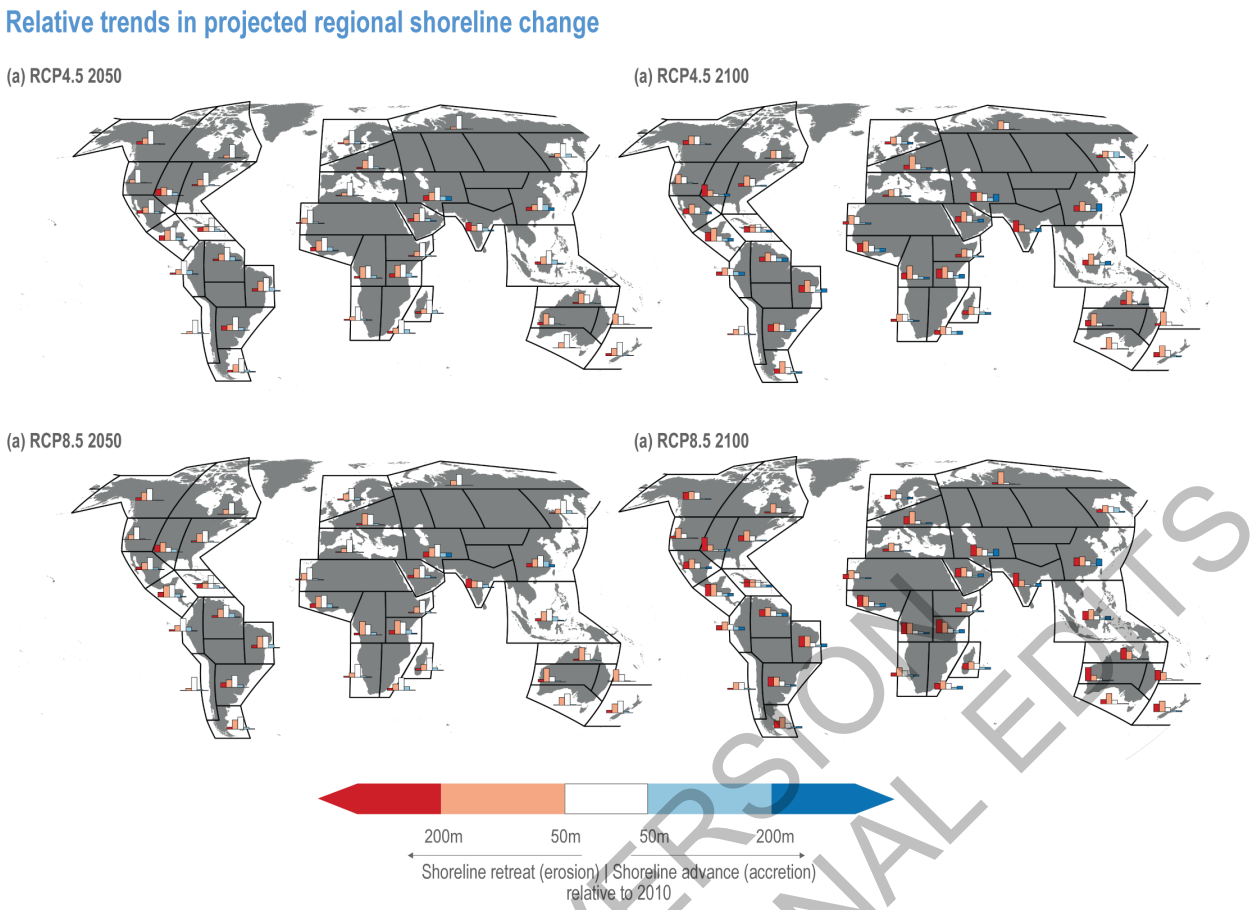

Figure AI.40 [INSERT CAPTION HERE]

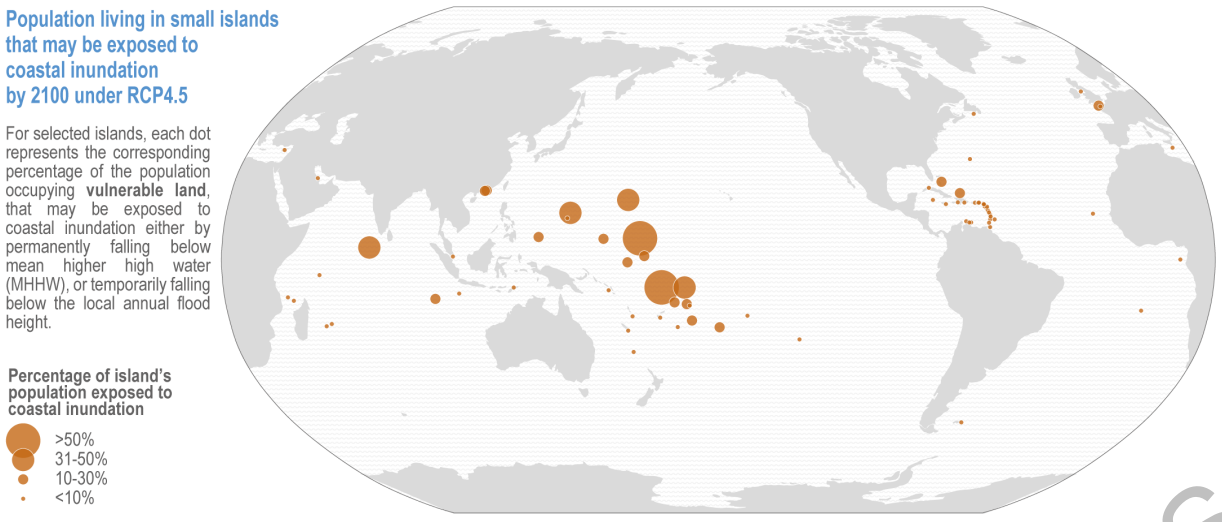

Figure AI.41 [INSERT CAPTION HERE]

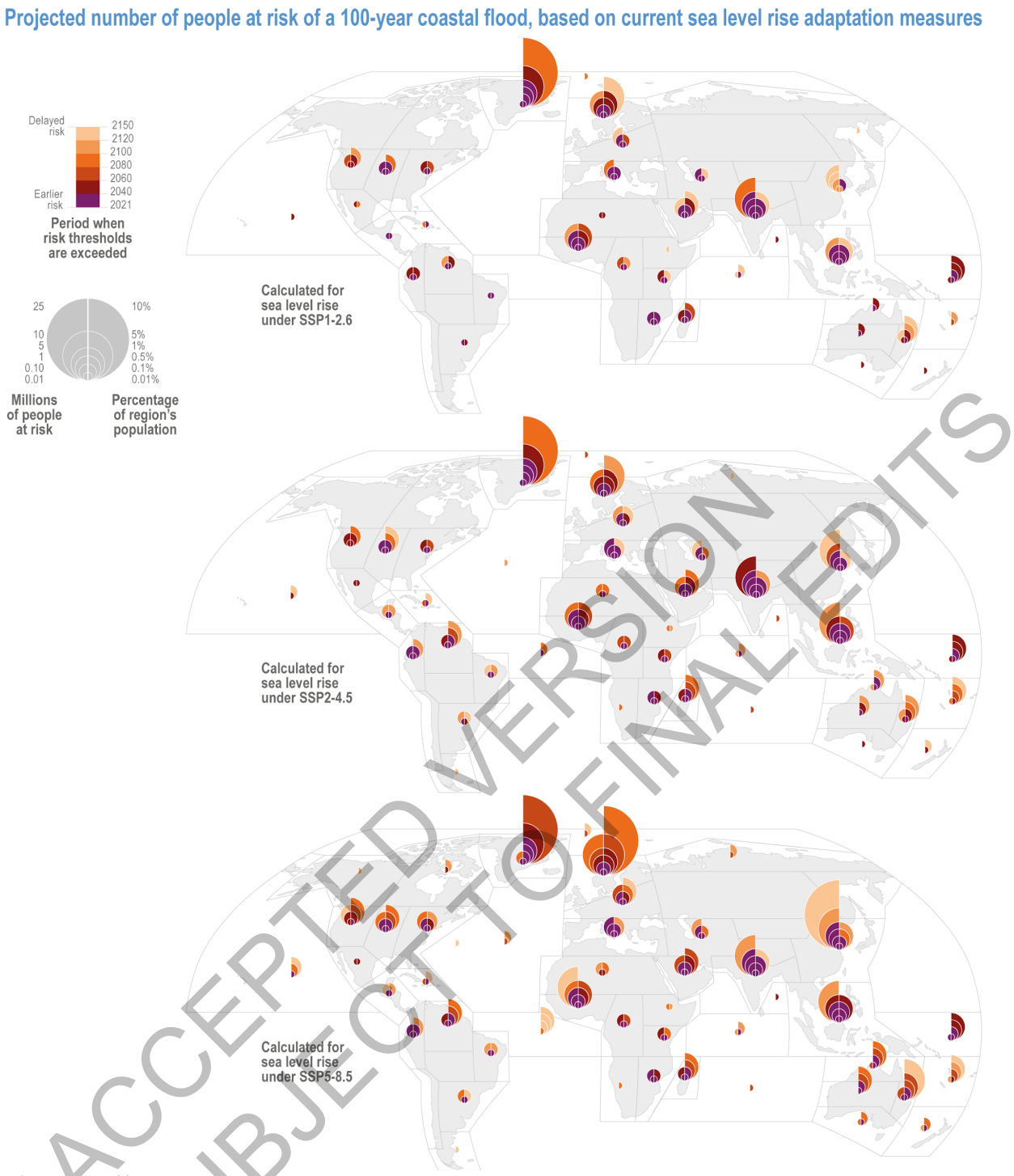

Figure AI.42 [INSERT CAPTION HERE]

Selected regions at risk of potential sea level rise

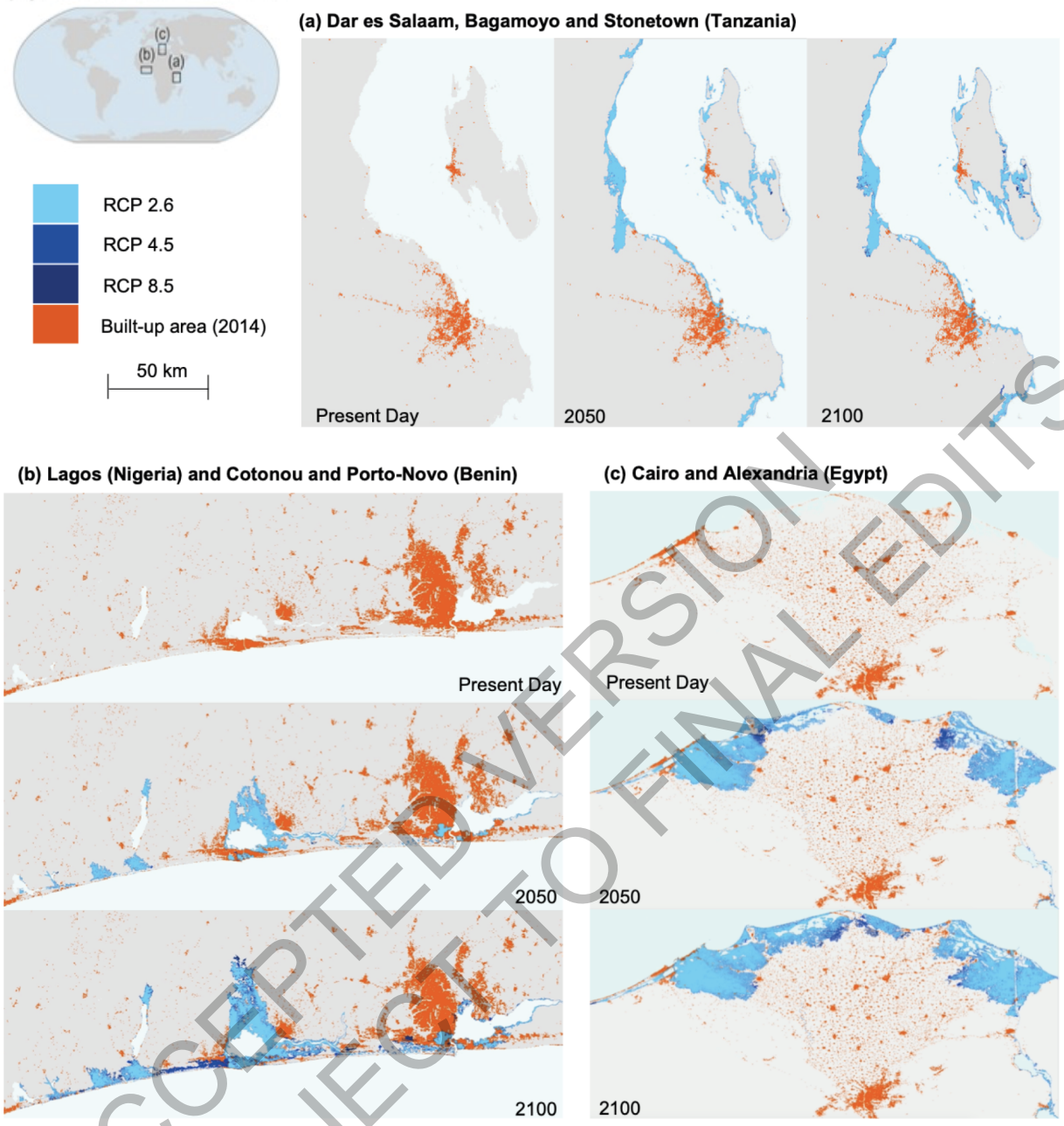

Figure AI.43 [INSERT CAPTION HERE]

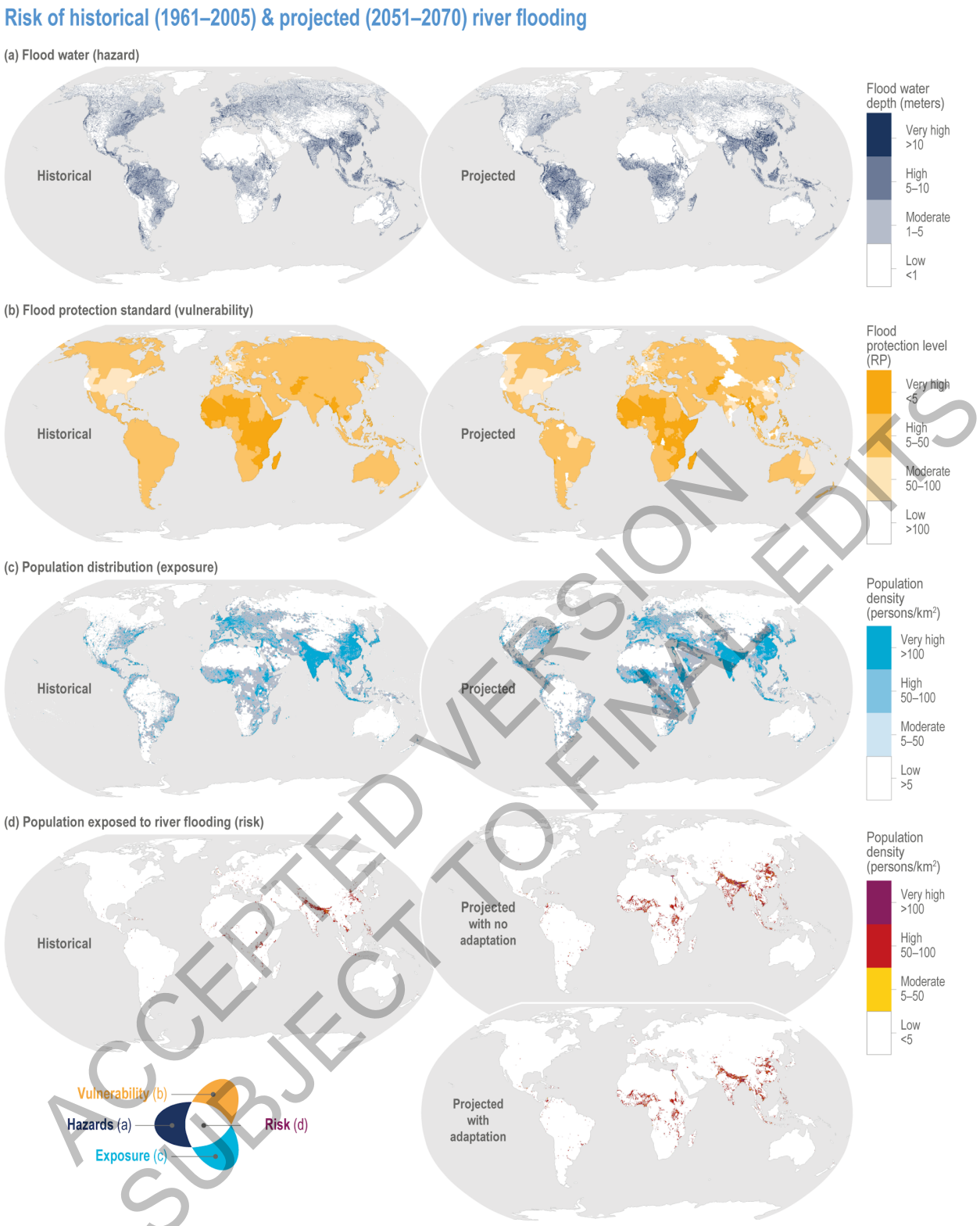

Figure AI.44 [INSERT CAPTION HERE]

Projected changes in river flooding

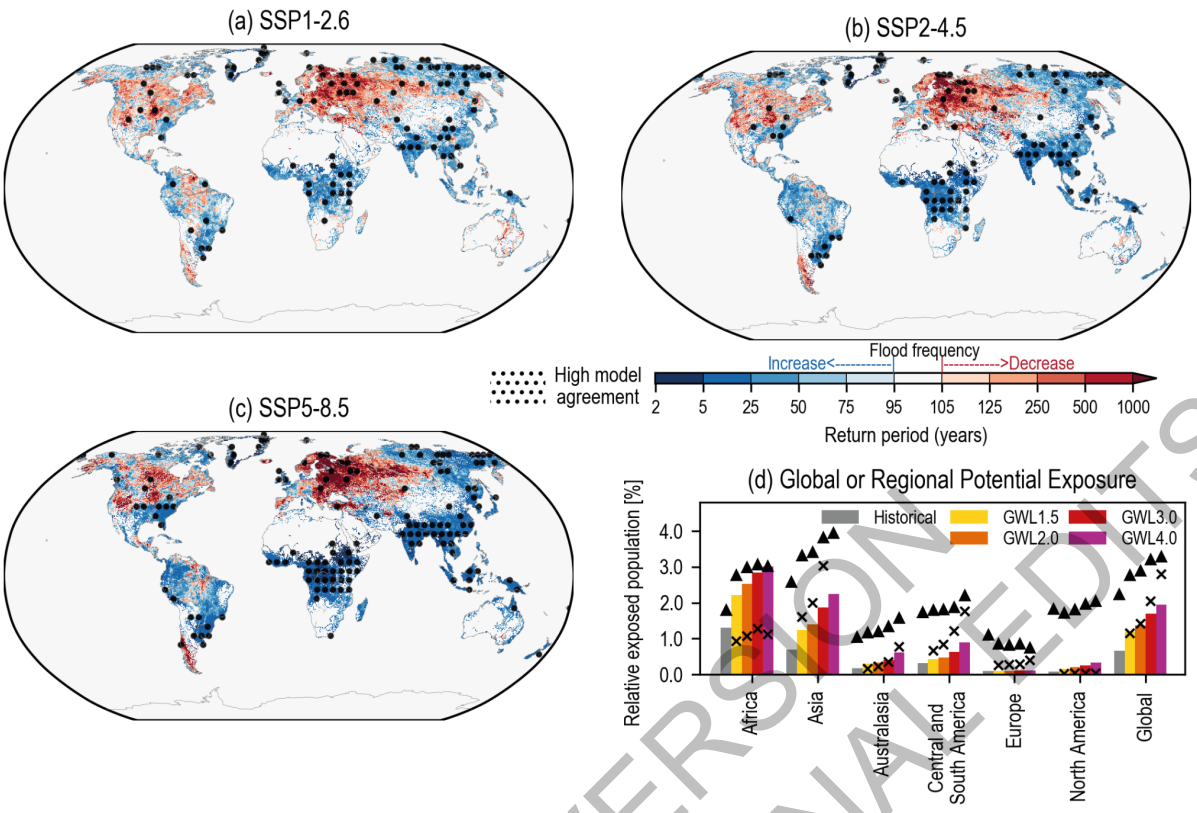

Figure AI.45 [INSERT CAPTION HERE]

AI.2.3 Global to Regional Risks (including Economic), Vulnerabilities, and Adaptive Capacities

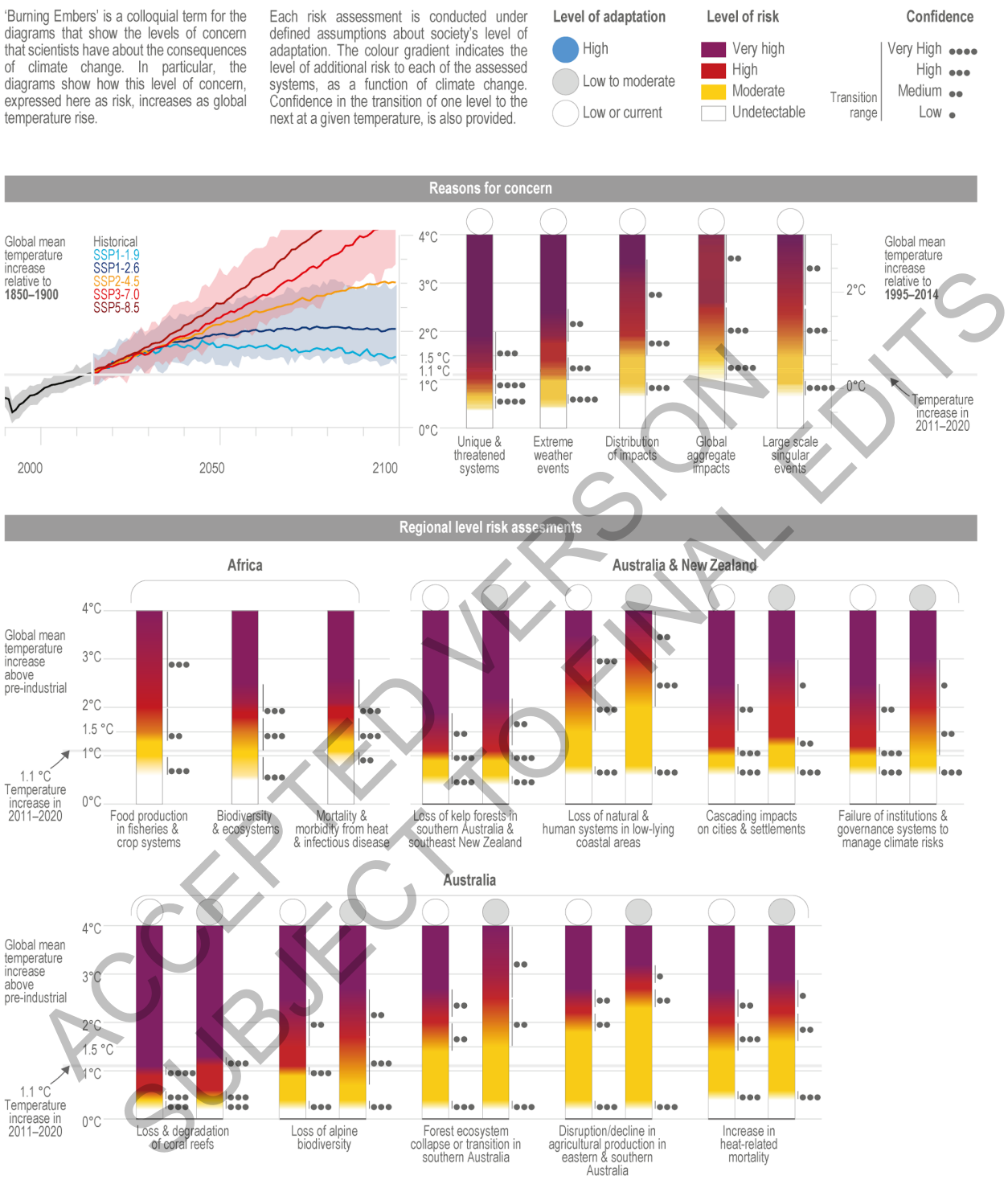

Figure AI.46a [INSERT CAPTION HERE]

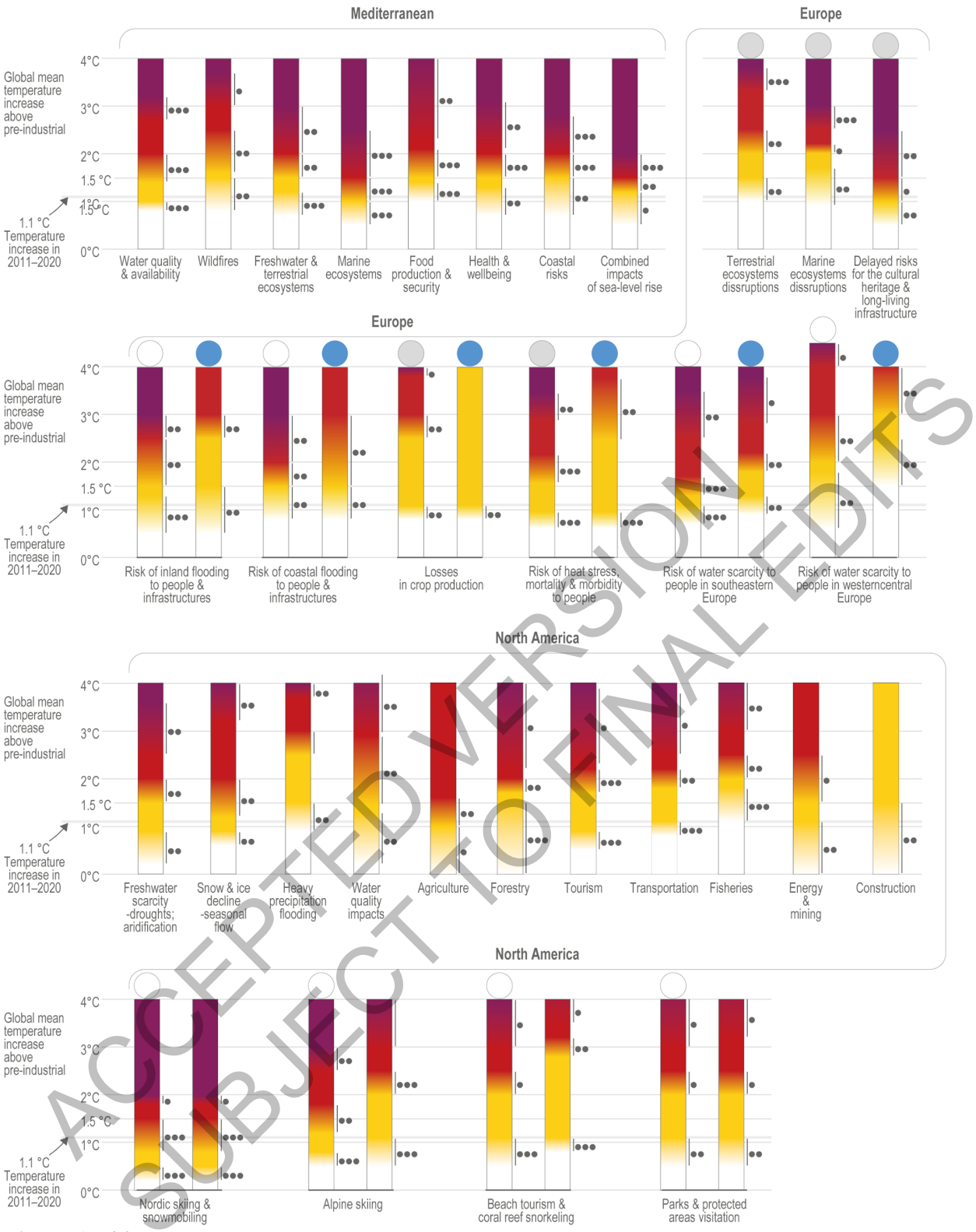

Figure AI.46b [INSERT CAPTION HERE]

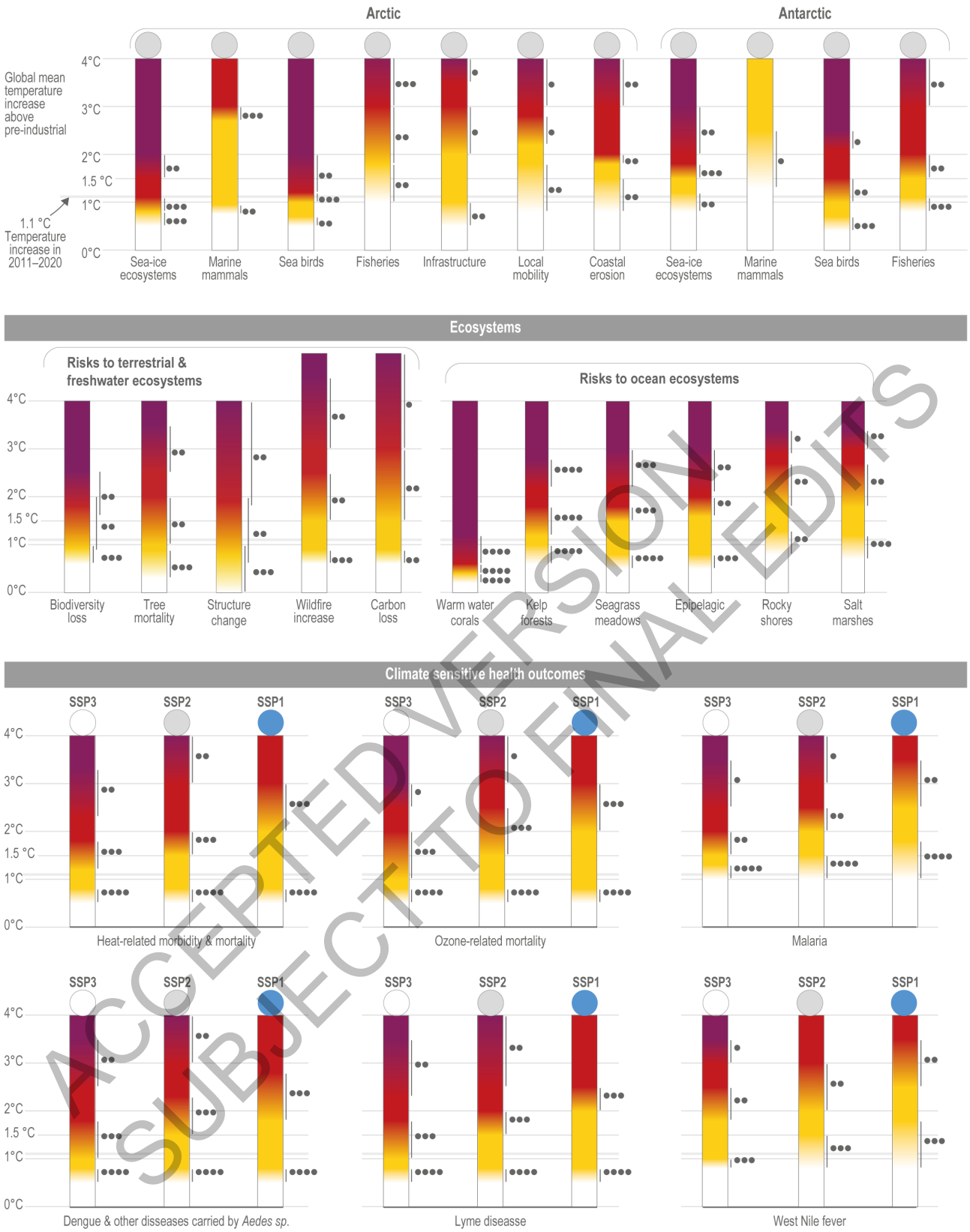

Figure AI.46c [INSERT CAPTION HERE]

AI.2.4 From Adaptation to Climate Resilient Development

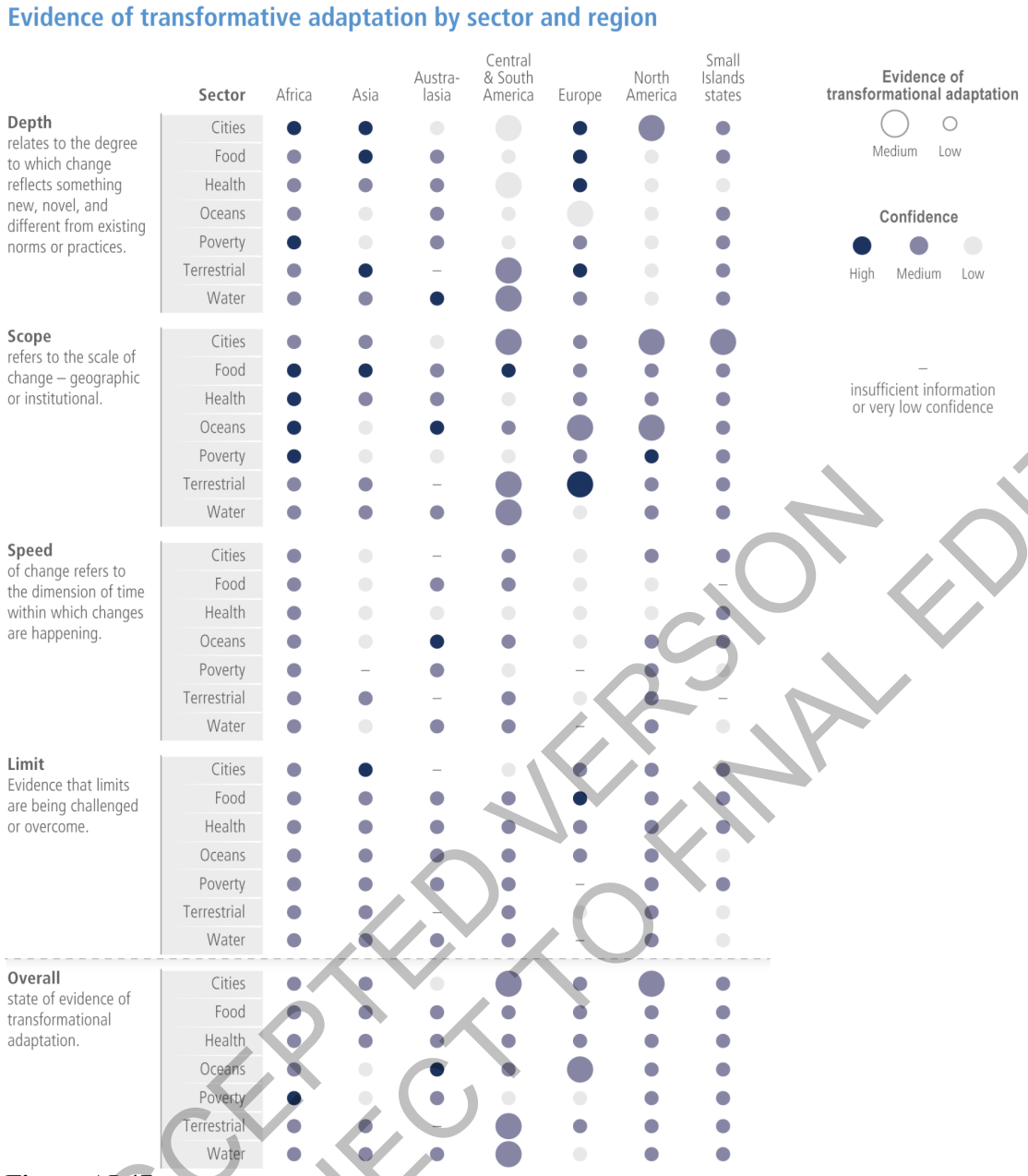

Figure AI.47 [INSERT CAPTION HERE]

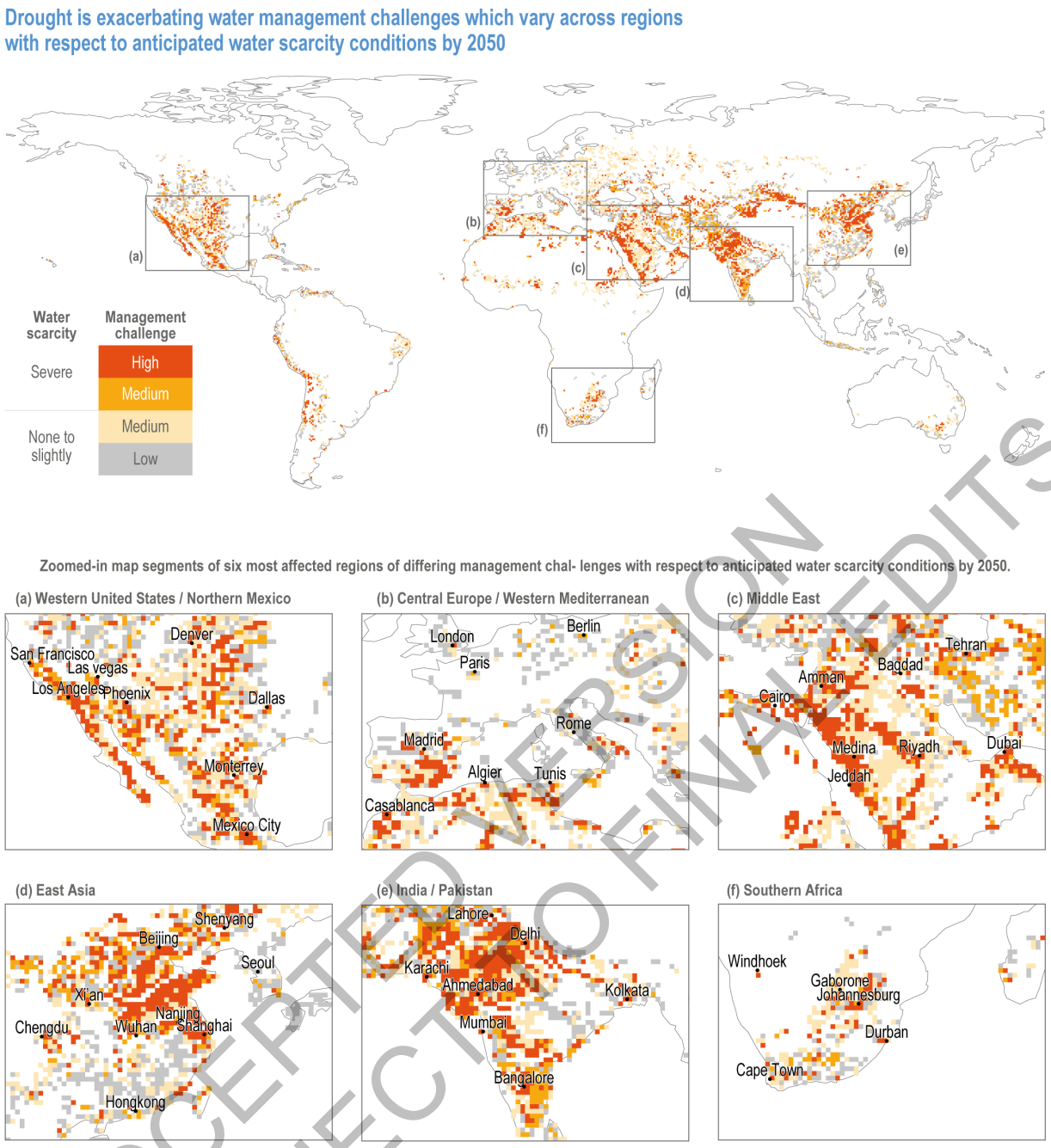

Figure AI.48 [INSERT CAPTION HERE]

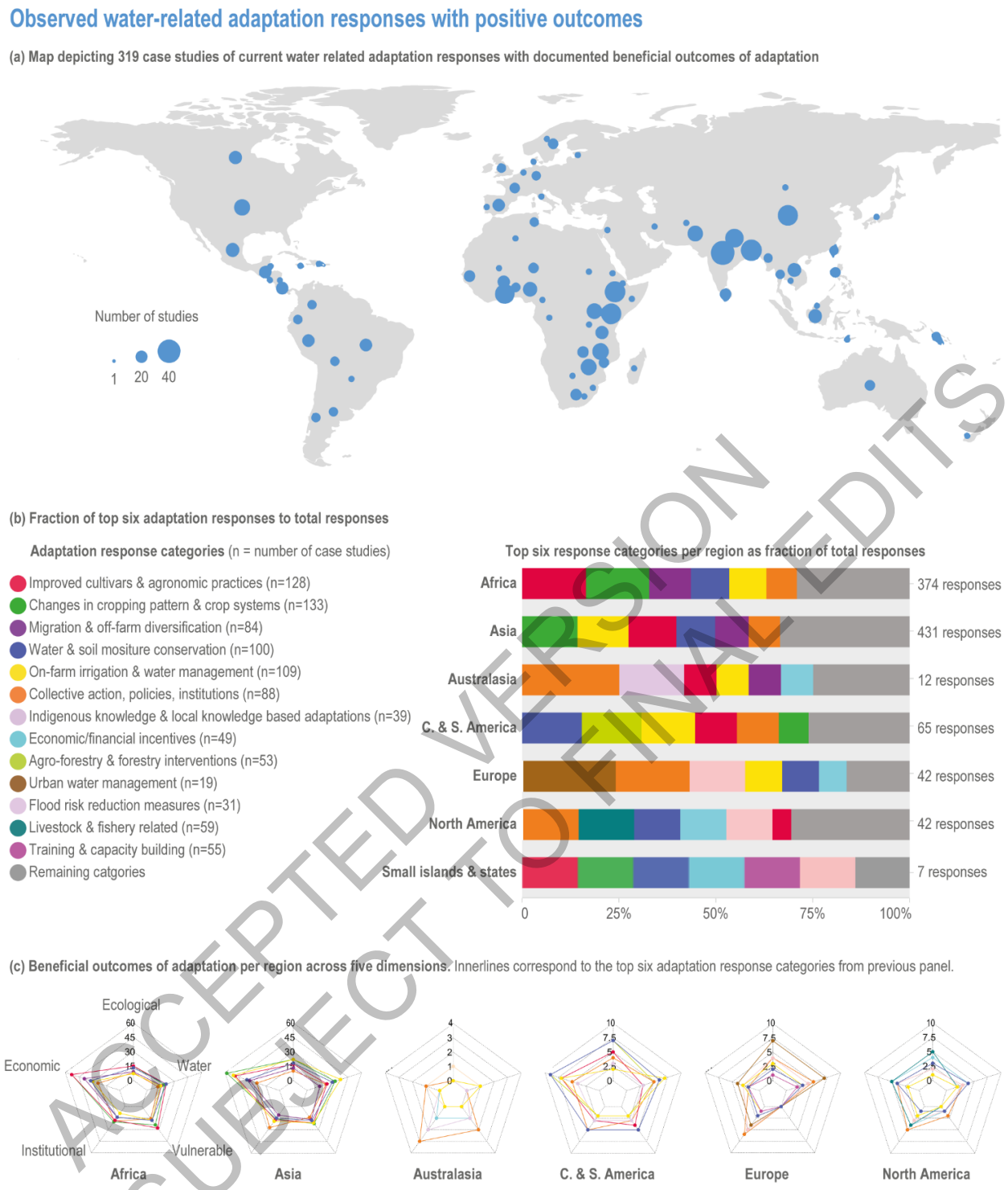

Figure AI.49 [INSERT CAPTION HERE]

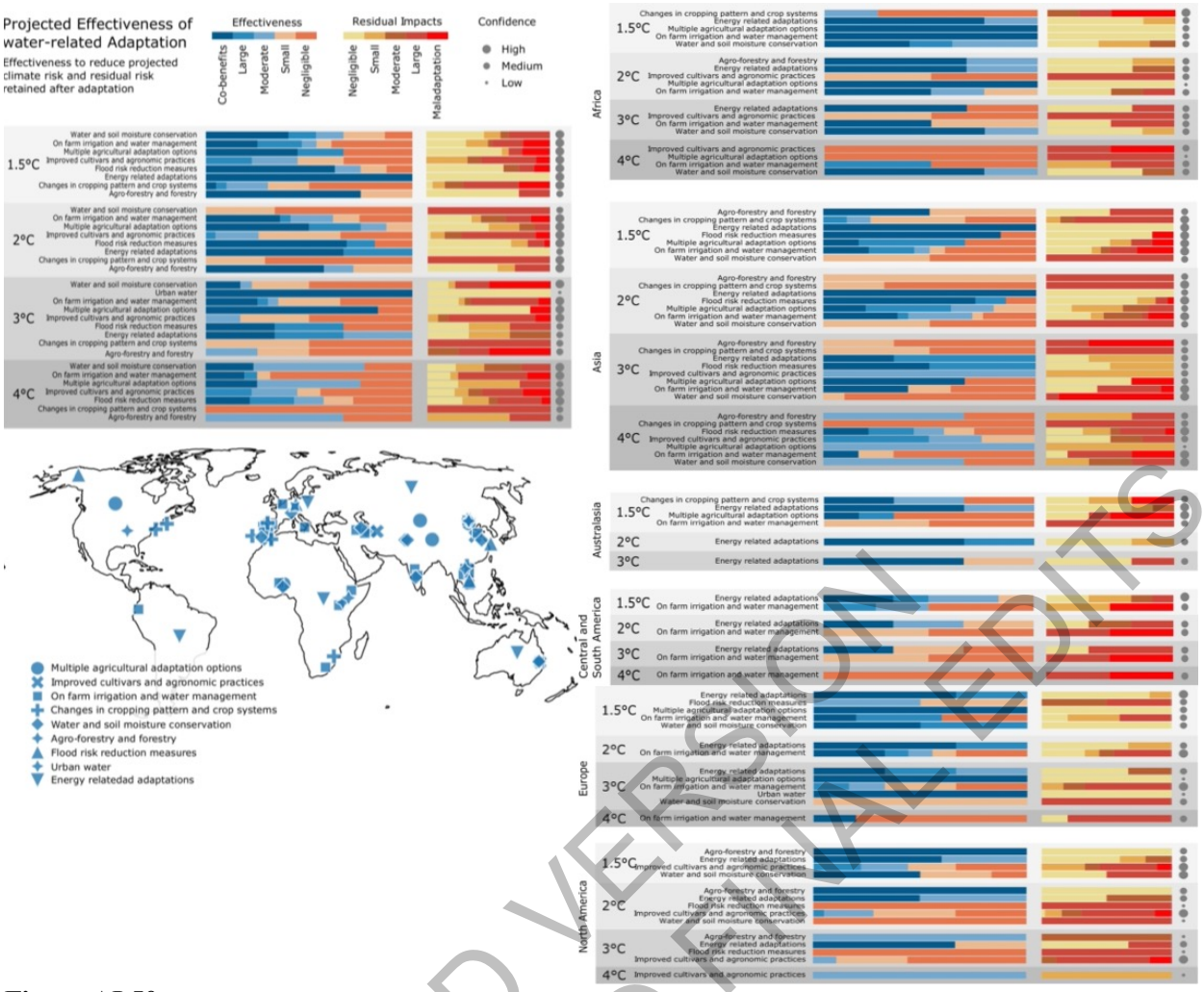

Figure AI.50 [INSERT CAPTION HERE]

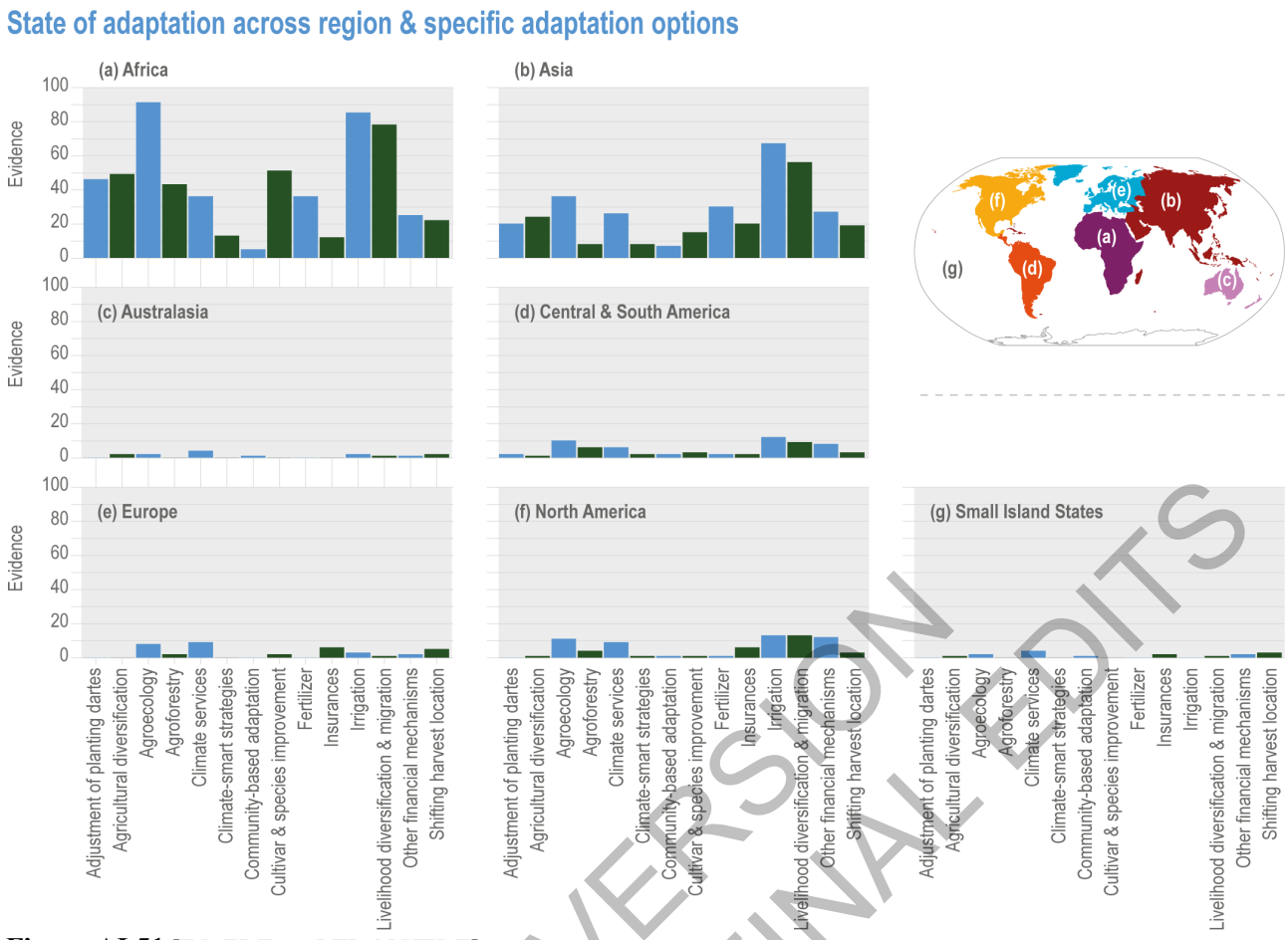

Figure AI.51 [INSERT CAPTION HERE]

Who is responding, by geographic region and sector?

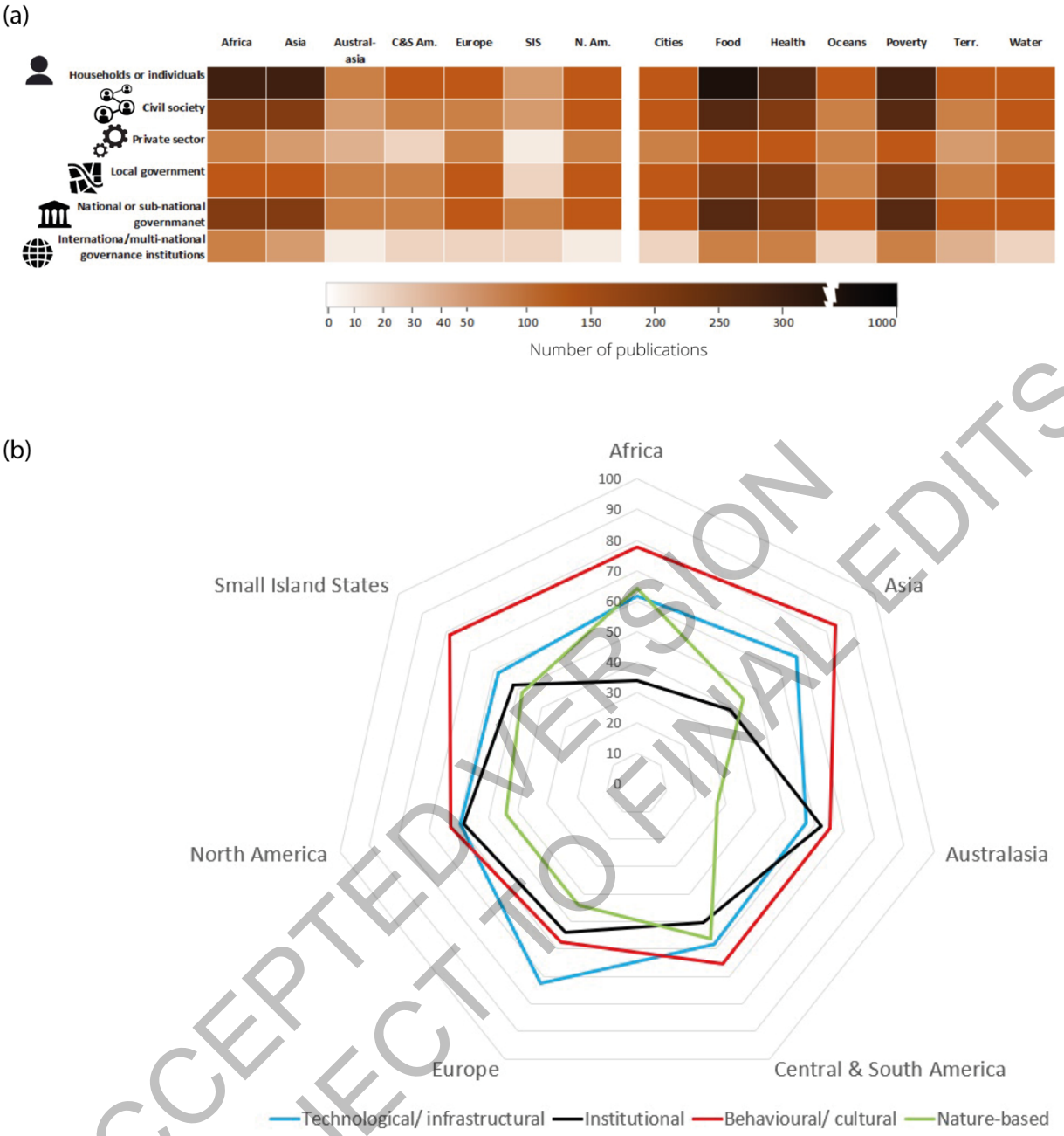

Figure AI.52 [INSERT CAPTION HERE]

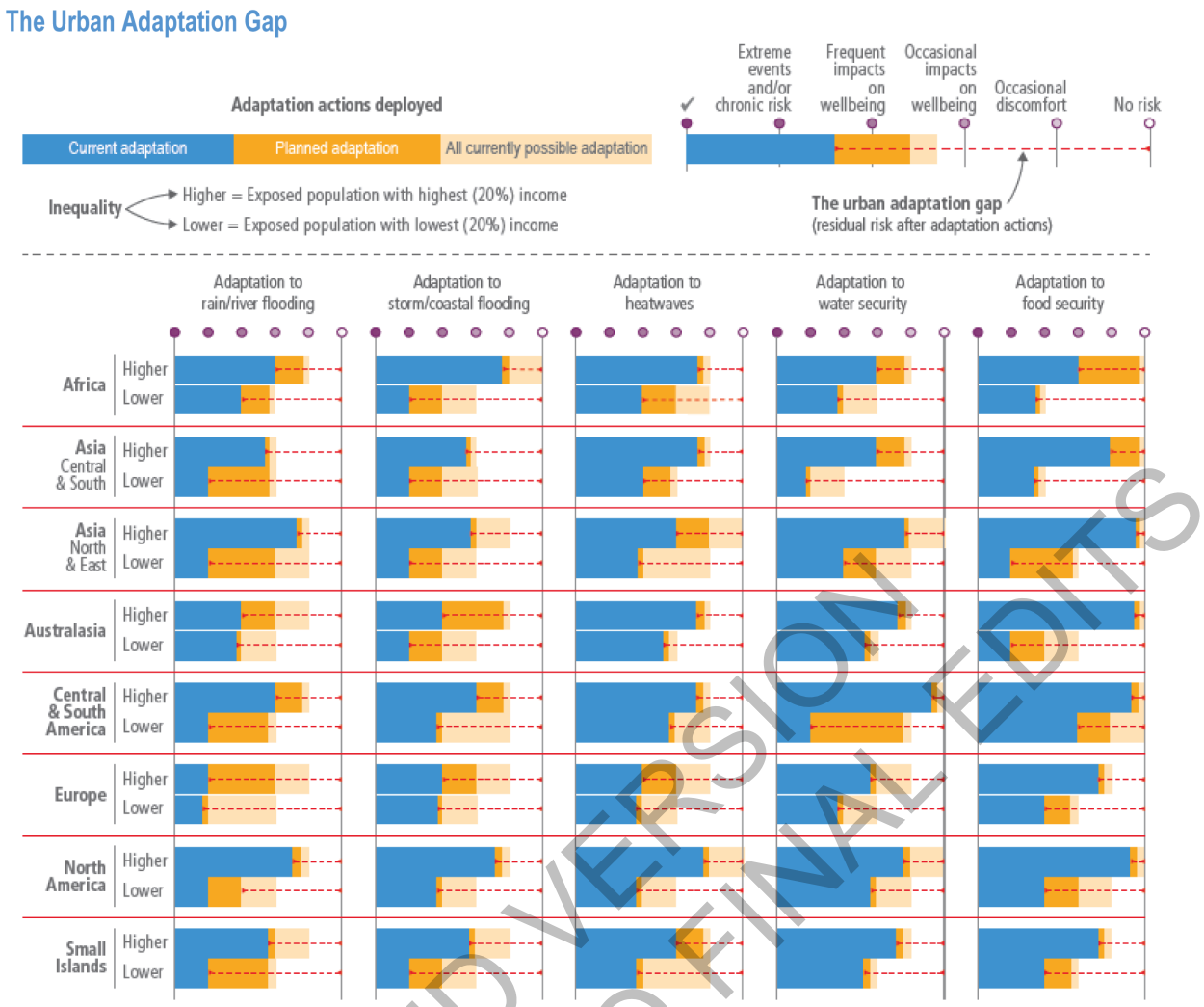

Figure AI.53 [INSERT CAPTION HERE]

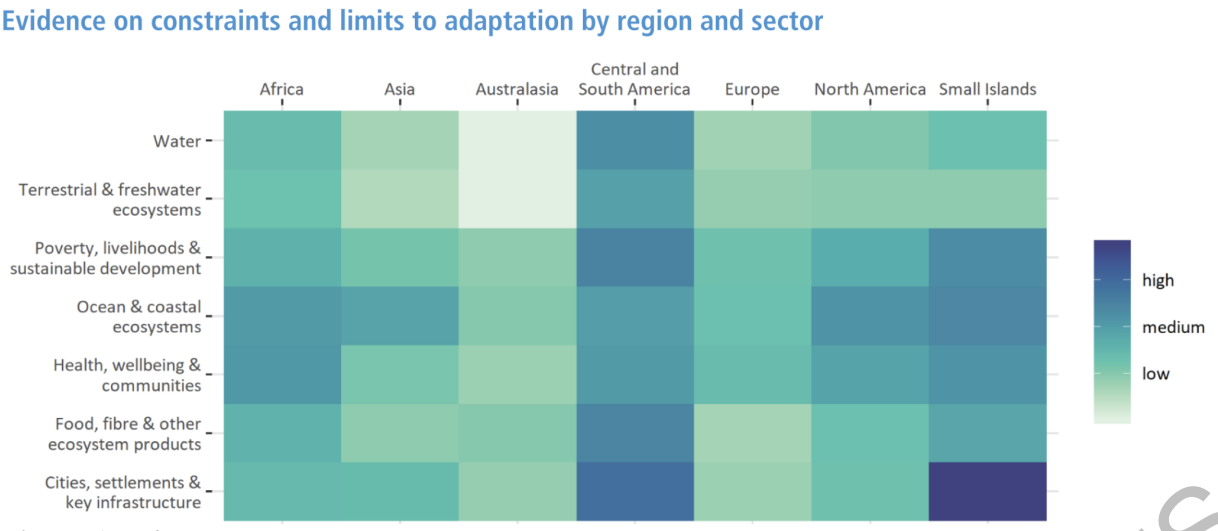

Figure AI.54 [INSERT CAPTION HERE]

Constraints associated with limits by region and sector

Figure AI.55 [INSERT CAPTION HERE]

Distribution of adaptation finance across different regions and different types of finance

(a) Distribution of adaptation finance across different regions and different types of finance in 2015–2016

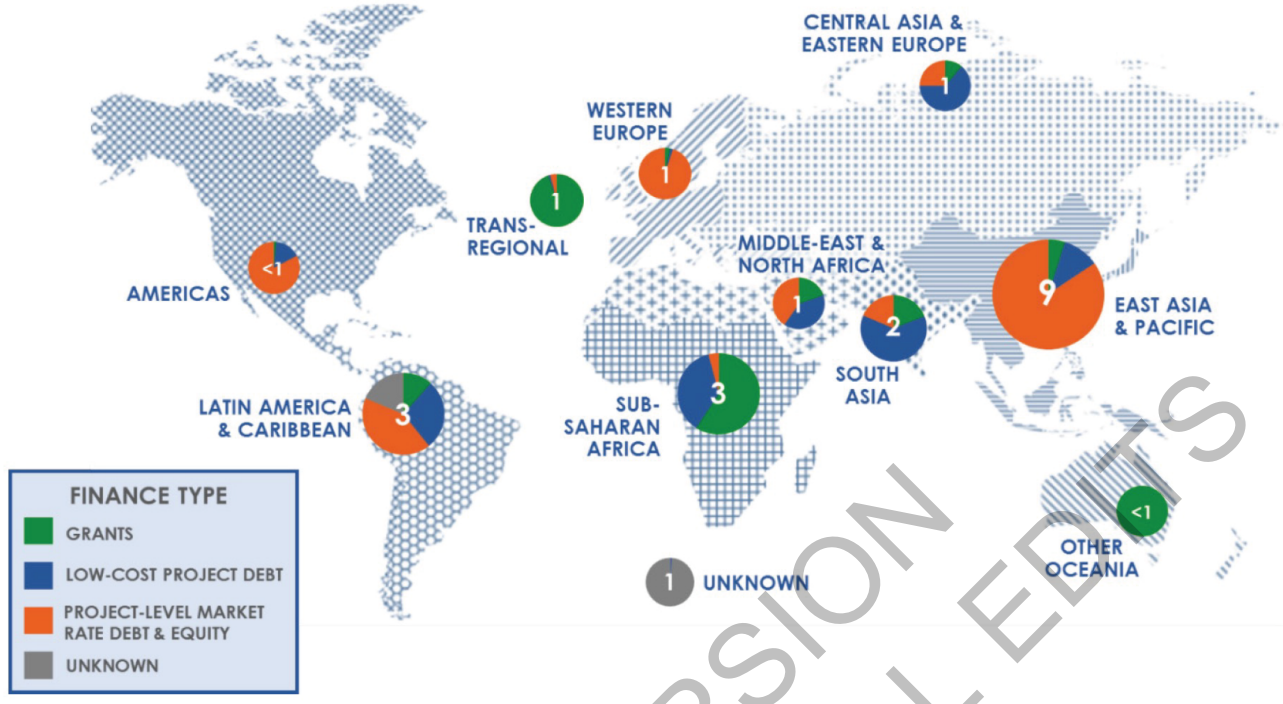

(b) Flow and distribution of globally tracked adaptation and resilience finance in 2018

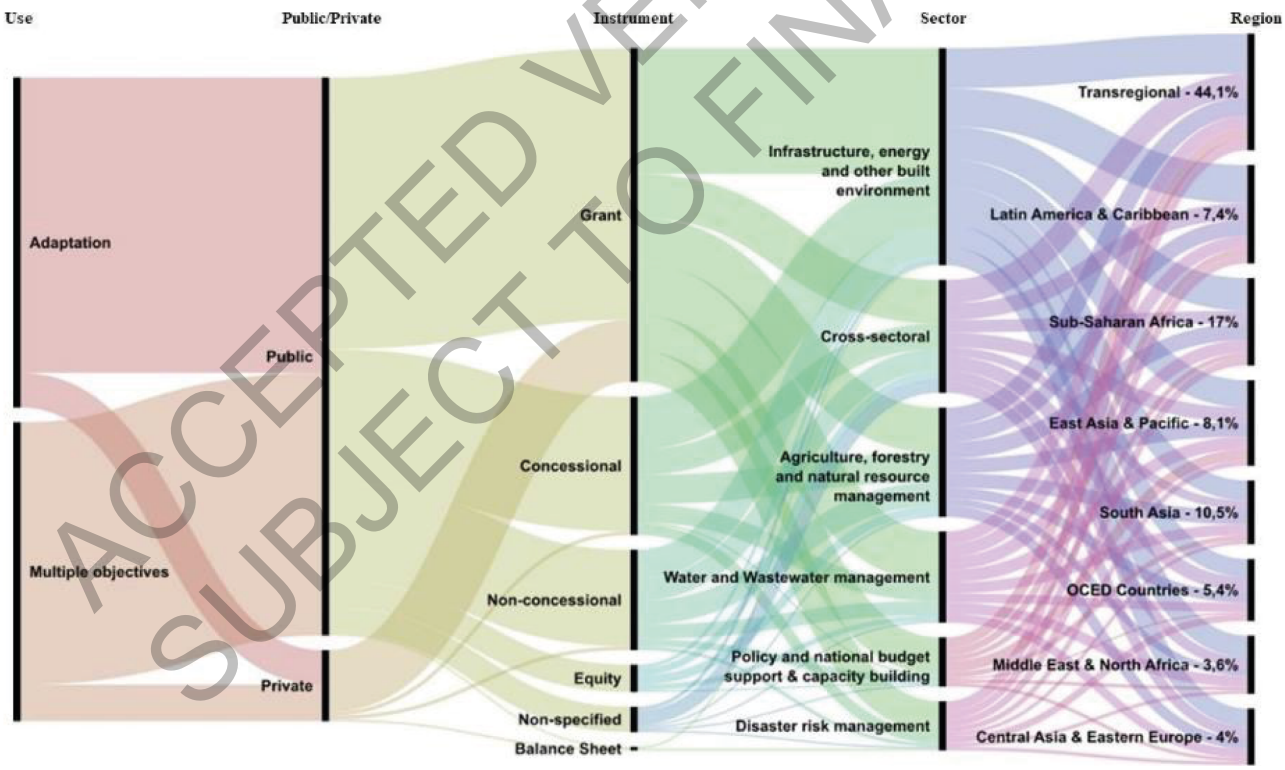

Figure AI.56 [INSERT CAPTION HERE]

Captions

Figure AI.01: Risk in IPCC assessments.
(a) An explicit risk framing emerged in the IPCC SREX and WGII AR5. (b) In the current AR6 assessment, the role of responses in modulating the determinants of risk is a new emphasis (the "wings" of the hazard, vulnerability, and exposure "propellers" represents the ways in which responses modulate each of these risk determinants {Figure 1.5}

Figure AI.02: Physical drivers of climate change: Temperature.
{AR6 WGI Interactive Atlas}

Figure AI.03: Physical drivers of climate change: Precipitation.
{AR6 WGI Interactive Atlas}

Figure AI.04: Physical drivers of climate change: Dissolved Oxygen in the Ocean.
{Assis et al., 2017}

Figure AI.05: Evidence of climate change impacts in many regions of the world.
Global density map shows climate impact evidence, derived by machine-learning from 77,785 studies. Bar charts show the number of studies per continent and impact category. Bars are coloured by the climate variable predicted to drive impacts. Colour intensity indicates the percentage of cells a study refers to where a trend in the climate variable can be attributed (partially attributable: >0% of grid cells, mostly attributable: >50% of grid cells) From Callaghan et al. (2021) {Figure 1.1}

Figure AI.6: Projected changes in global marine richness in 2100 compared to 2006.
Differences between current (year 2006) and projected (year 2100) cell species richness for Representative Concentration Pathways (RCPs) RCP4.5 and RCP8.5 (García Molinos et al. 2016).

Figure AI.07: Observed shifts in distribution of plant functional types.
Observed shifts in the distribution of plant functional types over the 1700–2020. Shifts in plant functional types are indicative of shift in biome function and structure {Box 2.1, Figure Box 2.1.1}

Figure AI.08: Projected responses of rangeland plants to CO_2 fertilization.
Regional percent changes in land cover and soil carbon from ensemble simulation results and plant responses to CO_2 fertilisation. Regions as defined by the United Nations Statistics Division. (Boone et al., 2018) {5.5.3; Figure 5.11}

Figure AI.09: People living in land area of high conservation importance:
{CCP1.2.1.3, Figures CCP1.1, CCP1.2}

Figure AI.10: Present & projected habitat losses of climatically suitable area in terrestrial biodiversity hotspots.
Projected loss for present-day (around 1°C warming) and at global warming levels of 1.5°C, 2°C and 3°C. Maps (right hand column) show the regional distribution of losses in five categories of loss (Very low loss 0–20%, Low loss 20–40%, Medium loss 40–60%, High loss 60–80%, Very high loss 80–100%). The clusters of circles (middle column) show losses in the five categories of loss in each of the 143 hotspot areas of high importance for terrestrial biodiversity conservation with circles scaled by area size. {CCP1, Figure CCP1.6; Table CCP1.1}

Figure AI.11: Projected change in marine animal biomass.
Simulated global biomass changes of animals. Spatial patterns of simulated change by 2090–2099 are calculated relative to 1995–2014 for SSP1-2.6 and SSP5-8.5. The ensemble projections of global changes in total animal biomass updated based on Tittensor et al. (2021) include 6–9 published global fisheries and marine ecosystem models from the Fisheries and Marine Ecosystem Model Intercomparison Project (Fish-MIP, Tittensor et al., 2018; Tittensor et al., 2021), forced with standardised outputs from two CMIP6 Earth System Models. {3.4.3; Fig. 3.21}

Figure AI.12: Projected change in marine zooplankton biomass.
Simulated global biomass changes of zooplankton. In the multi-model mean (solid lines) and *very likely range* (envelope) over 2000–2100 relative to 1995–2014, for SSP1-2.6 and SSP5-8.5. Spatial patterns of simulated change by 2090–2099 are calculated relative to 1995–2014 for SSP1-2.6 and SSP5-8.5. Confidence intervals can be affected by the number of models available for the Coupled Model Intercomparison Project 6 (CMIP6) scenarios and for different variables.The ensemble projections of global changes in zooplankton biomasses updated based on Kwiatkowski et al. (2019) include, under SSP1-2.6 and SSP5-8.5, respectively, a total of nine and 10 CMIP6 Earth System Models (ESMs). {3.4.3.4., Figure 3.21}

Figure AI.13: Spatial patterns of simulated change in total phytoplankton biomass.
Simulated global biomass changes of surface phytoplankton. In the multi-model mean (solid lines) and *very likely range* (envelope) over 2000–2100 relative to 1995–2014, for SSP1-2.6 and SSP5-8.5. Spatial patterns of simulated change by 2090–2099 are calculated relative to 1995–2014 for SSP1-2.6 and SSP5-8.5. Confidence intervals can be affected by the number of models available for the Coupled Model Intercomparison Project 6 (CMIP6) scenarios and for different variables. The ensemble projections of global changes in phytoplankton biomasses updated based on Kwiatkowski et al. (2019) include, under SSP1-2.6 and SSP5-8.5, respectively, a total of nine and 10 CMIP6 Earth System Models (ESMs). {3.4.3.4., Figure 3.21}

Figure AI.14: Spatial patterns of simulated change in total benthic animal biomass.
Simulated global biomass changes of seafloor benthos. In the multi-model mean (solid lines) and *very likely range* (envelope) over 2000–2100 relative to 1995–2014, for SSP1-2.6 and SSP5-8.5. Spatial patterns of simulated change by 2090–2099 are calculated relative to 1995–2014 for SSP1-2.6 and SSP5-8.5. Confidence intervals can be affected by the number of models available for the Coupled Model Intercomparison Project 6 (CMIP6) scenarios and for different variables. Globally integrated changes in total seafloor biomass have been updated based on Yool et al. (2017) with one benthic model (Kelly-Gerreyn et al., 2014) forced with the CMIP6 ESM.

Figure AI.15: Projected exposure of biodiversity.
Global warming levels (GMST) modelled across the ranges of more than 30,000 marine and terrestrial species. Figure based on Trisos et al 2020. {CCP 1; Figure 3.20}.

Figure AI.16: Projected loss of terrestrial and freshwater biodiversity compared to pre-industrial period.
Global warming levels (GSAT); change indicated by the proportion of species (modelled n=119,813 species globally) for which the climate is projected to become unsuitable across their current distributions. {Figure 2.6}

Figure AI.17: Regional impacts to major crop yields and food production loss events.
Trends in food production shocks in different food supply sectors from 1961-2-13 (Cottrell et al., 2019). Projected impacts are for RCP 4.5 mid 21st century, taking into account adaptation and CO_2 fertilisation for crop yield productivity {Figure 5.3; 5.5.3; 5.4.1; Figure FAQ 5.1; Figure 9.22; 15.3.4; 15.3.3}

Figure AI.18: Climatic and environmental stresses on global production of wheat.
The global effects of five climatic and environmental stresses on wheat yield. The combined effect of each stress on yield is presented as a Yield Constraint Score (YCS) on a five-category scale from low stress to high stress (Mills et al., 2018). Higher temperatures enhance not only ozone production but also ozone uptake by plants thus exacerbating yield loss and quality damage. Data are available at Sharps et al., (2020). All data are presented for the 1 × 1° (latitude and longitude) grid squares where the mean production of wheat was >500 tonnes (0.0005 Tg). {5.4.1; Fig. 5.5}

Figure AI.19: Climatic and environmental stresses on global production of soybean.
The global effects of five climatic and environmental stresses on soybean yield. The combined effect of each stress on yield is presented as a Yield Constraint Score (YCS) on a five-category scale from low stress to high stress (Mills et al., 2018). Higher temperatures enhance not only ozone production but also ozone

uptake by plants thus exacerbating yield loss and quality damage. Data are available at Sharps et al., (2020). All data are presented for the 1 × 1° (latitude and longitude) grid squares where the mean production of soybean was >500 tonnes (0.0005 Tg). {5.4.1; Fig. 5.5}

Figure AI.20: Climatic and environmental stresses on global production of rice.
The global effects of five climatic and environmental stresses on rice yield. The combined effect of each stress on yield is presented as a Yield Constraint Score (YCS) on a five-category scale from low stress to high stress (Mills et al., 2018). Higher temperatures enhance not only ozone production but also ozone uptake by plants thus exacerbating yield loss and quality damage. Data are available at Sharps et al., (2020). All data are presented for the 1 × 1° (latitude and longitude) grid squares. {5.4.1; Fig. 5.5}

Figure AI.21: Climatic and environmental stresses on global production of maize.
The global effects of five climatic and environmental stresses on maize yield. The combined effect of each stress on yield is presented as a Yield Constraint Score (YCS) on a five-category scale from low stress to high stress (Mills et al., 2018). Higher temperatures enhance not only ozone production but also ozone uptake by plants thus exacerbating yield loss and quality damage. Data are available at Sharps et al., (2020). All data are presented for the 1 × 1° (latitude and longitude) grid squares. {5.4.1; Fig. 5.5}

Figure AI.22: Projected changes in global maize production.
For maize production time series are shown as relative changes to the 1983-2013 reference period under SSP126 (green) and SSP585 (yellow). Shaded ranges illustrate the interquartile range of all climate and crop model combinations (5 GCMs x 8 GGCMs). The solid line shows the median climate and crop model response (and a 30yr moving average). Horizontal dashed lines mark the 5th and 95th percentile of the historical variability (1983-2013; ensemble median) and open circles highlight the "time of climate impact emergence" (TCIE), the year in which the smoothed median response exceeds the historical envelope. For context, the TCIE calculated from GC5 5 simulations is indicated in lighter shades above the TCIE based on GC6 (>2099 if no TCIE occurs by 2099). The maps (c, d) show median yield changes (2069-2099) under SSP585 across climate and crop models for current growing regions (>10 ha). Hatching indicates areas where less than 70% of the climate-crop model combinations agree on the sign of impact. Regional production time series (e) are similar to (a), but stratified for the four major KoeppenGeiger climate zones (temperature limited, temperate/humid, subtropical, and tropical). The percentage of the total global production contributed by each zone is indicated in the top right corner of the inlets. All data are shown for the default [CO_2] {Jägermeyr et al. 2021; 5.4.3.2}

Figure AI.23: Projected changes in global wheat production.
Production time series are shown as relative changes to the 1983-2013 reference period under SSP126 (green) and SSP585 (yellow). Shaded ranges illustrate the interquartile range of all climate and crop model combinations (5 GCMs x 8 GGCMs). The solid line shows the median climate and crop model response (and a 30yr moving average). Horizontal dashed lines mark the 5th and 95th percentile of the historical variability (1983-2013; ensemble median) and open circles highlight the "time of climate impact emergence" (TCIE), the year in which the smoothed median response exceeds the historical envelope. For context, the TCIE calculated from GC5 5 simulations is indicated in lighter shades above the TCIE based on GC6 (>2099 if no TCIE occurs by 2099). The maps (c, d) show median yield changes (2069-2099) under SSP585 across climate and crop models for current growing regions (>10 ha). Hatching indicates areas where less than 70% of the climate-crop model combinations agree on the sign of impact. Regional production time series (e) are similar to (a), but stratified for the four major KoeppenGeiger climate zones (temperature limited, temperate/humid, subtropical, and tropical). The percentage of the total global production contributed by each zone is indicated in the top right corner of the inlets. All data are shown for the default (CO_2) (Jägermeyr et al. 2021). {5.4.3.2}

Figure AI.24: Rainfed agriculture: drought risks, hazards, exposure & vulnerability indicators.
Hazard and exposure indicator score (a), vulnerability index (b) and drought risk index (c), for rainfed agricultural systems between 1986 and 2015. Drought hazard indicator is defined as the ratio of actual crop evapotranspiration to potential crop evapotranspiration, calculated for 24 crops. Vulnerability index is the country-scale weighted average of a total of 64 indicators including social and ecological susceptibility

indicators, and coping capacity. Risk index is calculated by multiplying hazard/exposure indicator score and vulnerability index (Meza et al., 2020). {Figure 5.5}

Figure AI.25: Extreme stress for livestock driven by temperature and humidity.
Change in the number of days per year above "extreme stress" values from 2000 to the 2090s for livestock globally. Extreme stress conditions estimated using the Temperature Humidity Index (THI). Distributions of livestock in 2090s assumed to be the same as historical global distribution. {Fig 5.12}

Figure AI.26: Temperature and humidity-driven reduction in physical work capacity for humans working outdoors
Projected increase in the number of days per year where physical work capacity is less than 50% based on average daily air temperature and relative humidity. Physical work capacity is defined as the maximum physical work output that can be reasonably expected from an individual performing moderate to heavy work in a 'cool' reference environment of 15oC. {Figure 5.17}

Figure AI.27: Full mortality risk and climate change.
Change in full risk mortality due to increases in temperatures. Estimates come from a model accounting for both the costs and the benefits of adaptation, and the map shows the climate model weighted mean estimate across Monte Carlo simulations conducted on 33 climate models (Carleton et al., 2018). {Figure 9.35, 9.10.1}

Figure AI.28: Projected geographical shift of the human temperature niche.
Geographical position of the human temperature niche projected on the current situation and the RCP8.5 projected 2070 climate. Those maps represent relative human distributions (summed to unity) for the imaginary situation that humans would be distributed over temperatures following the stylized double Gaussian model fitted to the modern data. Difference between the maps, visualizing potential source and sink areas for the coming decades if humans were to be relocated in a way that would maintain this historically stable distribution with respect to temperature. (Xu et al., 2020) {Table 8.7; 8.4.5.6}

Figure AI.29: Global population exposed to hyperthermia from extreme heat.
Global distribution of population exposed to hyperthermia from extreme heat and humidity. Maps indicate the historical and projected number of days in a year in which conditions of air temperature and humidity surpass a common threshold beyond which conditions turned deadly and pose a risk of death (Mora et al., 2017). Largest fifteen urban areas by population size/number of citizens during 2020, 2050, and 2100 respectively as projected by Hoornweg and Pope (2017) {Figure 6.3; 6.2.3.1}"

Figure AI.30: Present-day global distribution of camps for refugees & internally displaced people.
The global distribution of the United Nations High Commissioner for Refugees (UNHCR) refugee and internally displaced people (IDP) settlements (as of 2018) overlaid with annual mean near surface air temperature (°C) in 2040-2059 under RCP8.5. {Figure Box 8.1.1; Box 8.1}

Figure AI.31: Estimated relative human dependence on marine ecosystems.
Relative human dependence on marine resources for coastal protection, nutrition, fisheries economic benefits and overall. Each bar represents an index value that semi-quantitatively integrates the magnitude, vulnerability to loss and substitutability of the benefit. Indices synthesize information on people's consumption of marine protein and nutritional status, gross domestic product, fishing revenues, unemployment, education, governance and coastal characteristics. Overall dependence is the mean of the three index values after standardization from 0–1 (Details are found in Table 1 and supplementary material of (Selig et al., 2019)). This index does not include the economic benefits from tourism or other ocean industries, and data limitations prevented including artisanal or recreational fisheries or the protective impact of saltmarshes (Selig et al., 2019). Values for reference regions established in the WGI AR6 Atlas (Gutiérrez et al., 2021) were computed as area-weighted means from original country-level data. {Figure 3.1}

Figure AI.32: Regional vulnerabilities to impacts of current and projected climate change on marine fishery and terrestrial livestock resources.
(a) Ocean areas are delineated into FAO (Food and Agricultural Organization of the United Nations) regions. Ocean sensitivity is calculated from aggregated sensitivities from Blasiak et al. (2017) S1 country data based on number of fishers, fisheries exports, proportions of economically active population working as fishers, total fisheries landings and nutritional dependence, which was subsequently reanalyzed for each FAO region depicted here. Arrows denote projected average commercial (light blue) and artisanal (orange arrows) fishing resource shifts in location under RCP2.6 and under RCP8.5 (dark blue and red arrows respectively) scenarios by 2100. Text boxes highlight examples of vulnerabilities (Bell et al., 2018a), conflicts (Miller et al., 2013; Blasiak et al., 2017; Østhagen et al., 2020), or opportunities for marine resource usage (Robinson et al., 2015; Stuart-Smith et al., 2018; Meredith et al., 2019). (b) Projected changes in the number of extreme heat stress days per year for cattle (Bos taurus, temperate sub-regions, grey background; Bos indicus, tropical sub-regions, orange background) from 2000 to the 2090s, shown as arrows rooted in the most affected area in each IPCC sub-region pointing to the nearest area of reduced or no extreme heat stress. Arrows are shown only for sub-regions where > 1 million additional animals affected. Areas in green are those with >5000 animals per 0.5 degree grid cell (Thornton et al., 2021). {Cross-Chapter Box MOVING PLATE Figure 1}

Figure AI.33: Current fisheries adaptive capacity to climate change and regional dependence on seafood micronutrients in human diets.
Global documented fisheries management adaptive capacity to climate change and regional dependencies on micronutrients from fisheries. 1. Fisheries management adaptive capacity is a function of: averaged GDP World Development Indicators for 2018 (World Bank, 2020); climate awareness assessments of 30 of the FAO (Food and Agricultural Organization of the United Nations) recognized most recent Regional Fisheries Management Organizations with direct fisheries linkages; governance effectiveness index based on six aggregate indicators (voice and accountability, political stability and absence of violence / terrorism, government effectiveness, regulatory quality, rule of law, control of corruption) from 2018 World Governance Indicator (World Bank, 2019) data, and; heterogeneity of countries within each FAO zone (highly heterogeneous regions are less likely to establish sustainable and efficient fisheries management for the entire FAO zone). Adaptative capacity index ranges from 1 (high) to 0 (no adaptative capacity). Ocean areas are delineated into FAO regions. 2. Nutritional dependence of regional human populations on micronutrient supply from marine fisheries. Nutritional dependence scale ranges from 100 (full dependence) to 0 (no dependence). (Beal et al. 2017). {Cross-Chapter Box MOVING PLATE Figure 3 in Chapter 5}

Figure AI.34: Climate change risk to fisheries in Africa.
Inland fisheries (panels a-e): (a) Countries' reliance on inland fisheries was estimated by catch (total, tonnes) (FAO, 2018b; Fluet-Chouinard et al., 2018), per capita catch (kg/person/year) (FAO, 2018b), percent reliance on fish for micronutrients, and percent consumption per household (Golden et al., 2016). Z-scores of each metric were averaged for each country to create a composite index describing 'current dependence on freshwater fish' for each country with darker blue colours indicating higher dependence. (b–c) Projected concentrations (numbers) of vulnerable freshwater fishery species averaged within freshwater ecoregions under >2°C global warming (b) and >4°C global warming (c) estimated from recent past (1961–1992) to the end of the 21st century (2071 to 2100) (Nyboer et al., 2019). Numbers of vulnerable fish species translate to an average of 55–68% vulnerable at >2°C and 77–97% vulnerable at <4°C global warming. Darker reds indicate higher concentrations of vulnerable fish species. (d–e) Countries (in green) that have an overlap between high dependence on freshwater fish and high concentrations of fishery species that are vulnerable to climate change under two warming scenarios. Inland fisheries (panels f–j) comparing countries' current percent dependence on marine foods for nutrition compared with projected change in maximum catch potential (MCP) from marine fisheries. (f) The percentage of animal sources foods consumed that originate from a marine environment. Countries with higher dependence are indicated by darker shades of blue (Golden et al., 2016). (g–h) Projected percent change in maximum catch potential (MCP) of marine fisheries under 1.6°C global warming (g) and >4°C global warming (h) from recent past (1986–2005) to end of 21st century (2081-2100) in countries' Exclusive Economic Zones (EEZs) (Cheung William et al., 2016). Darker red indicates greater percent reduction [negative values]. (i–j) Countries (in green) that have overlap between high nutritional dependence and high reduction in MCP under two warming scenarios. {Figure 9.25, Figure 9.26}

Figure AI.35: Regional synthesis of changes in water and consequent impacts on ecosystems and human systems.
For physical changes, increase/decrease refers to changes in the amount or frequency of the measured variable, and the level of confidence refers to confidence that the change has occurred. For impacts on ecosystems and human systems, plus or minus marks depicts whether an observed impact of hydrological change is positive (beneficial) or negative (adverse), respectively, to the given system, and the level of confidence refers to confidence in attributing an impact on that system to a climate-induced hydrological change. Circles indicate that within that region, both increase and decrease of physical changes are found, but are not necessarily equal; or beneficial and adverse assessed impacts on ecosystems and human systems. 'na' indicates variables not assessed due to limited evidences. Agriculture refers to impacts on crop production. Energy refers to impacts on hydro and thermoelectric power generation. {Figure 4.20}

Figure AI.36: Current global drought risk. Current global drought risk and its components.
(a) Drought hazard computed for the events between 1901– 2010 by the probability of exceedance the median of global severe precipitation deficits, using precipitation data from the Global Precipitation Climatology Center (GPCC) for 1901–2010. (b) Drought vulnerability is derived from an arithmetic composite model combining social, economic, and infrastructural factors proposed by UNISDR (2004). (c) Drought exposure computed at the sub-national level with the non-compensatory DEA (Data Envelopment Analysis) model (Cook et al., 2014). (d) Drought risk based on the above components of hazard, vulnerability and exposure, scored on a scale of 0 (lowest risk) to 1(highest risk) with the lowest and highest hazard, exposure, and vulnerability (Carrão et al., 2016). {Figure 4.9}

Figure AI.37: Dependence of land surface areas and population on mountain water resources 1961–2050.
Results are shown as decadal averages for lowland population in each category of dependence on mountain water from no surplus and negligible to essential. (a) Global mountain regions and their differentiated importance for lowland water resources. (b) Lowland population and their differentiated dependence on mountain water resources, both for the scenario combination SSP2-RCP6.0 and for the time period 2041–2050. (c) Number of lowland population and their differentiated dependence on mountain water resources from the 1960's to the 2040's for three different scenario combinations (based on Viviroli et al., 2020). {Figure CCP5.2}

Figure AI.38: Risk to livelihoods and the economy from changing mountain water resources.
The majority of studies assessed focus on impacts up to mid-century (2030–2060) and for RCP-2.6, RCP-4.5 and RCP-6.0, which was converted into the corresponding warming level range 1.5-2.0°C GWL (see CCB CLIMATE). Methodological details are provided in Section SMCCP5.4, Figure SMCCP5.1, Table SMCCP5.16 and SMCCP5.18. Due to the limited evidence available to determine risks against high Global Warming Levels (GLWs), and the relatively high uncertainties associated with future irrigation trends for the second half of the century (see e.g. Viviroli et al., 2020), assessment of risks associated with GLWs greater than 2.0°C GWL was not conducted. {Figure CCP5.6}

Figure AI.39: The effect of regional sea level rise on extreme sea level events at coastal locations.
(a) Schematic illustration of extreme sea level events and their average recurrence in the recent past (1986–2005) and the future. As a consequence of mean sea level rise, local sea levels that historically occurred once per century (historical centennial events, HCEs) are projected to recur more frequently in the future. (b) The year in which HCEs are expected to recur once per year on average under RCP8.5 and RCP2.6, at the 439 individual coastal locations where the observational record is sufficient. The absence of a circle indicates an inability to perform an assessment due to a lack of data but does not indicate absence of exposure and risk. The darker the circle, the earlier this transition is expected. The likely range is ±10 years for locations where this transition is expected before 2100. White circles (33% of locations under RCP2.6 and 10% under RCP8.5) indicate that HCEs are not expected to recur once per year before 2100. (c) An indication at which locations this transition of HCEs to annual events is projected to occur more than 10 years later under RCP2.6 compared to RCP8.5. As the scenarios lead to small differences by 2050 in many locations results are not shown here for RCP4.5 but they are available in Chapter 4. {4.2.3, Figure 4.10, Figure 4.12}

Figure AI.40: Relative trends in projected regional shoreline change.

Advance/retreat relative to 2010. Frequency distributions of median projected change by (a,c) 2050 and (b,d) 2100 under (a,b) RCP4.5 and (c,d) RCP8.5. Projections account for both long-term shoreline dynamics and sea-level rise and assume no impediment to inland transgression of sandy beaches. Data for small island states are aggregated and plotted in the Caribbean. Data from Vousdoukas et al. (2020b). Values for reference regions established in the WGI AR6 Atlas (Gutiérrez et al., 2021) were computed as area-weighted means from original country-level data. For model assumptions and associated debate, see Vousdoukas et al. (2020a) and Cooper et al. (2020a).{Figure 3.14}

Figure AI.41: Population living in small islands that may be exposed to coastal inundation.
Projected percentage of current population in selected small islands occupying vulnerable land (the number of people on land that may be exposed to coastal inundation—either by permanently falling below Mean Higher High Water, or temporarily falling below the local annual flood height) (adapted from Kulp et al. 2019, using the CoastalDEM_Perm_p50 model). Positions on the map are based on the capital city or largest town. {Figure 15.3}

Figure AI.42: Projected number of people at risk of a 100-year coastal flood.
The size of the circle represents the number of people at risk per IPCC region and the colours show the timing of risk based on projected sea-level rise (Haasnoot et al., 2021) under three different Shared Socioeconomic Pathways (SSPs). Darker colours indicate earlier in setting risks. The left side of the circles shows absolute population at risk and the right side the share of the population in percentage. {Figure CCP2.4; Figure 13.6; Figure 15.3}.

Figure AI.43: Selected African cities exposed to sea level rise.
Selected African cities exposed to sea level rise include (a) Dar es Salaam, Bagamoyo, and Stone Town in Tanzania (East Africa), (b) Lagos in Nigeria, and Cotonou and Porto-Novo in Benin (West Africa), and (c) Cairo and Alexandria in Egypt (North Africa). Orange shows built-up area in 2014. Shades of blue show permanent flooding due to sea level rise by 2050 and 2100 under low (RCP2.6), medium (RCP4.5) and high (RCP8.5) greenhouse gas emissions scenarios. Darker colours for higher emissions scenarios show areas projected to be flooded in addition to those for lower emissions scenarios. The figure assumes failure of coastal defences in 2050 and 2100. Some areas are already below current sea level rise and coastal defences need to be upgraded as sea level rises (e.g., in Egypt), others are just above mean sea levels and they do not necessarily have high protection levels, so these defences need to be built (e.g., Dar Es Salam and Lagos). Blue shading shows permanent inundation surfaces predicted by Coastal DEM and SRTM given the 95th percentile K14/RCP2.6, RCP4.5, and RCP8.5, for present day, 2050, and 2100 sea level projection for permanent inundation (inundation without a storm surge event), and RL10 (10-year return level storm) (Kulp and Strauss, 2019). Low-lying areas isolated from the ocean are removed from the inundation surface using connected components analysis. Current water bodies are derived from the SRTM Water Body Dataset. Orange areas represent the extent of coastal human settlements in 2014 (Corbane et al., 2018). See Figure CCP4.7 for projections including subsidence and worst-case scenario projections for 2100. {Figure 9.29}.

Figure AI.44: Risk of historical and projected river flooding.
(a) Vulnerability. Modelled mean global fluvial flood water depth (Tanoue et al., 2016; Tanoue et al., 2021) based on a land surface model and a river and inundation model driven by reanalysis climate forcing of 5 CMIP5 GCMs (metres). The annual maximum daily river water was allocated along elevations, and inundation depth was calculated for each year and averaged for the target period. (b) Hazard. Local flood protection standard (return period) at sub-country scale (Scussolini et al., 2016) based on published reports and documents, websites and personal communications with experts. Note that the vulnerability of this map reflects local flood protection such as complex infrastructure and does not fully reflect the other source of vulnerabilities, including exposure. (c) Exposure. Population distribution per 30 arc second grid cell (Klein Goldewijk et al., 2010; Klein Goldewijk et al., 2011). (d) Risk as population exposed to flood (number of people where inundation occurs) per 30 arc-second grid cell. Population under inundation depth > 0 m (a) was counted when the return period of annual maximum daily river water exceeds the flood protection standard (c). {Figure 4.8}

Figure AI.45: Projected changes in river flooding.
Multi-model median return period (years) in the 2080s for the 20th-century 100-year river flood, based on a global river and inundation model, CaMa-Flood, driven by runoff output of 9 CMIP6 Models in the SSP1-2.6 (a), SSP2-4.5 (b) and SSP5-8.5 (c) scenario respectively. All changes are estimated in 2071-2100 relative to 1970-2000. A dot indicates regions with high model consistency (more than 7 models out of 9 show the same direction of change). (d) Global or regional potential exposure (% to the total population affected by flooding) under different warming levels with constant population scenario of CMIP5 (Alfieri et al., 2017) and with population scenario of SSP5 of CMIP6 (bar chart, (Hirabayashi et al., 2021b)). Inundation is calculated when the magnitude of flood exceeds current flood protection (Scussolini et al., 2016). Note that number of GCMs used to calculate Global Warming Level (GWL) 4.0 is less than that for other SWLs, as the global mean temperature of some GCMs did not exceed 4°C. {Figure 4.17}

Figure AI.46 Burning ember diagrams of regional & global risk assessments.
{Reasons for concern: 16.6.3.1 – 16.6.3.5; 16.6.4; Table SM16.18 in Supplementary Material SM16.6 presents the consensus values of the transition range and median estimate in terms of global warming level by risk level for each of the five RFC embers. Africa: 9.2; Table 9.2; For range of global warming levels for each risk transition used to make this figure see Supplementary Material Table SM 9.1. Australia and New Zealand/ Australia: The assessment is based on available literature and expert judgement, summarized in Table 11.14 and described in Supplementary Material SM 11.2. Mediterranean: See CCP4.3.2-8 and Supplementary Tables SMCCP4.2a-h for details. Europe: 13.10.2; More details on each burning ember are provided in Sections 13.10.2.1-13.10.2.4 and SM13.10. North America: 14.6.2; 14.6.3; Table 14.3, see SM14.4. for detailed information. Arctic: CCP6.3.1; Table CCP6.5; The supporting literature and methods are provided in SMCCP6.6. Ecosystems: Terrestrial and freshwater: Tables 2.5 and 2.S.4 provide details of the key risks and temperature levels for the risk transitions. Ocean: Special Report on the Ocean and Cryosphere in a Changing Climate (SROCC). Health: 7.3.1; Based on (Ebi et al., 2021).}

Figure AI.47: Evidence of transformative adaptation by sector and region.
Evidence of transformational adaptation does not imply effectiveness, equity, or adequacy. Evidence of transformative adaptation is assessed based on the scope, speed, depth, and ability to challenge limits of responses reported in the scientific literature Studies relevant to multiple regions or sectors are included in assessment for each relevant sector/region. {16.3.2; Figure 16.6}.

Figure AI.48: Drought is exacerbating water management challenges which vary across regions with respect to anticipated water scarcity conditions by 2050.
Local levels of policy challenges for addressing water scarcity by 2050, considering both the central estimate (median) and the changing uncertainty in projections of the Water Scarcity Index (WSI) from the present day to 2050. Projections used five CMIP5 climate models, three global hydrological models from ISIMIP, and three Shared Socioeconomic Pathways (SSPs).Reproduced from (Greve et al., 2018). {Figure Box 4.1.1; Box 4.1}.

Figure AI.49: Observed water-related adaptation responses with positive outcomes.
(a) Location of case studies of water-related adaptation responses (996 data points from 319 studies). In these 996 data points, at least one positive outcome was recorded in one of the five outcome indicators. These outcome indicators are economic/financial, outcomes for vulnerable people, ecological/environmental, water-related, and socio-cultural and institutional. (b) In most instances, the top six adaptation categories include nearly 3/4th of the studies. (c) Due to a small number of studies in small island states, a spider diagram was not generated for the Small Island States. {Figure 4.27}

Figure AI.50: Projected effectiveness of water-related adaptation options.
Effectiveness in returning the system to a study-specific baseline state relative to the projected climate impact; and level of residual risk retained after adaptation, relative to baseline conditions. Regional summaries are based on IPCC regions. Warming levels refer to the global mean temperature (GMT) increase relative to a 1850-1900 baseline. For each data point, the study-specific GMT increase was calculated to show effectiveness at 1.5°C, 2°C, 3°C and 4°C. Based on the ability of an implemented option to return the system to its baseline state, the effectiveness is classified based on the share of risk the option can reduce: Large (>80%); Moderate (80-50%); Small (<50-30%); Insufficient (<30%). Where the system state is

improved relative to baseline, Co-benefits are identified. Residual impacts show the share of remaining impacts after adaptation has been implemented: Negligible (<5%); Small (5 to <20%); Moderate (20 to <50); Large (50% and more). Where risks increase after adaptation, data points are shown as maladaptation. All underlying data is provided in SM4.8. {Figure 4.28}

Figure AI.51: Evidence of observed adaptation across regions in food, fibre, and other ecosystem products.
Stage of implementation; Type of adaptation; Inclusion of Indigenous knowledge and local knowledge (IK and LK) based on Global Adaptation Mapping Initiative (GAMI) database – (Berrang-Ford et al., 2021a). The bars indicate the number of evidence for the options x region. {Figure 5.21}

Figure AI.52: Who is responding, by geographic region and sector?
(a) Cell contents indicate the number of publications reporting engagement of each actor in adaptation-related responses. Darker colours denote a high number of publications. (b) Percentages reflect the number of articles mentioning each type of adaptation over the total number of articles for that region. Radar values do not total 100% per region since publications frequently report multiple types of adaptation; for example, construction of drainage systems (infrastructural), changing food storage practices by households (behavioural), and planting of tree cover in flood prone areas (nature-based) in response to flood risk to agricultural crops. Data updated and adapted from (Berrang-Ford et al., 2021b), based on 1682 scientific publications reporting on adaptation-related responses in human systems. {Figure 16.4; Figure 16.5}

Figure AI.53: The Urban Adaptation Gap.
This is a qualitative assessment presenting individual, non-comparative data for world regions from 25 AR6 Contributing Lead Authors and Lead Authors, the majority from regional chapters. Respondents were asked to make expert summary statements based on the data included within their chapters and across the AR6 report augmented by their expert knowledge. Multiple iterations allowed opportunity for individual and group judgement. Urban populations and risks are very diverse within regions making the presented results indicative only. Variability in data coverage leads to the overall analysis having medium agreement – medium evidence. Major trends identified in 6.3.1 at least meet this level of confidence. Analysis is presented for current observed climate change associated hazards and for three adaptation scenarios: (1) current adaptation (based on current levels of risk management and climate adaptation), (2) planned adaptation (assessing the level of adaptation that could be realised if all national, city and neighbourhood plans and policies were fully enacted), (3) transformative adaptation (if all possible adaptation measures were to be enacted). Assessments were made for the lowest and highest quintile by income. Residual risk levels achieved for each income class under each adaptation scenario are indicated by five adaptation levels: no risk, occasional discomfort, occasional impacts on wellbeing, frequent impacts on wellbeing, extreme events and/or chronic risk. The urban adaptation gap is revealed when levels of achieved adaptation fall short of delivering 'no risk'. The graphic uses IPCC Regions, and has split Asia into two regions: North and East Asia, and Central and South Asia. {Figure 6.4}

Figure AI.54: Evidence on constraints and limits to adaptation by region and sector.
Data from (Thomas et al. 2021), based on 1682 scientific publications reporting on adaptation-related responses in human systems. See 16.A.1 for methods. Low evidence: <20% of assessed literature has information on limits, literature mostly focuses on constraints to adaptation Medium evidence: between 20-40% of assessed literature has information on limits, literature provides some evidence of constraints being linked to limits High evidence: > 40% of assessed literature has information on limits, literature provides broad evidence of constraints being linked to limits. {Figure 16.7}

Figure AI.55: Constraints associated with limits by region and sector.
Data from (Thomas et al. 2021), based on 1682 scientific publications reporting on adaptation-related responses in human systems. See 16.A.1 for methods. Constraints are categorized as: (1) Economic: existing livelihoods, economic structures, and economic mobility; (2) Social/cultural: social norms, identity, place attachment, beliefs, worldviews, values, awareness, education, social justice, and social support; (3) Human capacity: individual, organizational, and societal capabilities to set and achieve adaptation objectives over time including training, education, and skill development; (4) Governance, Institutions & Policy: existing laws, regulations, procedural requirements, governance scope, effectiveness, institutional arrangements, adaptive capacity, and absorption capacity; (5) Financial: lack of financial resources; (6)

Information/Awareness/Technology: lack of awareness or access to information or technology; (7) Physical: presence of physical barriers; and (8) Biologic/climatic: temperature, precipitation, salinity, acidity, and intensity and frequency of extreme events including storms, drought, and wind. Insufficient data: there is not enough literature to support an assessment (less than 5 studies available); Minor constraint: <20% of assessed literature identifies this constraint; Secondary constraint: 20-50% of assessed literature identifies this constraint; Primary constraint: >50% of assessed literature identifies this constraint. {Figure 16.8}

Figure AI.56: Distribution of adaptation finance across different regions and different types of finance. (a) Data for period 2015-2016, as tracked the Climate Policy Initiative. (b) Data for year 2018 from different sources, through different instruments into different sectors and regions as collated by (CPI, 2020). Each strand shows the relative proportion of finance flowing from one category to another (for example from private or public sources to different instruments). Categories from left to right are: Use = whether the finance is solely for adaptation or for adaptation and other objectives, including mitigation; Public/Private = whether the finance comes from public or private sources; Instrument, the financing instrument; Sector = the broad sectoral allocation; Region = the geographical distribution of funding (proportion of total in % and per-capita allocation). {Figure Cross-Chapter Box FINANCE.2; Figure FAQ17.2.1}

References

Alfieri, L. et al., 2017. Global projections of river flood risk in a warmer world. *Earth's Future*, 5 (2), 171-182, doi:10.1002/2016ef000485.

Assis, J., et al., 2017. Bio-ORACLE v2.0: Extending marine data layers for bioclimatic modelling. *Glob. Ecol. Biogeogr*. 27, 277–284. doi:10.1111/geb.12693.

Barragán, J.M. and de Andrés, M., 2015. Analysis and trends of the world's coastal cities and agglomerations. Ocean & Coastal Management, 114: 11-20.

Beal, T. et al., 2017. Global trends in dietary micronutrient supplies and estimated prevalence of inadequate intakes. *PLoS One*, 12(4), e0175554, doi:10.1371/journal.pone.0175554.

Bell, J. D. et al., 2018a. Climate change impacts, vulnerabilities and adaptations: Western and Central Pacific Ocean marine fisheries. In: Impacts of Climate Change on Fisheries and Aquaculture: Synthesis of Current Knowledge, Adaptation and Mitigation Options [Barange, M., T. Bahri, M. C. M. Beveridge, K. L. Cochrane, S. Funge-Smith and F. Poulain (eds.)]. Food and Agriculture Organization of the United Nations,, Rome, Italy, pp. 305-324. ISBN 9789251306079.

Berrang-Ford, L. et al., 2021a. The Global Adaptation Mapping Initiative (GAMI): Part 1 – Introduction and overview of methods. protocolexchange, doi:10.21203/rs.3.pex-1240/v1.

Berrang-Ford, L. et al., 2021b. A systematic global stocktake of evidence on human adaptation to climate change. Nat. Clim. Change,(in press).

Blasiak, R. et al., 2017. Climate change and marine fisheries: Least developed countries top global index of vulnerability. *PLoS One*, 12(6), e0179632, doi:10.1371/journal.pone.0179632.

Boone, R., et al., 2018. Climate change impacts on selected global rangeland ecosystem services. *Global Change Biology,* 24(3), 1382-1393, DOI:10.1111/gcb.13995.

Callaghan, M., et al., 2021. Machine learning-based evidence and attribution mapping of 100,000 climate impact studies. Nature Climate Change.

Carleton, T. et al., 2018. Valuing the Global Mortality Consequences of Climate Change Accounting for Adaptation Costs and Benefits. University of Chicago, Becker Friedman Institute for Economics Working Paper No. 2018-51., doi:10.2139/ssrn.3224365.

Carrão, H., G. Naumann and P. Barbosa, 2016. Mapping global patterns of drought risk: An empirical framework based on sub-national estimates of hazard, exposure and vulnerability. *Global Environmental Change*, 39, 108-124, doi:https://doi.org/10.1016/j.gloenvcha.2016.04.012.

Cheung William, W. L., G. Reygondeau and L. Frölicher Thomas, 2016. Large benefits to marine fisheries of meeting the 1.5°C global warming target. *Science (New York, N.Y.)*, 354(6319), 1591-1594, doi:10.1126/science.aag2331.

Cottrell, R. S. et al., 2019. Food production shocks across land and sea. Nat. Sustain., 2(2), 130-137, doi:10.1038/s41893-018-0210-1.

Cook, W. D., K. Tone and J. Zhu, 2014. Data envelopment analysis: Prior to choosing a model. *Omega*, 44, 1-4, doi:https://doi.org/10.1016/j.omega.2013.09.004.

Cooper, J. A. G. et al., 2020a: Sandy beaches can survive sea-level rise. *Nature Climate Change*, 10(11), 993-995, doi:10.1038/s41558-020-00934-2.

Corbane, C. et al., 2018: GHS built-up grid, derived from Landsat, multitemporal (1975-1990-2000-2014), R2018A, European Commission, Joint Research Centre (JRC), Brussels.

CPI, 2020: Updated View of the Global Landscape of Climate Finance 2019. Rob Macquarie, Baysa Naran, Paul Rosane, Matthew Solomon, Cooper Wetherbee, Climate Policy, I., London. Available at: https://www.climatepolicyinitiative.org/publication/updated-view-on-the-global-landscape-of-climate-finance-2019 (accessed 2021/06/26).

Ebi, K. et al., 2021: Burning embers: synthesis of the health risks of climate change. Environmental Research Letters, 16(4), doi:10.1088/1748-9326/abeadd.

FAO, 2018b: *The State of World Fisheries and Aquaculture: Meeting the sustainable development goals* [Barange, M., J. Alder, U. Barg, S. Funge-Smith, P. Mannini, M. Taconet and J. Plummer (eds.)]. The State of World Fisheries and Aquaculture (SOFIA), FAO, Rome, Italy, 277 pp. Available at: http://www.fao.org/3/i9540en/i9540en.pdf.

Fluet-Chouinard, E., S. Funge-Smith and P. B. McIntyre, 2018: Global hidden harvest of freshwater fish revealed by household surveys. *Proceedings of the National Academy of Sciences*, 115(29), 7623, doi:10.1073/pnas.1721097115.

García Molinos, J., et al., 2016: Climate velocity and the future global redistribution of marine biodiversity. Nature Climate Change, 6,: 83-88. DOI: 10.1038/NCLIMATE2769

Golden, C. D. et al., 2016: Nutrition: Fall in fish catch threatens human health. *Nature*, 534(7607), 317-320, doi:10.1038/534317a.

Greve, P. et al., 2018: Global assessment of water challenges under uncertainty in water scarcity projections. *Nature Sustainability*, 1 (9), 486-494, doi:10.1038/s41893-018-0134-9.

Gutiérrez, J. M. et al., 2021: Atlas. In: *Climate Change 2021: The Physical Science Basis. Contribution of Working Group I to the Sixth Assessment Report of the Intergovernmental Panel on Climate Change* [Masson-Delmotte, V., P. Zhai, A. Pirani, S. L. Connors, C. Péan, S. Berger, N. Caud, Y. Chen, L. Goldfarb, M. I. Gomis, M. Huang,

K. Leitzell, E. Lonnoy, J. B. R. Matthews, T. K. Maycock, T. Waterfield, O. Yelekçi, R. Yu and B. Zhou (eds.)]. Cambridge University Press.
Haasnoot, M., et al., 2019a. Generic adaptation pathways for coastal archetypes under uncertain sea-level rise. Environmental Research Communications, 1(7): 071006.
Haasnoot, M. et al., 2021: Long-term sea-level rise necessitates a commitment to adaptation: A first order assessment. Climate Risk Management, 34, doi:https://doi.org/10.1016/j.crm.2021.100355.
Hirabayashi, Y. et al., 2021b: Global exposure to flooding from the new CMIP6 climate model projections. *Scientific Reports*, 11 (1), 3740, doi:10.1038/s41598-021-83279-w.
Hoornweg, D. and Pope, K. (2017): Population predictions for the world's largest cities in the 21st century', *Environment and Urbanization,* 29(1), pp. 195-216.
Jägermeyr, J. et al., 2021: Climate change signal in global agriculture emerges earlier in new generation of climate and crop models". Nat. Food, in press, doi:10.21203/rs.3.rs-101657/v1.
Jurgilevich, A., Räsänen, A., Groundstroem, F. and Juhola, S., 2017. A systematic review of dynamics in climate risk and vulnerability assessments. Environmental Research Letters, 12(1): 013002.
Kay, R. and and Adler, J., 2017. Coastal planning and management. CRC Press.
Kelly-Gerreyn, B. A. et al., 2014: Benthic biomass size spectra in shelf and deep-sea sediments. *Biogeosciences*, 11(22), 6401-6416, doi:10.5194/bg-11-6401-2014.
Kienberger, S., Blaschke, T. and Zaidi, R.Z., 2013. A framework for spatio-temporal scales and concepts from different disciplines: the 'vulnerability cube'. Natural Hazards, 68(3): 1343-1369.
Klein Goldewijk, K., A. Beusen and P. Janssen, 2010: Long-term dynamic modeling of global population and built-up area in a spatially explicit way: HYDE 3.1. *The Holocene*, 20 (4), 565-573.
Klein Goldewijk, K., A. Beusen, G. Van Drecht and M. De Vos, 2011: The HYDE 3.1 spatially explicit database of human-induced global land-use change over the past 12,000 years. *Global Ecology and Biogeography*, 20 (1), 73-86.
Kulp, S. and B. Strauss, 2019: New elevation data triple estimates of global vulnerability to sea-level rise and coastal flooding. *Nature Communications*, 10(4844), doi:10.1038/s41467-019-12808-z.
Kwiatkowski, L., O. Aumont and L. Bopp, 2019: Consistent trophic amplification of marine biomass declines under climate change. *Global Change Biology*, 25(1), 218-229, doi:10.1111/gcb.14468.
Meredith, M. et al., 2019: Polar Regions. In: *IPCC Special Report on the Ocean and Crysosphere in a Changing Climate* [Pörtner, H. O., D. C. Roberts, V. Vmasson-Delmotte, P. Zhai, M. Tignor, E. Poloczanska, K. Mintenbeck, A. Alegría, M. Nicolai, A. Okem, J. Petzold, B. Rama and N. M. Weyer (eds.)], pp. 203-320.
Meza, I. et al., 2020: Global-scale drought risk assessment for agricultural systems. Nat. Hazards Earth Syst. Sci., 20(2), 695-712, doi:10.5194/nhess-20-695-2020.
Miller, K. A., G. R. Munro, U. R. Sumaila and W. W. L. Cheung, 2013: Governing marine fisheries in a changing climate: a game-theoretic perspective. *Can. J. Agric. Econ.*, 61(2), 309-334, doi:10.1111/cjag.12011.
Mills, G. et al., 2018: Closing the global ozone yield gap: quantification and cobenefits for multistress tolerance. Glob Chang Biol, 24(10), 4869-4893, doi:10.1111/gcb.14381. {AI.21, AI.22, AI.23, AI.Mora, C., Dousset, B., Caldwell, I. R., Powell, F. E., Geronimo, R. C., Bielecki, Coral R., Counsell, C. W. W., Dietrich, B. S., Johnston, E. T., Louis, L. V., Lucas, M. P., McKenzie, M. M., Shea, A. G., Tseng, H., Giambelluca, T. W., Leon, L. R., Hawkins, E. and Trauernicht, C. (2017b) 'Global risk of deadly heat', *Nature Climate Change,* 7, pp. 501.
Mora, C., Dousset, B., Caldwell, I. R., Powell, F. E., Geronimo, R. C., Bielecki, Coral R., Counsell, C. W. W., Dietrich, B. S., Johnston, E. T., Louis, L. V., Lucas, M. P., McKenzie, M. M., Shea, A. G., Tseng, H., Giambelluca, T. W., Leon, L. R., Hawkins, E. and Trauernicht, C. (2017b) 'Global risk of deadly heat', Nature Climate Change, 7, pp. 501.
Nyboer, E. A., C. Liang and L. J. Chapman, 2019: Assessing the vulnerability of Africa's freshwater fishes to climate change: A continent-wide trait-based analysis. *Biological Conservation*, 236, 505-520, doi:https://doi.org/10.1016/j.biocon.2019.05.003.
Østhagen, A., J. Spijkers and O. A. Totland, 2020: Collapse of cooperation? The North-Atlantic mackerel dispute and lessons for international cooperation on transboundary fish stocks. *Marit. Stud.*, 19(2), 155-165, doi:10.1007/s40152-020-00172-4.
Robinson, L. M. et al., 2015: Rapid assessment of an ocean warming hotspot reveals "high" confidence in potential species' range extensions. *Glob. Environ. Change*, 31, 28-37, doi:10.1016/j.gloenvcha.2014.12.003.
Rufat, S., Tate, E., Burton, C.G. and Maroof, A.S., 2015. Social vulnerability to floods: Review of case studies and implications for measurement. International Journal of Disaster Risk Reduction, 14: 470-486.
Scussolini, P. et al., 2016: FLOPROS: an evolving global database of flood protection standards. *Nat. Hazards Earth Syst. Sci.*, 16 (5), 1049-1061, doi:10.5194/nhess-16-1049-2016.
Selig, E. R. et al., 2019: Mapping global human dependence on marine ecosystems. Conservation Letters, 12(2), e12617, doi:10.1111/conl.12617.
Sharps, K. et al., 2020: Yield Constraint Score (YCS) for the effect of five crop stresses on global production of four staple food crops, NERC Environmental Information Data Centre. Available at: https://doi.org/10.5285/d347ed22-2b57-4dce-88e3-31a4d00d4358.
Spielman, S.E., et al., 2020. Evaluating social vulnerability indicators: criteria and their application to the Social Vulnerability Index. Natural Hazards, 100(1): 417-436.

Stuart-Smith, J. et al., 2018: Southernmost records of two Seriola species in an Australian ocean-warming hotspot. *Marine Biodiversity*, 48(3), 1579-1582, doi:10.1007/s12526-016-0580-4.
Taberna, A., Filatova, T., Roy, D. and Noll, B., 2020. Tracing resilience, social dynamics and behavioral change: a review of agent-based flood risk models. Socio-Environmental Systems Modelling, 2: 17938.
Tanoue, M., Y. Hirabayashi and H. Ikeuchi, 2016: Global-scale river flood vulnerability in the last 50 years. *Scientific Reports*, 6, 36021, doi:10.1038/srep36021.
Tanoue, M., R. Taguchi, H. Alifu and Y. Hirabayashi, 2021: Residual flood damage under intensive adaptation. *Nature Climate Change*, In Press.
Thomas, A. et al., 2021: Global evidence constraints and limits to human adaptation. *Regional Environmental Change*, 21, doi:doi.org/10.1007/s10113-021-01808-9.
Thornton, P. K., G. C. Nelson, D. Mayberry and M. Herrero, 2021: Increases in extreme heat stress in domesticated livestock species during the twenty-first century. *Global Change Biol.*, doi:10.1111/gcb.15825.
Tittensor, D. P. et al., 2018: A protocol for the intercomparison of marine fishery and ecosystem models: Fish-MIP v1.0. *Geoscientific Model Development*, 11(4), 1421-1442, doi:10.5194/gmd-11-1421-2018.
Tittensor, D. P. et al., 2021: Next-generation ensemble projections reveal higher climate risks for marine ecosystems. *Nature Climate Change*, Accepted.
Trisos, C. H., C. Merow and A. L. Pigot, 2020: The projected timing of abrupt ecological disruption from climate change. *Nature*, 580(7804), 496-501, doi:10.1038/s41586-020-2189-9.
UNISDR, 2004: Living with risk: A global review of disaster reduction initiatives: Version 1. In: Living with risk: A global review of disaster reduction initiatives: Version 1. UN. International Strategy for Disaster Reduction (ISDR). Secretariat; World ….
Viviroli, D. et al., 2020: Increasing dependence of lowland populations on mountain water resources. *Nature Sustainability*, doi:10.1038/s41893-020-0559-9.
Vousdoukas, M. I. et al., 2020a: Reply to: Sandy beaches can survive sea-level rise. *Nature Climate Change*, 10(11), 996-997, doi:10.1038/s41558-020-00935-1.
Vousdoukas, M. I. et al., 2020b: Sandy coastlines under threat of erosion. *Nature Climate Change*, 10(3), 260-263, doi:10.1038/s41558-020-0697-0.
World Bank, 2019: *The World Governance Indicators*. Available at: https://info.worldbank.org/governance/wgi/.
World Bank, 2020: *The World Development Indicators: GDP (current US$)*. Available at: https://data.worldbank.org/indicator/NY.GDP.MKTP.CD.
Xu, C. et al., 2020: Future of the human climate niche. *Proceedings of the National Academy of Sciences*, 117(21), 11350-11355, doi:https://doi.org/10.1073/pnas.1910114117.
Yool, A. et al., 2017: Big in the benthos: future change of seafloor community biomass in a global, body size-resolved model. *Global Change Biology*, 23(9), 3554-3566, doi:10.1111/gcb.13680.